Clinically Oriented Translational Cancer Multilevel Modelling

Deliverable D5.1

Glioma model for prediction of cell survival probabilities in response to radio- and chemotherapy

Project Number:	FP7--IST-*223979*
Deliverable Id:	D5.1
Deliverable Name:	Glioma model for prediction of cell survival probabilities in response to radio- and chemotherapy
Submission Date:	31/07/2009

COVER AND CONTROL PAGE OF DOCUMENT	
Project Acronym:	CONTRACANCRUM
Project Full Name:	Clinically Oriented Translational Cancer Multilevel Modelling
Document id:	D5.1
Document name:	Glioma model for prediction of cell survival probabilities in response to radio- and chemotherapy
Document type	RE
Version:	0.1
Submission date:	31/07/2009
Editor: Organisation: Email:	Amos Folarin UCL a.folarin@cancer.ucl.ac.uk

Document type PU = public, INT = internal, RE = restricted

ABSTRACT:

Deliverable 5.1 details the preliminary therapy sensitivity prediction for glioma. These models will enable the incorporation of individualized patient molecular profiles within the ContraCancrum simulator by the perturbation of cell survival in the proliferation model at the tissue level of simulation. Here we discuss the data available for such a statistical models and the methodological approach.

Using drug (temozolomide/dacarbazine) and radiation sensitivity data, coupled with microarray expression data, we have defined a signature capable of predicting *in-vitro* response to therapy as a measure of cell-survival probability. This method provides a means to incorporate molecular information within the context of *in-silico* simulation of patient specific therapy as part of the ContraCancrum.

KEYWORD LIST: glioma, lung cancer, in silico oncology, cancer modelling, expression profiling, therapy response prediction

MODIFICATION CONTROL			
Version	Date	Status	Author
0.1	05/05/2009	Draft	Amos Folarin

List of Contributors

Sylvia Nagl UCL

Georgios S. Stamatakos ICCS

Norbert M. Graf USAAR

Contents

1 Publishable Executive Summary

This document details the deliverable D5.1 – *Glioma model for prediction of cell survival probabilities in response to radio- and chemotherapy* for the ContraCancrum project. The primary goal here relates to the integration of molecular data into the Glioma model thereby enabling the simulation of tumour growth based on individualized patient molecular profiles. At present the focus remains is on the incorporation of expression data derived from microarray experiments on cell lines and real patient tumours, these data are drawn from retrospective datasets, further data will be available for validation through prospective studies generated by the University Hospital of Saarland as part of the clinical validation study.

Numerous studies have demonstrated a link between specific molecular profiles and response to therapy in tumours. This provides an opportunity to incorporate this prognostic information in a multi-scale simulation setting, allowing the impact of molecular profiles of sensitivity and resistance to be considered *in-silico*.

A review of the methods is provided followed by a summary of the available data. Workflows for the modelling process are discussed. And finally an application of these methods in the generation of molecular signatures in Glioma is presented in detail.

2 Introduction

This document describes the glioma response to therapy model. D5.1 details the data and methods used in the preliminary model for predicting cell-survival probabilities in response to radio and chemotherapy regimes. It is our intention that this is a data driven approach, here we will leverage the publicly available databases of microarray and drug screen data as the basis of the model, and where possible we will use independent datasets for validation.

The molecular state of the cell is an important factor in the therapeutic outcome of tumour therapy [9,26,30,38]. A number of studies have demonstrated association between specific molecular profiles and response to therapy in tumours[4,11,28]. This provides an opportunity to incorporate prognostic information from the molecular level into a multi-scale simulation setting, allowing for the impact of different molecular profiles of sensitivity and resistance to be considered *in-silico*. The objective of WP-5(T5.2) is to utilize high throughput datasets to establish models of molecular determinants of response to therapy in the two exemplar tumour types. With expression profiling is now becoming commonplace in clinical trials, these approaches have the capacity to produce a picture of the cancer at the molecular level.

At present, a mechanistic molecular model is not possible as it is not fully understood how the components of individual patient's response to therapy are manifest. We therefore consider this to be beyond the scope of possibility for the project. Our method is therefore based on a comparison of patient molecular profile to a database of *in-vitro* drug response data. A statistical model is constructed based on a correlation between gene expression and therapy induced inhibition of cell growth (e.g. GI_{50}). Such data exist for glioma & lung cancer cell lines in the NCI-60 database and other published literature. This statistical model will be used to assess a given patients molecular profile, thus enabling the estimation of cellular therapy response. This will then be used to modify a 'cell kill probability' for a given tumour and radiation/drug dose. It is this cell kill probability that will form the interface between the molecular (WP-5) and cellular scale models (WP-4).

3 Objectives

Our objectives for the glioma model include:

1. The definition of a suitable modelling methodology.
2. Acquisition of appropriate data for glioma model generation and validation.
3. Model development and testing.
4. Model integration w.r.t. ContraCancrum multi-level simulations.
5. Evaluation of model performance in the multi-level scenario.

Additionally, it is suggested that characteristic defects in the tumour biology may manifest at the level of biological pathways, we will therefore also consider perturbation of a number of key pathways using a large database of clinical glioma expression profiles and consider the differential expression of pathway specific genes from normal brain tissue controls.

4 Glioma Therapy and Molecular Classification

Gliomas tumours include: ependymoma, oligodendroglioma and astrocytoma (of which glioblastoma multiforme is the most common); these are derived respectively from ependymal, oligodendrocytes and astrocytes cells. Mixed tumours such as oligoastrocytomas also exist including a mix of cells further complicating the diagnosis and treatment of these tumours.

Freije *et al.* showed that gene expression profiling (85 samples) could be utilised as a means to predict glioma patient survival, here defining a 44 gene classifier that accurately classifies gliomas into prognostic groups[9]. This idea was further explored by using a large agglomerated microarray dataset (267 samples) to show a clear molecular basis for different subtypes of glioblastoma and a subset that have improved prognosis[19] and found that this approach outperforms histological based classification[25].

Current treatments for gliomas often include combined approaches using surgery, radiotherapy and chemotherapy[35] the effects of which have been shown to be either additive or supra-additive depending on the tumour type *in-vitro*[37] and *in-vivo*[8,35]. Temozolomide, an alkylating agent that is able to cross the blood-brain barrier effectively is the current choice chemotherapeutic agent. Temozolomide is a member of a class of drugs that includes Dacarbazine (DTIC) these are prodrugs of MTIC (3-methyl-(triazen-1-yl)imidazole-4-carboxamide) which is able to alkylate the O-6 position of guanine residues. This chemical modification results in DNA lesions during cellular DNA replication, followed by cell death triggered through the DNA damage response pathway. Response to radiotherapy with concomitant and adjuvant temozolomide depends on tumour O6-methylguanine methyltransferase (MGMT) status (a protein which reacts stoichometrically to remove drug-induced alkylguanine adducts from DNA). Around half of patients with glioblastomas will not benefit from this combination because of effective MGMT-based repair of DNA base damage[13,24]. This dependency of MITC on MGMT has also been demonstrated *in-vitro* in colon and melanoma[4] cancer lines. There is also evidence that MGMT may be regulated by methylation status of the gene promoter[13].

Among the factors reported to contribute to temozolomide resistance are base excision repair (BER), in particular poly(ADP-ribose) polymerase 1(PARP1), and mismatch repair (MMR). Analogous to MGMT, the BER pathway plays an important role in repairing the cytotoxic methyl DNA adducts created by temozolomide, and high BER activity can confer tumour resistance to the effects of the drug. On the other hand, a deficiency in the MMR pathway can lead resistance as a continuation of DNA replication, results in the loss of the cytotoxic effects of temozolomide[10]. It has been also suggested that MGMT may be targeted to alleviate temozolomide resistance through the use of O6-benzylguanine, or RNA interference-mediated gene silencing of MGMT[14,16].

5 Pharmacogenomic Data Sources

5.1 NCI-60 Cell Line Data & Drug/Radiological Response Data

5.1.1 The NCI-60 Panel

The US National Cancer Institute NCI-60 consists of a series 60 human tumour cell lines derived from 9 cancer types (leukaemia, colon, lung, CNS, renal, melanoma, ovarian, breast and prostate) which has been used to assess *in-vitro* performance of cancer therapies. This panel of cell lines was developed in the late 1980s as an in vitro drug-discovery tool intended to replace the use of transplantable animal tumours in anticancer drug screening [33]. The panel has been tested for sensitivity to more than 100,000 potential chemotherapy agents and profiled comprehensively at the DNA, RNA, protein, functional, and pharmacologic levels. For a tabulated description of the cell lines see **[Appendix Table 8.1 and Table 8.2].**

5.1.2 Microarray Data

Basal NCI-60 expression levels have been collected using various platforms. For the following work, we used the most current Affymetrix chipset HG-U133A/B data [31].

Manufacturer: Affymetrix
Platform: HG-U133
Molecular Target: RNA
Platform Description: 44,000 probeset 2-chip set

Expression data for one of the 60 cell lines (LC:NCI_H23) was not available to download as HGU133 array cel file was missing corresponding to "13440HG133B21.cel", we have discounted this sample from the analyses, therefore only using 59 of the 60 NCI-60 cell lines.

Amundson *et al.* have also made available transcriptional response to radiation microarray data, GEO accession (GSE7505), using NHGRI Homo sapiens 6K chip [2]. In contrast to reported basal gene expression patterns, changes in expression in response to radiation showed little tissue-of-origin effect, apart from differentiating the lymphoblastoid cell lines from other cell types.

5.1.3 Drug Sensitivity Data

For the NCI-60 panel, drug sensitivity data were collated from the Developmental Therapeutics Program (DTP) screen[23] and through CellMiner[3,32]. Here sensitivity determined by Sulforhodamine assay was conducted at least 4 times for 1429 molecules with known 2D structure and known mechanism of action for many of the drugs[3]. Although other screen data are available with either larger number of replicates or larger compounds, this dataset represented the best available compromise between number of replicates and number of screened compounds.

The drug response parameters include: 50% Growth Inhibition (GI_{50}) and 50% Lethal Concentration (LC_{50}), a cytotoxic measure, are extrapolated from dose-response curves by linear interpolation. The Total Growth Inhibition (TGI), a cytostatic measure, is read as the x-axis intercept. The higher GI_{50}, LC_{50}, and TGI the

greater the resistance to treatment is. These are all measures of drug resistance and are frequently inverted to give drug sensitivities, taken as e.g. –(log10(GI_{50})). It should be noted that as 4 drug concentration values are used, some approximation is required where the criteria is not satisfied: including, e.g. for GI_{50}, the case where the drug concentrations used are not high enough to reach the putative e.g. 50% inhibition mark then the highest concentration is assigned (occurring in 3% of the screen), and where the e.g. 50% mark is reached below the first concentration measure - then the lowest concentration used is assigned.

So for *T*=optical density at time (48 or 0 hrs), and *C*=control optical density at 48hrs, the GI_{50} LC_{50} and TGI are given by the test drug concentration:

$$GI_{50} = (T_{48} - T_0)/(C - T_0) \times 100 = 50 \quad [5.1]$$

$$LC_{50} = (T_{48} - T_0)/(T_0) \times 100 = -50 \quad [5.2]$$

$$TGI = (T_{48} - T_0)/(C - T_0) \times 100 = 0 \quad [5.3]$$

Standard dilutions span a four -log concentration range, here: 1 = $1E^{-5.2}$, 2 = $1E^{-4.2}$, 3 = $1E^{-3.2}$, 4 = $1E^{-2.2}$ and 5 = $1E^{-1.2}$. In the example in [**Figure 5.1**] for the cell line EKVX, the GI_{50} = $1E^{-4.05}$, the TGI = $1E^{-3.49}$ and the LC_{50} was not reached (>$1E^{-1.2}$, the maximum concentration tested). Full discussions of the DTP screening process are beyond the scope of this document and can be found on their website [23].

The highest concentration in the DTP screen for both dacarbazine and temozolomide are $1E^{-4}$ which does not resolve the bulk of LC_{50} and TGI values, GI_{50} was therefore selected as the sensitivity indicator for this study as the value is more likely to have been reached within the range of assessed drug concentrations.

The NCI-60 drug screen does not include temozolomide; we have therefore elected to use the data from the dacarbazine screen. Data from two sources are available on dacarbazine sensitivity the DTP website[23] directly or from CellMiner[3]. We see that the data are poorly characterized for some of CellMiner download where values appear as 4 [**Appendix Table 8.3**]. Accordingly we have selected the DTP dataset for this study as it is most current.

Figure 5.1 Growth Inhibition Curves

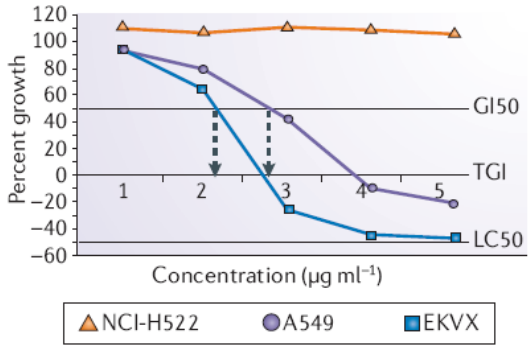

Example drug concentration vs. growth curves, showing GI_{50} LC_{50} and TGI. Adapted from [33]. 0% = starting cellular population T_0.

5.1.4 Radiation Sensitivity Data

Data on radiation sensitivity was taken from the recent study by Amundson *et al*. [2], in this study cells from the NCI-60 panel were exposed to 0, 8, or 16 Gy of ionizing γ-rays and assessed by clonogenic survival experiments to establish radiation survival curves [**Figure 5.2 (A)**]. D_0 and extrapolation number *n*, are two variables used to describe the shape of survival curves. D_0 is the dose required to reduce survival by 37% (a factor of e) in the linear part of the curve. The extrapolation number, a measure of the initial shoulder of the survival curve, is the y-intercept obtained by extrapolating the linear part of the curve back to the axis [**Figure 5.2 (B)**].

Survival fraction is calculated as the fraction of viable cells. Where the *PE*=plating efficiency (percentage of cells that go on to form colonies) and *SF*=survival fraction is given by:

$$PE = \frac{\text{Number of colonies counted}}{\text{Number of cells seeded}} \times 100 \qquad [5.4]$$

$$SF = \frac{\text{Colonies counted}}{\text{Cells seeded} \times (\text{PE}/100)} \qquad [5.5]$$

Baseline doubling time (T2) without irradiation as well as survival fractions after 24hrs are given for single γ-rays radiation doses of 2, 5 and 8 Gy. Caspase activity was determined by flow cytometry as an estimate of apoptosis induction. Caspase activity levels at 24hr time after 8- and 16 Gy doses relative to untreated controls are reported. The Amundson dataset has been collated in [**Appendix Table 8.4**]. From this data, we have

extrapolated the 50% Lethal Dose in Gy (LD_{50}) by fitting a linear quadratic model, **[5.6]** to the radiation survival data for 0,2,5 and 8 Gy [**Figure 5.3**] and then solving for LD_{50} **[5.7]**, where *D*=Dose (Gy), α and β are constants.

$$SF = e^{-\alpha D - \beta D^2} \quad [5.6]$$

$$LD_{50} = -\alpha + \sqrt{\frac{\alpha^2 - 4\beta \ln(0.5)}{2\beta}} \quad [5.7]$$

D_0 and LD_{50} are analogous to LC_{50} in measuring a dose cytotoxic effect of drugs (i.e. no growth control is used as is the case with GI50 and TGI). D_0 tends to reflect the higher dose SF8 and LD_{50} the lower SF2. We have used LD_{50} as it appears to give a better approximation of the radiation curve correlating much better with SF than any single one of the SF parameters [**Figure 5.3 (B)**], and so a better overall representative of radio-sensitivity. The inversion $-\log(LD_{50})$ is taken as a radiation sensitivity measure.

Figure 5.2 Radiation Survival Fraction Curves

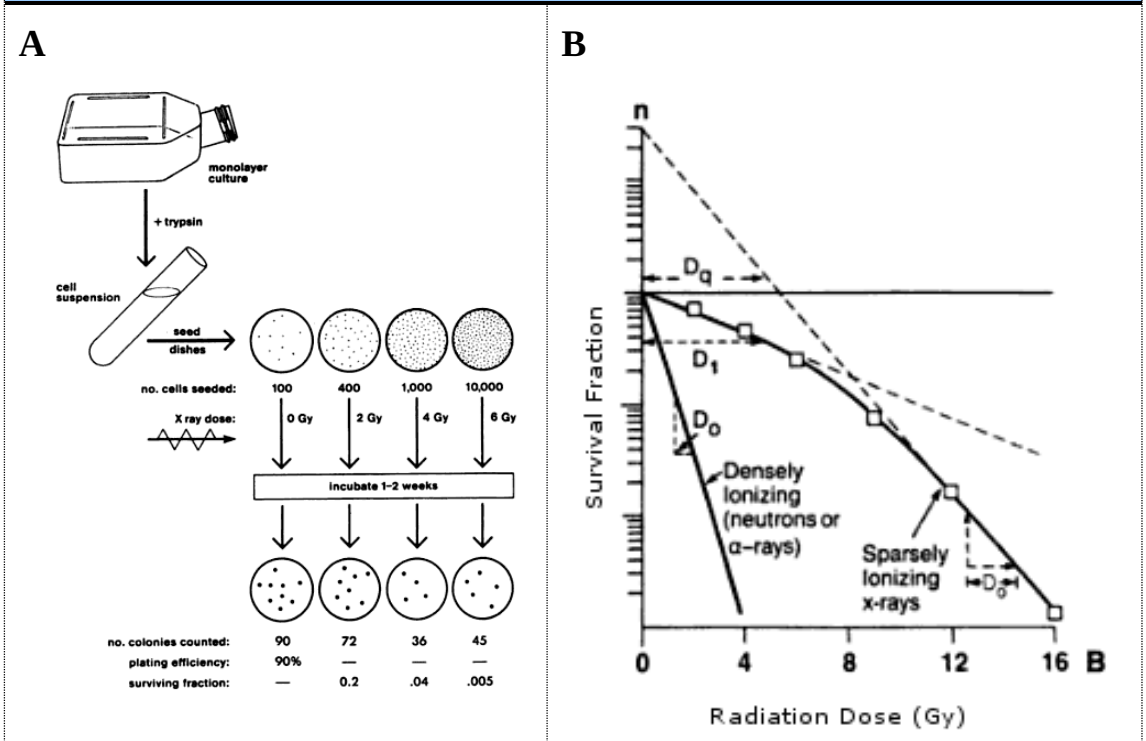

(A) Cells from stock culture are used to produce a survival curve and (B) Shape of survival curve for mammalian cells exposed to radiation, square markers indicate the line for sparsely ionizing radiation such as x-rays and γ-rays, parameters D_0 and D_1 describe the linear parts of the curve. Adapted from "*Radiobiology for the Radiologist*"[12].

Figure 5.3 Radiation Response Parameters

A

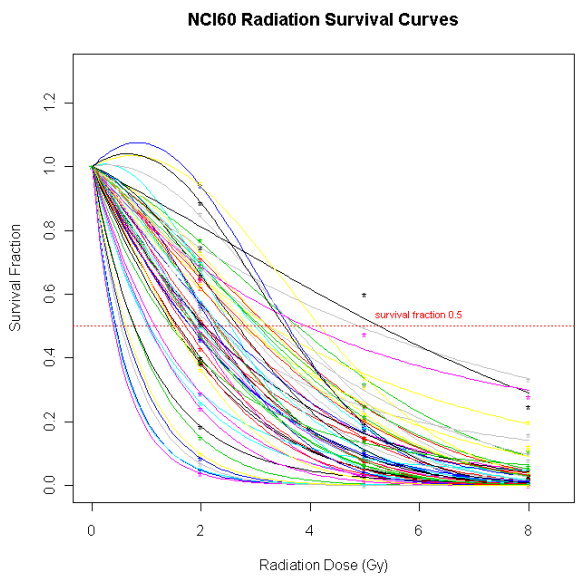

B

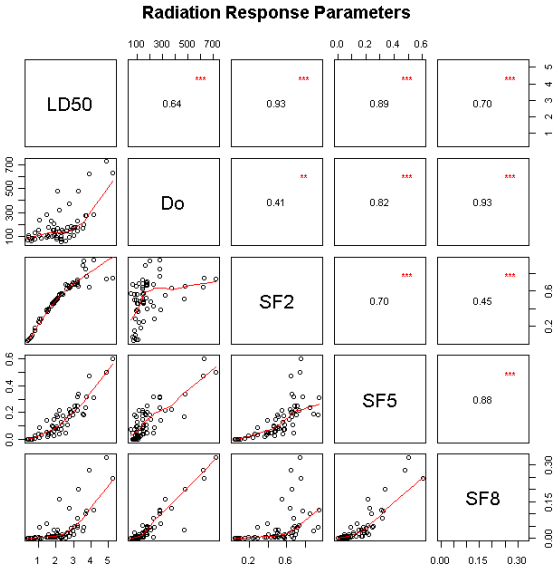

(A) Linear quadratic survival curves fitted to SF:0,2,5,8 Gy, the LD_{50} values are taken at vertical intersections with the red 50% line. (B) Correlation between of survival parameters LD50, D0, SF2-8 are all measurements of radiation response; the Pearson's correlation value and scatter-plots are given in the upper and lower triangular matrix respectively.

5.2 Prospective Glioma Cell Line Data

We have secured a collaboration with the Wellcome Trust Centre for Stem Cell Research and Department of Biochemistry at University of Cambridge to carry out a glioma temozolomide and dacarbazine *in-vitro* drug screen using their adherent cell platform (Incucyte)[27]. This collaboration will involve Steven Pollard and Davide Danovi who have kindly agreed to make available glioma neural stem-cell (CNS) panel for the purpose of running carrying out the screen. The work could not however be organised until mid-September 2009 so is not discussed in detail, other than to say, the objective for this data will be to provide validation for the NCI60 derived gene signature. This independent glioma cell line screen could be used in an analogous manner to the lung docetaxel screen used by Potti et al. independent dataset that measured docetaxel sensitivity in a series of 29 lung cancer cell lines (Gene Expression Omnibus (GEO) database (see URLs) accession number GSE4127) [28] and the melanoma temozolomide screen used by Augustine et al. [4].

Human brain tumours appear to have a hierarchical cellular organization suggestive of a stem cell foundation and interest in these cells is of growing importance. Recently, cells with the CD133 putative cancer stem cell marker have been shown to be both more resistant to DNA damaging therapy and to have a greater clonongenic potential compared to CD133- cells [6].

This will presently focus on drug screening data. We may later extend this to radiation response using methods described by as used by Amundson *et al.* [2].

A list of the proposed cell lines to be included in the study is listed below **[Table 5.1]**.

Table 5.1 Cell Lines In Planned Study

Cell Line	Description	Microarray Data	Reference
G144	Glioblastoma GNS	Source: GEO: GSE15209 Type: HGU133plus2	Pollard et al. 2009[27]
G166	Glioblastoma GNS		
GliNS2	Glioblastoma GNS		
G174	Oligoastrocytoma GNS		
CB660	Glioblastoma GNS		
NORM#12	Non-malignant Human Cortex		
HS27	Fibroblast (use as control for normal tissue response)		
T98G	Temozolomide Resistant	Source: [34] Type: HGU133plus2, HGU133A	Short et al. 2007[34] Kanzawa et al. 2003[16]
U373	Temozolomide Sensitive		
A7	Glioblastoma		
U87	Glioblastoma		
SF-268	NCI60 CNS	Source: [31] Type: HGU133A/B, HGU95A	Shoemaker et al. 2006[33]
SF-295	NCI60 CNS		
SF-539	NCI60 CNS		
SNB19	NCI60 CNS		
SNB75	NCI60 CNS		
U251	NCI60 CNS		
D384	*Possible inclusion*		Van Rijn et al. 2000 [37]

Cell lines to be used in a proposed drug response screen. This data can then be used as part of the validation for the temozolomide response profile. One of the normal cell lines can be substituted for NORM12 if necessary, this list is not finalized yet.

5.3 CMAP Cell Line Data

A further data resource of *in-vitro* drug response is the Connectivity Map (CMAP), which is a collection of genome-wide transcriptional expression data from cultured human cells treated with bioactive small molecules[17]. The CMAP contains more than 7,000 expression profiles and the drug screen data from 1,309 compounds including temozolomide. Data are from a range of 5 cell lines **[Table 5.2]**. Presently, we are in the process of evaluating if the temozolomide drug response data would be of value.

Table 5.2 CMAP Cell Lines

Cell Line	Description
MCF7 (ATCC# HTB-22)	Human breast epithelial adenocarcinoma cell line derived from pleural effusion.
PC3 (ATCC# CRL-1435)	Epithelial cell line established from human prostate adenocarcinoma
SKMEL5 (ATCC# HTB-70)	Human malignant melanoma cell line derived from a metastatic axillary node
HL60 (ATCC# CCL-240)	Human promyelocytic cell line established by leukopheresis from promyelocytic leukemia
MCF7	MCF7 cells

Cell lines used in the production of the CMAP connectivity matrix. Drug response and microarray expression data is available for download from the CMAP site.

5.4 REpository for Molecular BRAin Neoplasia DaTa (REMBRANDT)

REMBRANDT is a collaborative project between the National Institute of Health (NIH)'s National Cancer Institute (NCI) and the National Institute of Neurological Disorders and Stroke (NINDS) [21]. As a repository for clinical and functional genomics data REMBRANDT provides a publicly available bioinformatics knowledge base derived from clinical trials specifically for glioma tumours[20].

For the purposes of the ContraCancrum interests, we are interested in the large collection of expression data collected from glioma biopsies and the associated response-to-therapy parameters for these patients. Microarray Data provided in REMBRANDT uses the Affymetrix HGU133plus2 platform. Of the REMBRANDT set we have currently 277 samples with matching clinical data.

Looking at high level parameters that may be reflective of patient response to therapy we have considered two in particular 1) MRI description and 2) survival time. We see however that survival time and MRI do not correlate (this was based on the subset of samples with available data) **[Figure 5.4 (A)]**. The survival time however appears as a bimodal distribution for the combined data **[Figure 5.4(B)]** this can be resolved further

to show that the major poor prognosis component is due to glioblastoma multiforme, where other tumours such as oligodendroglioma have better prognosis, in concurrence with Lee *et al.* [19]. The glioblastoma multiforme survival time distribution does still appear to be slightly bimodally distributed, again suggestive of a possibly distinct population **[Figure 5.4 (C)]**.

Selected response variables are discussed in [**Table 5.3**]:

Figure 5.4 Possible Indicators of Therapy Performance in REMBRANDT

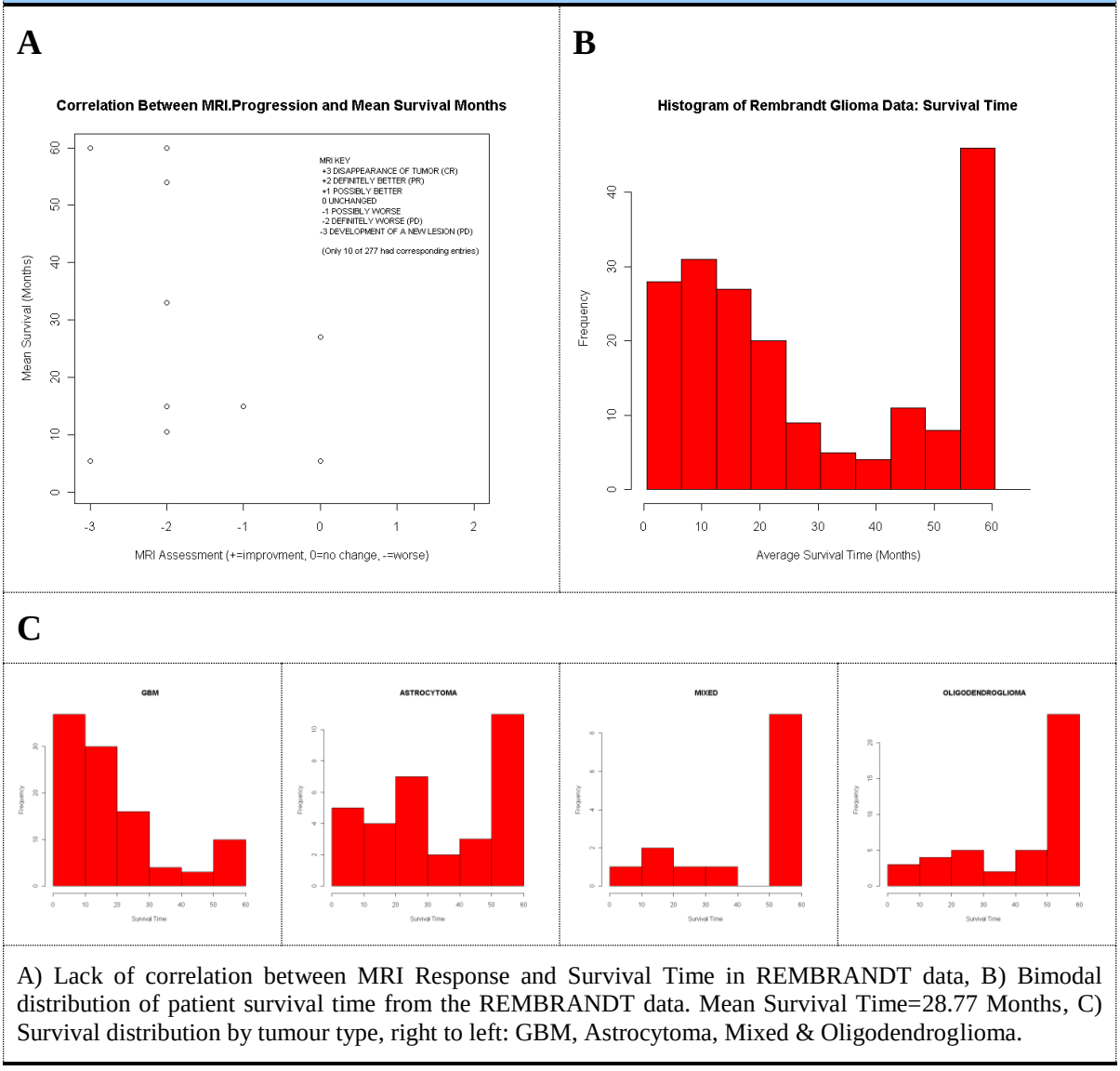

A) Lack of correlation between MRI Response and Survival Time in REMBRANDT data, B) Bimodal distribution of patient survival time from the REMBRANDT data. Mean Survival Time=28.77 Months, C) Survival distribution by tumour type, right to left: GBM, Astrocytoma, Mixed & Oligodendroglioma.

Table 5.3 REMBRANDT Clinical Response Parameters	
MRI.Desc	Response to treatment as determined by MRI imaging Relates to the disease evaluation as measured by scan (MRI/CT). Score definitions are the following: +3 DISAPPEARANCE OF TUMOR (CR) +2 DEFINITELY BETTER (PR) +1 POSSIBLY BETTER 0 UNCHANGED -1 POSSIBLY WORSE -2 DEFINITELY WORSE (PD) -3 DEVELOPMENT OF A NEW LESION (PD)
X.Survival.months.	Survival time in Months
Karnofsky	Score from the Karnofsky Performance status scale, representing the functional capabilities of a person.
Lansky	Score from an enumerated set of values representing performance status according to the Lansky scale. The Lansky scale is intended for use only with subjects under 12 years old.
MRI.Desc is not defined for all samples in the above format, some samples are given a descriptive entry which is not consistant with the metadata. A full list of the metadata is available at the REMBRANDT portal site.	

5.5 The Cancer Genome Atlas (TCGA)

The Cancer Genome Atlas (TCGA) is a collaborative pilot project between the National Cancer Institute (NCI) and the National Human Genome Research Institute (NHGRI) to understand the genomic changes that occur in cancer. This large project collected clinical and functional genomic data from patients with Glioblastoma Multiforme, Ovarian and Lung Cancers as part of the pilot project. The gene expression data is provided by TCGA on a number of platforms **[Table 5.4]**, for WP-5 we will make use of the transcriptional profiling data on HGU133A chips in order to remain consistent with the other studies of interest (REMBRANDT and NCI-60). Of these samples for glioblastoma, we have selected 273 samples which have matching clinical data.

Table 5.4 TCGA profiling datasets

Platform	**Data Type**
Affymetrix Human Exon 1.0 ST Array	Expression-Gene
Affymetrix Human Exon 1.0 ST Array	Expression-Exon
Affymetrix Genome-Wide Human SNP Array 6.0	SNP
Affymetrix Genome-Wide Human SNP Array 6.0	Copy Number Results
Affymetrix Genome-Wide Human SNP Array 6.0	LOH
Illumina DNA Methylation OMA002 Cancer Panel 1	DNA Methylation
Illumina DNA Methylation OMA003 Cancer Panel 1	DNA Methylation
Illumina 550K Infinium HumanHap550 SNP Chip	SNP
Illumina 550K Infinium HumanHap550 SNP Chip	Copy Number Results
Illumina 550K Infinium HumanHap550 SNP Chip	LOH
Biospecimen Metadata - Complete Set	Complete Clinical Set
Biospecimen Metadata - Minimal Set	Minimal Clinical Set
Agilent Human Genome CGH Microarray 244A	Copy Number results
Agilent Whole Human Genome Microarray Kit, 4 x 44K	Expression-Genes
Agilent 8 x 15K Human miRNA-specific microarray	Expression-miRNA
Agilent Human Genome CGH Microarray 44K	Copy Number Results
Agilent Whole Human Genome, 1 x 44K	Expression-Genes
Agilent Human miRNA Microarray	Expression-miRNA
Agilent 244K Custom Gene Expression G4502A-07-1	Expression-Genes
Applied Biosystems Sequence data	Trace-Gene-Sample Relationship
Applied Biosystems Sequence data	Mutations
Parallel data modalities collected as part of TCGA project	

Clinical covariates including (family history, medical history, onset and course of illness, nature and time of medical, surgical, and radiological treatments, responses to therapy, and outcome of disease) are collected by the TCGA data centres, pseudo-anonymised and are held in public and private repositories. Through negotiation with the NCI we have secured access to the private clinical data which include a number

of possible clinical response parameters **[Table 5.5]**. The private dataset however come with certain obligations and restrictions as detailed on the TCGA website's data access regulations [22].

Some possible therapy response variables are detailed in **[Table 5.5]**:

Table 5.5 TCGA Clinical Response Parameters

NUMBERPROLIFERATINGCELLS	Sample locations include both top and bottom of tumour section. However variability is high for this parameter
PERCENTNECROSIS	A measure of the percentage of necrosis present in the tumour. This may not be suitable as the selection criterion for samples requires that samples have (GBM <50% necrosis (others tumours < 20%) & At least 80% tumour Nuclei)
PROGRESSIONSTATUS	An indicator of tumour progression/recurrence after initial treatment
SURVIVALTIME	This parameter is currently calculated from DATEOFPROCEDURE rather than the INITIALPATHOLOGICDIAGNOSISDATE which had some errors in a number of the recorded fields

6 Modelling Cell Survival Probabilities

6.1 Therapy Sensitivity/Resistance Gene Expression Signatures

D5.1 will focus on producing a model for predicting cell-survival probabilities in response to radio and chemotherapy regimes. Here we take a pharmacogenomic approach, where the primary goal is the integration of molecular data into the ContraCancrum glioma model, thereby enabling the simulation of tumour growth based on individualized patient molecular profiles. This requires both gene expression and drug/radiation sensitivity data on cell lines which are determined *in-vitro*. To achieve this we classify cell lines from the NCI60 as resistant or sensitive to either radio or chemo therapies in the form of γ-radiation and temozolomide/dacarbazine respectively. We then select the genes that best discriminate resistant and sensitive cell lines. Next we construct a statistical model based the selected genetic features that predict response (e.g. GI_{50} or LD_{50} index). Then using gene expression profiles from patient microarray data and the statistical model we are able to estimate cell survival probability by extrapolating the predicted therapy sensitivity back to the raw confluence dose response curve.

6.1.1 The Potti-Augustine Method

We utilize the method laid out by Anil Potti whose group/collaborators have extensively studied the use of gene expression in the prediction of therapeutic response[28], of particular relevance to the ContraCancrum project were their application in lung cancer[29] and temozolomide signatures in melanoma [4] Potti *et al.* determined the gene expression signature that are both highly variable and differentially expressed between the low sensitivity and high sensitivity cell lines. This method relies on the availability of 1) being able to delineate the sensitive and resistant cell lines and 2) the gene expression profiles of these cell lines.

To develop an *in-vitro* gene expression based predictor of sensitivity/resistance from the pharmacologic data used in the NCI-60 drug screen studies, cell lines were chosen within the NCI-60 panel that would represent the extremes of sensitivity to a given chemotherapeutic agent (mean GI50 +/- 1SD). Additionally, as the TGI and LC50 dose also represent the cytostatic and cytotoxic measures of a given drug, the log transformed TGI and LC50 dose of the sensitive and resistant subsets was then correlated with the respective GI50 data to establish consistency across TGI, LC50 and GI50 dose response data. The hypothesis, being, that such rigorous selection would identify cell lines that represent the extremes of sensitivity to a given drug. However, it should be noted that the drug screening data on the NCI-60 panel in conjunction with matched expression data did not always yield predictors of chemotherapy response for certain drugs. In the approach used, the presence of high quality dose response data is critical. For instance, there needs to be enough samples representing the extremes of sensitivity to any given agent. Thus, if a drug screening experiment did not result in variable GI50 and/or LC50 data, the generation of a genomic predictor would not be possible (e.g. cis/carboplatin and methotrexate).

For the generation of a temozolomide sensitivity signature, a subset of 10 cell lines was selected from the NCI-60 panel of cancer cell lines that represented two extremes of sensitivity to temozolomide; five of these cell lines were classified as ‘‘resistant’’ and five as ‘‘sensitive’’. Using the gene expression profiles of these cell lines, 150 genes were identified that showed significantly different expression patterns between the ‘‘resistant’’ and ‘‘sensitive’’ cell lines **[Figure 6.1]** 93 genes (red) were more highly expressed in the resistant than in the sensitive cell lines, whereas 57 genes (blue) were more highly expressed in the sensitive than in the resistant cell lines. Prior processing of the gene expression data excluded probesets with signals present at background noise levels and those that did not vary significantly across samples.

The drug sensitivity and resistance data from the selected NCI60 cell lines was then used in a supervised analysis using binary regression methodologies. The signature summarizes its constituent genes as a single expression profile, and is here taken as the top principal components of the set of genes. When predicting the chemosensitivity patterns or pathway activation of cancer cell lines or tumour samples, gene selection and identification is based on the training data (gene expression profiles of the selected cell line classes), and then metagene values are computed using the principal components of the training data and the additional cell line or tumour expression data. Bayesian fitting of a binary probit regression model to the training data then enables an assessment of the relevance of the metagene signatures in within-sample classification, and estimation and uncertainty assessments for the binary regression weights mapping metagenes to probabilities.

To prevent over-fitting given the disproportionate number of variables to samples, a leave-one-out cross validation (LOOCV) analysis was performed to test the stability and predictive capability of the model. Each sample was left out of the data set one at a time, the model refitted (both the metagene factors and the partitions used) using the remaining samples, and the phenotype of the held out case was then predicted and the certainty of the classification was calculated.

Figure 6.1 Genes Differentially Discriminating Temozolomide Sensitivity And Resistance

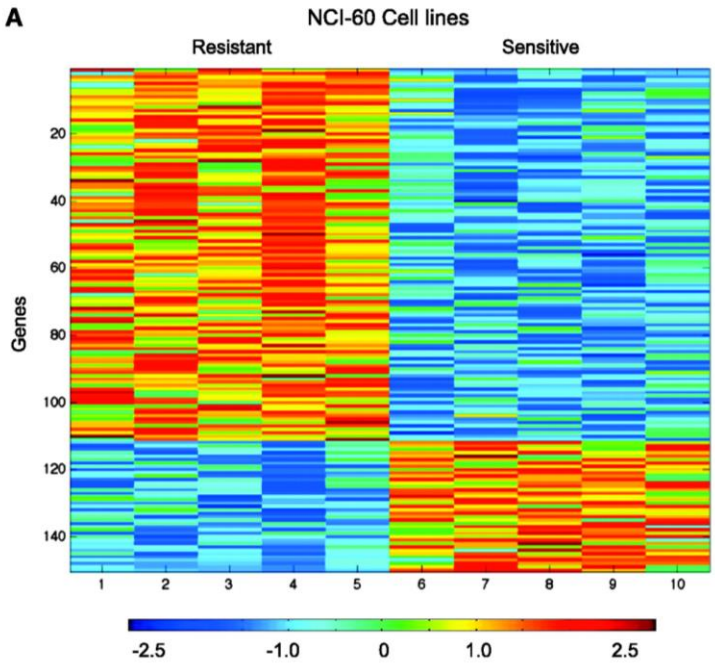

Gene expression signature of temozolomide resistance derived from 10 cell lines in the NCI-60 panel, showing a heatmap representation of genes that are differentially expressed across temozolomide-sensitive and temozolomide-resistant cell lines. Red and blue, genes that are expressed at high and low levels, respectively. The scale below shows the fold change difference in expression across the colour spectrum. Adapted from [4].

6.1.2 The Workflow

The general schema for the classification scheme for estimating cellular therapy sensitivity is outlined here for drug therapy (Temozolomide/Dacarbazine) **[Figure 6.2]** and Radio-therapy **[Figure 6.3]**. Evaluation a cell line or patient profile for analysis is detailed in **[Figure 6.4 A&B]**.

Figure 6.2 Workflow for Dacarbazine/Temozolomide Sensitivity Classification

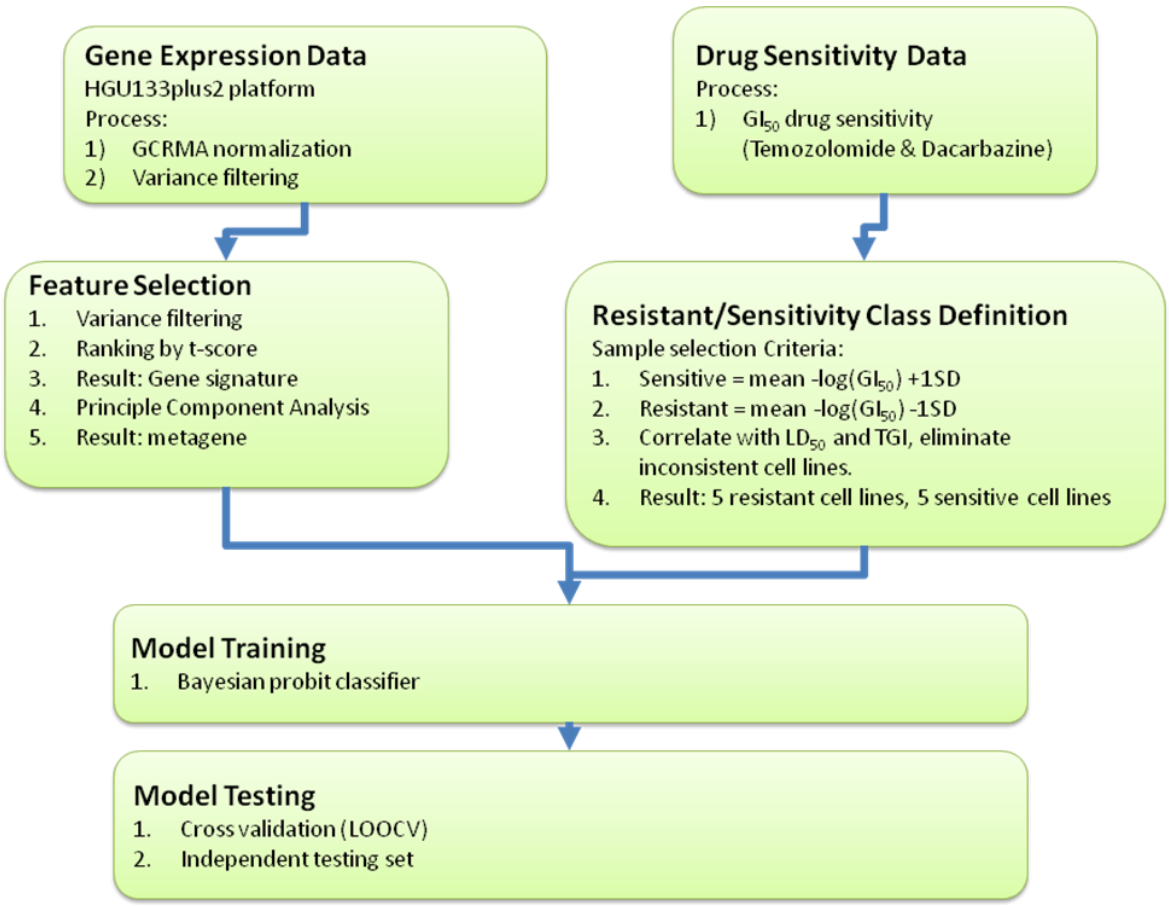

Process sequence used in the production of a classifier for predicting MITC based therapy sensitivity.

Figure 6.3 Workflow for Radiation Sensitivity Classification

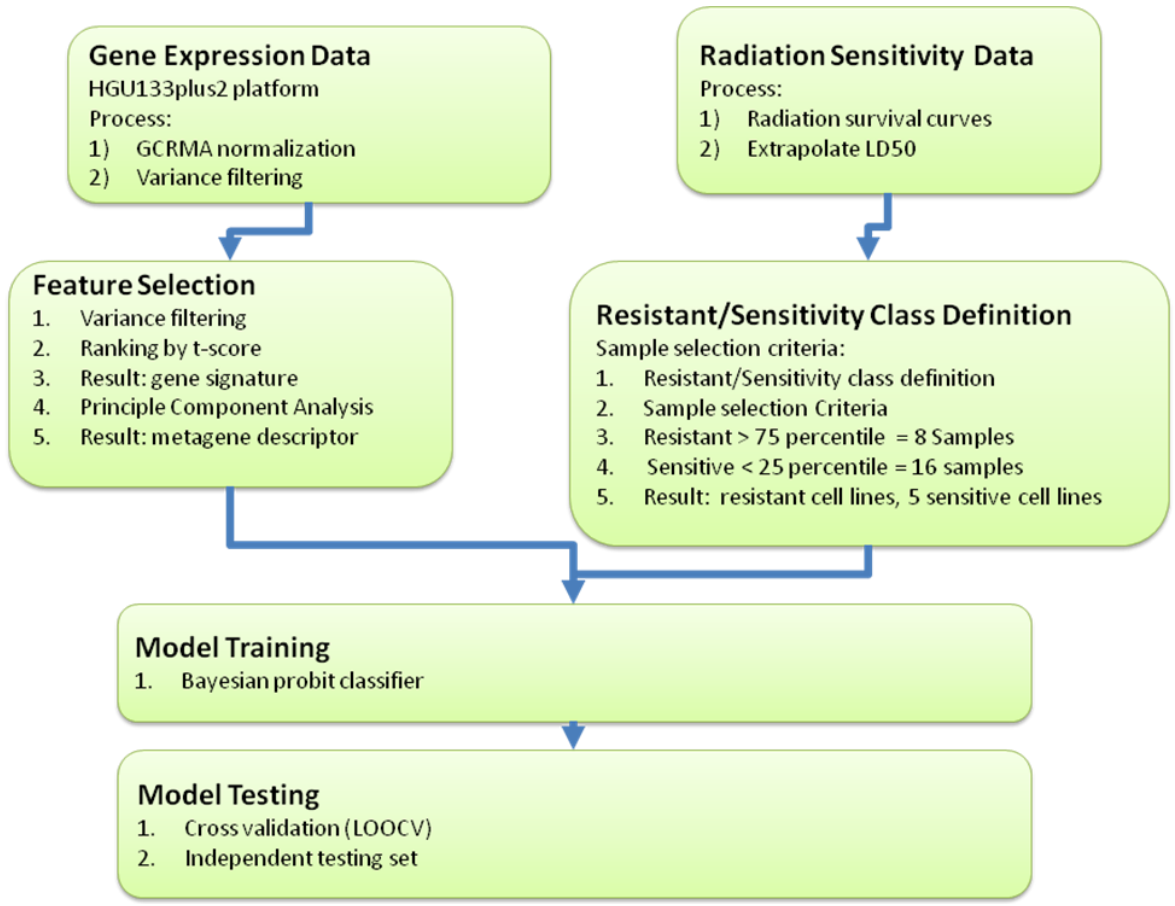

Process sequence used in the production of a classifier for predicting radiation based therapy sensitivity.

Figure 6.4 Assessment of Therapy Sensitivity

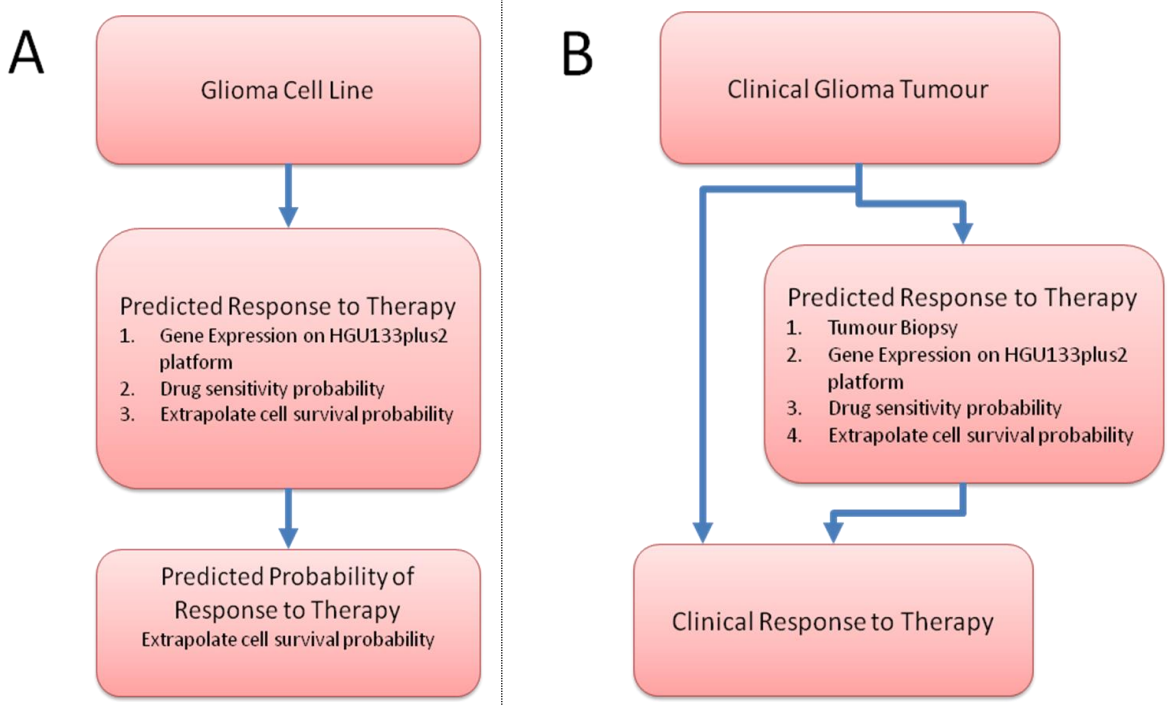

Strategy for assessment of performance of the classifier in (A) independent cell line data and (B) a clinical setting. Therapy sensitivity is used to extrapolate the cell survival probability by extrapolating back to the dose response curves.

6.1.3 Glioma Temozolomide Sensitivity Prediction

We have carried out preliminary work following the protocol detailed above [**Figure 6.2**]. Using these methods we have identified the genes signature listed in **[Figure 6.5]**, as show these genes (features) are sufficient to separate classes of resistant and sensitive, but also we see that the principle components here clearly also place the intermediate sensitivity cell lines in between the two extremes, these samples were not used in to construction of the classifier and so are an independent test set; this can be compared to the use of a random selection of genes which do not provide any coherent separation of the two classes **[Figure 6.6]**.

We started the work here by collating data from the DTP screen of 1429 compounds.

We used the following sensitivity to therapy measures:

- -(log10(GI_{50})) measure increases with of the sensitivity to drug compounds
- Later we plan to incorporate TGI and LC_{50} data in the class definition step; however, we have not been able to do this yet.

Currently we are exploring different classifiers for processing the data, this is currently ongoing.

Using a Leave one out cross validation scheme (LOOCV) and a trained support vector machine with a linear kernel (SVM) classification performance was estimated. Fairness of the cross validation test was guaranteed by splitting the training and test samples prior to any feature selection or training. On this basis an accuracy of 70% was achieved.

Figure 6.5 Dacarbazine Sensitivity Signature

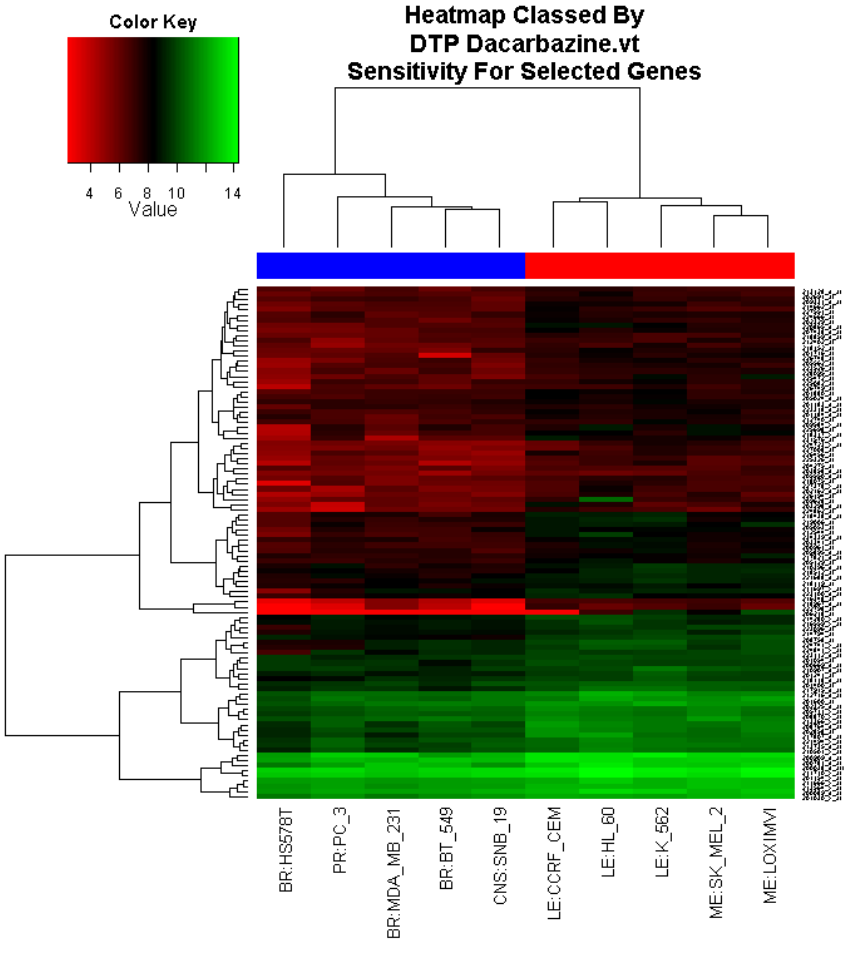

Profile of the top 100 differentially expressed genes between sensitive and resistant cell lines. Genes are given as rows, cell lines as columns. The horizontal bar shows the different classes of cell line columns (Red=Sensitive, Blue=Resistant). Array feature PIDs (RHS row labels) in **[Appendix Table 8.5]**.

Figure 6.6 Sensitivity Class Distribution in Principle Component Space

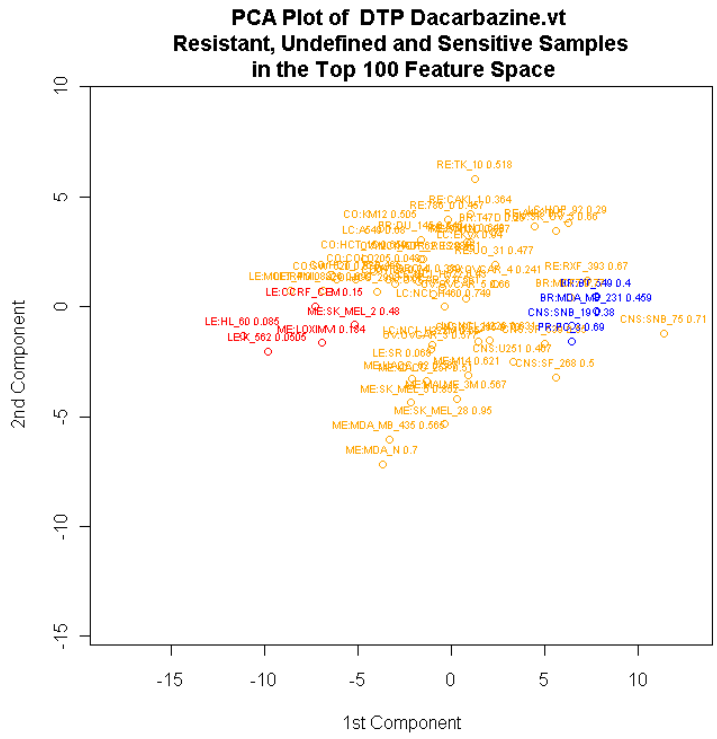

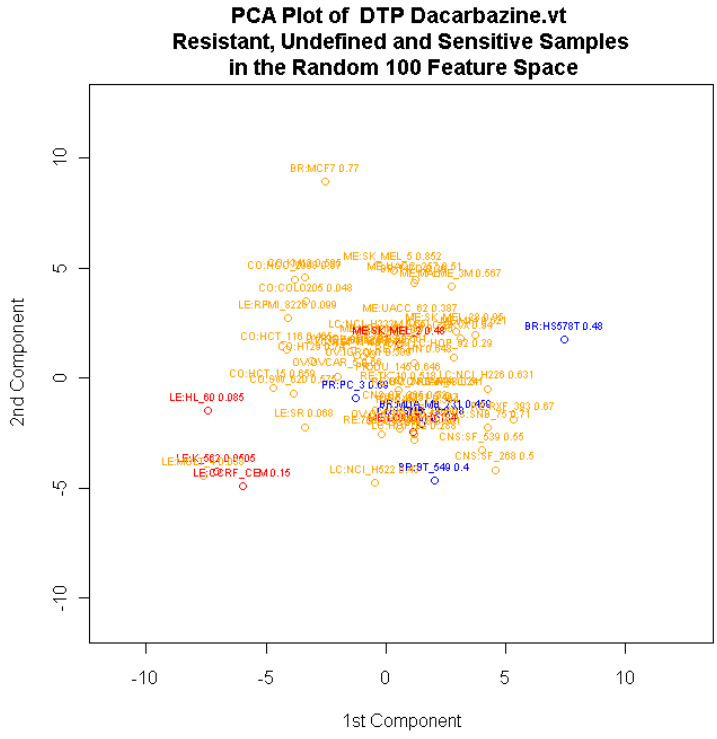

Projection of the samples along the first two principal components of 100 genes. (top panel) A clear separation is seen where the gene selection criteria is used, compared with the (bottom panel) where 100 random genes are used. Red=Sensitive, Blue=Resistant and Orange=Intermediate Sensitivity Samples.

6.1.4 Glioma Radiation Sensitivity Prediction

Similarly with the work carried out on **[6.1.3]**, we first identified a set of classification features that differentiate the two classes **[Figure 6.7]** then using the decomposition of this sub-set of expression profiles we demonstrate the class separation **[Figure 6.8]**.

We started the work here by collating data from Amundson et al.'s NCI60 radiation sensitivity screen **[Section 5.1.4]**.

We use the following sensitivity to therapy measure:

- $-(\log10(LD_{50}))$ measure increases with of the sensitivity to radiation

We proceeded to look at the features of the microarray data that distinguished the resistant and sensitive cell lines, using the workflow from **[Figure 6.3]**.

Using a selected smaller set of the topmost 100 genes ranked by t-score (resistant vs. sensitive) **[Figure 6.7]**, we see a better separation of the two classes **[Figure 6.8]**. This can be compared to the use of a random selection of genes which do not provide any coherent separation of the two classes.

Using a Leave one out cross validation scheme (LOOCV) and a trained support vector machine with a linear kernel (SVM) classification performance was estimated. Fairness of the cross validation test was guaranteed by splitting the training and test samples prior to any feature selection or training. On this basis an accuracy of 63.63636% was achieved. With a more stringent variance filter, feature selection criteria we have however found that this accuracy of class prediction accuracy is raised to 72.72727%).

Figure 6.7 Radiation Sensitivity Signature

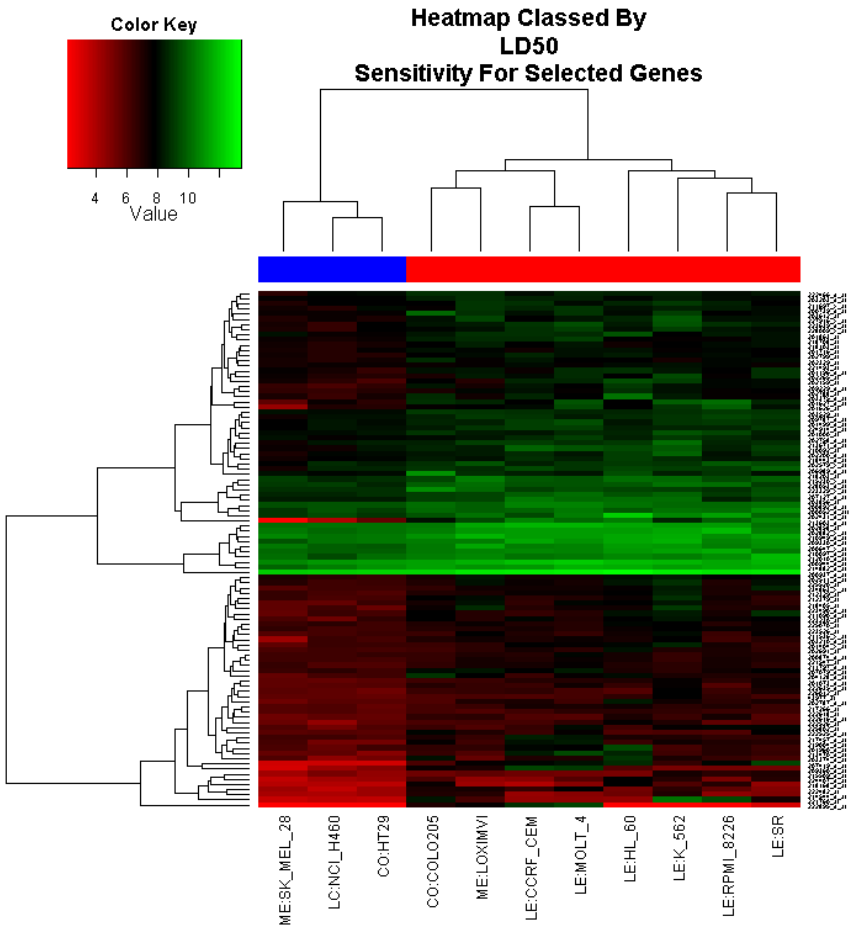

Profile of the top 100 differentially expressed genes between sensitive and resistant cell lines. Genes are given as rows, cell lines as columns. The horizontal bar shows the different classes of cell line columns (Red=Sensitive, Blue=Resistant). Array feature PIDs (RHS row labels) in **[Appendix Table 8.6]**.

Figure 6.8 Radiation Class Distribution in Principle Component Space

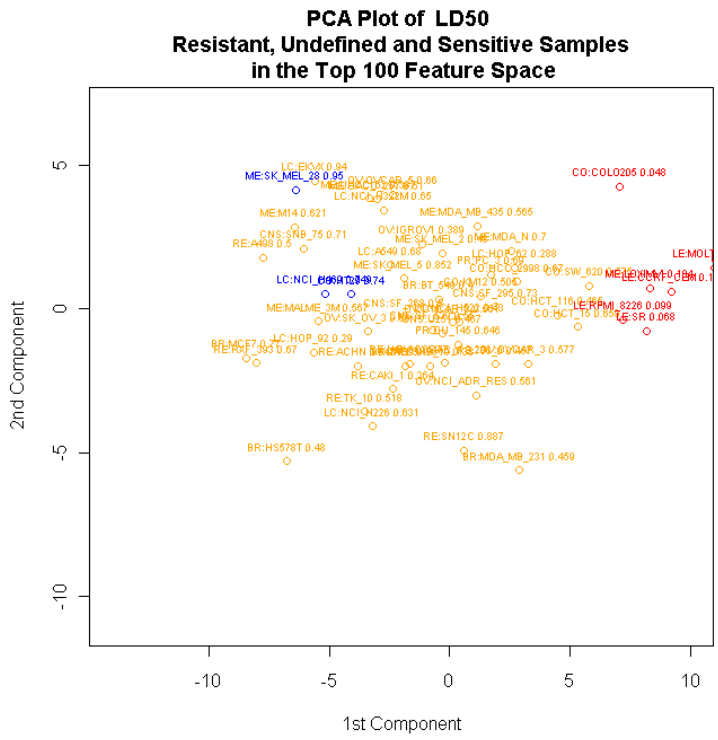

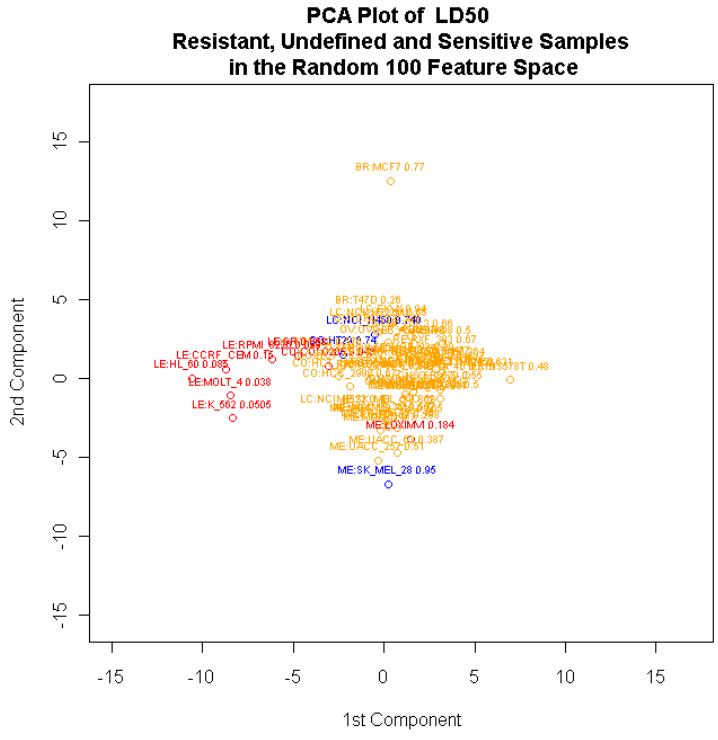

Projection of the samples along the first two principal components of 100 genes. (top panel) A clear separation is seen where the gene selection criteria is used, compared with the (bottom panel) where 100 random genes are used. Red=Sensitive, Blue=Resistant and Orange=Intermediate Sensitivity Samples.

6.2 Preliminary Analysis of Relevant Pathway Perturbations

Pathways are effectively discrete entities, often, these are associated with one or more functions within the cell. The loss (or in some cases gain) of these functions can occur as a result of any number of defects in the components of the pathway. This is important as single gene attempts to study cancer related defects are likely to miss the larger molecular picture of this disease [18].

We have begun analysis of pathway level effects and are considering different methods by which will be used from an analysis standpoint. Initially, we have simply considered a number of pathways that are 1) known to be involved in drug mode of action and 2) glioma etiology; we will aim to look at this in expression data from both clinical samples and cell lines. At present we extracted the probesets of the relevant pathways can either be mapped onto pathways or we can consider how these pathways are differentially expressed from cancers in 1) sub- classes of cancer or 2) normal tissues. Another interesting approach will be to determine if these pathway level effects can be generalized to produce a pathway/network activation scoring system.

NCI60 expression profiles of two central pathways and key elements involved in temozomide resistance (see **Chapter 4**) are the mismatch repair pathway **[Figure 6.9]** and the base excision repair pathway **[Figure 6.10]**.

Turning to the clinical information, it is clear that certain pathways are associated with different glioma sub-types and these have different mortality rates and therapeutic outcomes. Here we show that a 44 gene signature can delineate with accuracy, the different subtypes of glioma found in the REMBRANDT database. The genes in this 44 gene profile are primarily from specific subset gene ontology categories of Mitosis, Neurogenesis and Extra-cellular matrix [9].

Figure 6.9 Mismatch DNA Repair

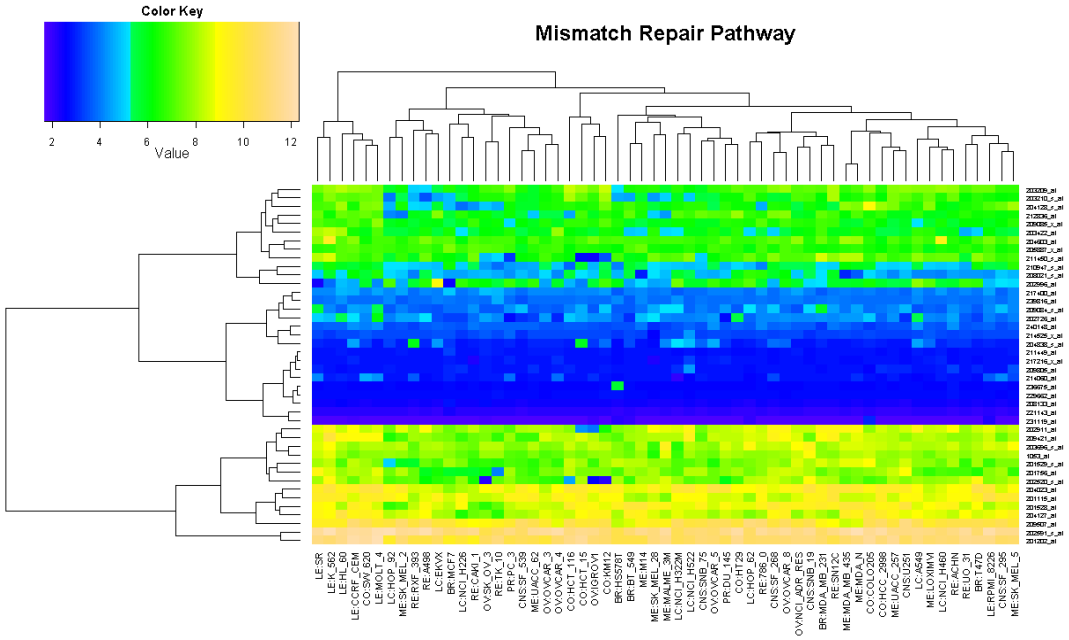

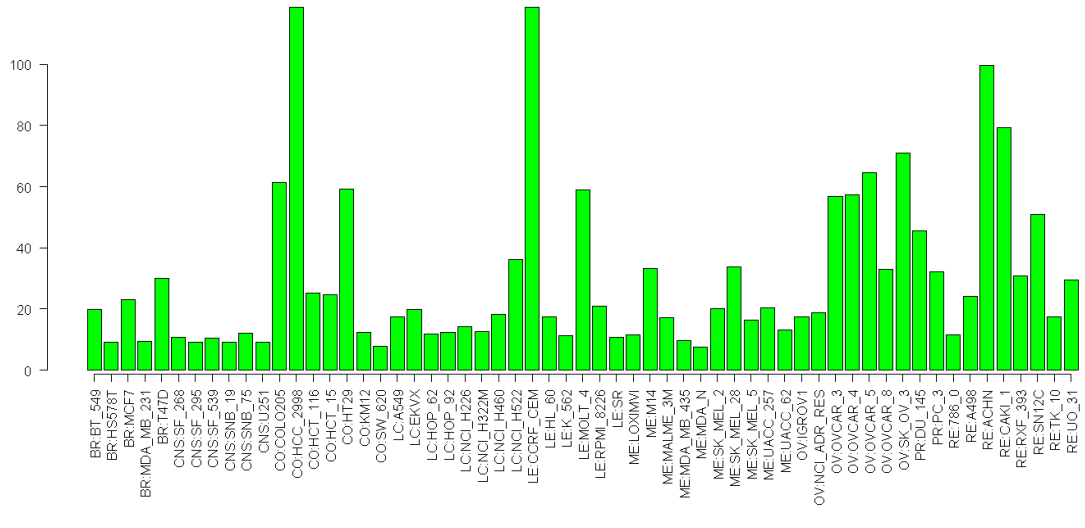

Mismatch repair pathway gene expression across the NCI60 panel (above). MGMT principal temozolomide resistance mechanism expression (bottom).

Figure 6.10 Base Excision DNA Repair

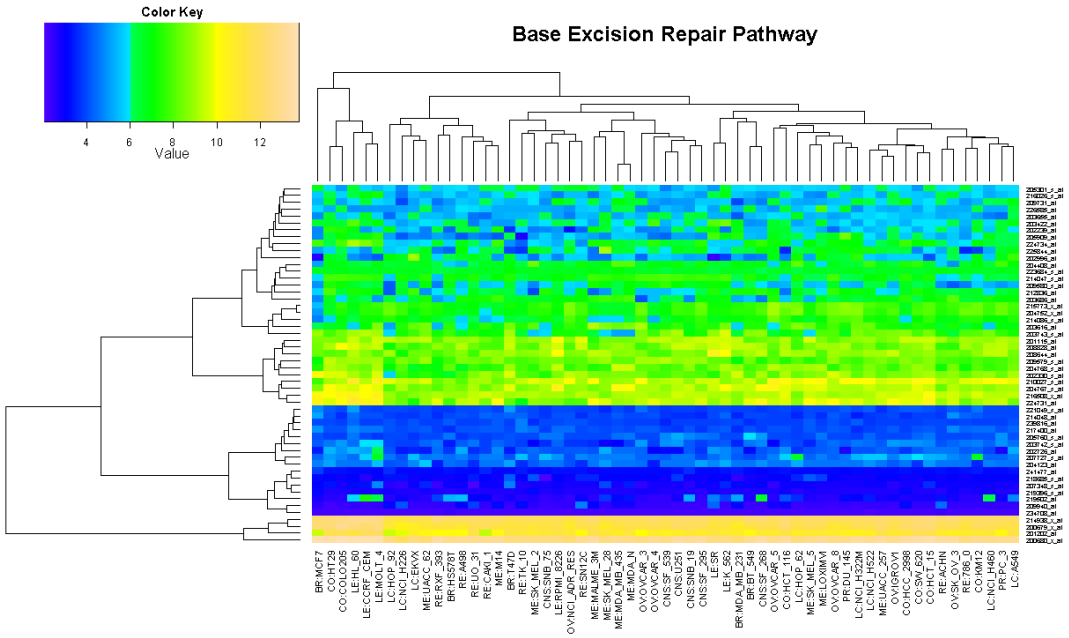

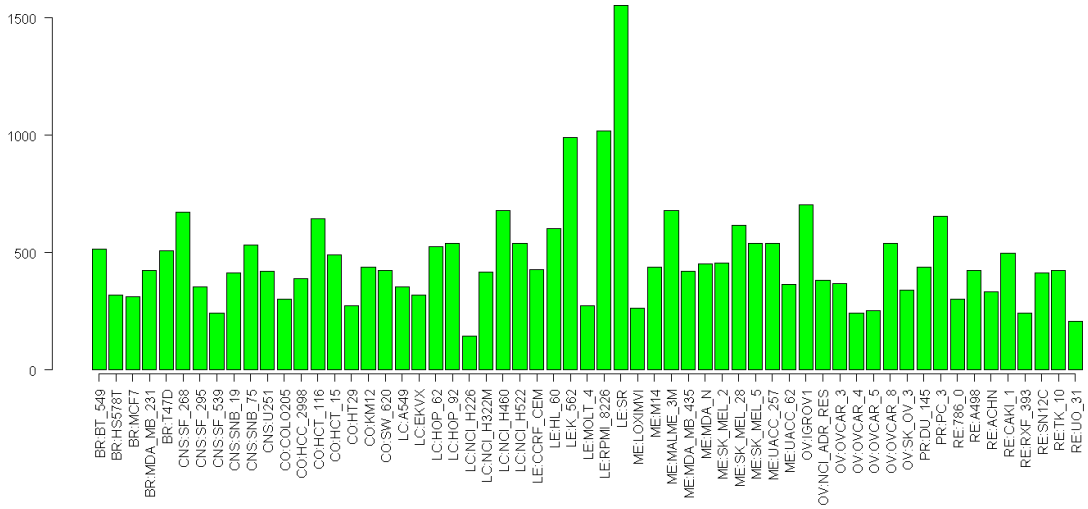

Base excision repair pathway gene expression across the NCI60 panel (above). PARP-1 expression (bottom).

Figure 6.11 Delineation of Expression REMBRANDT Glioma Types By 44-Gene Set

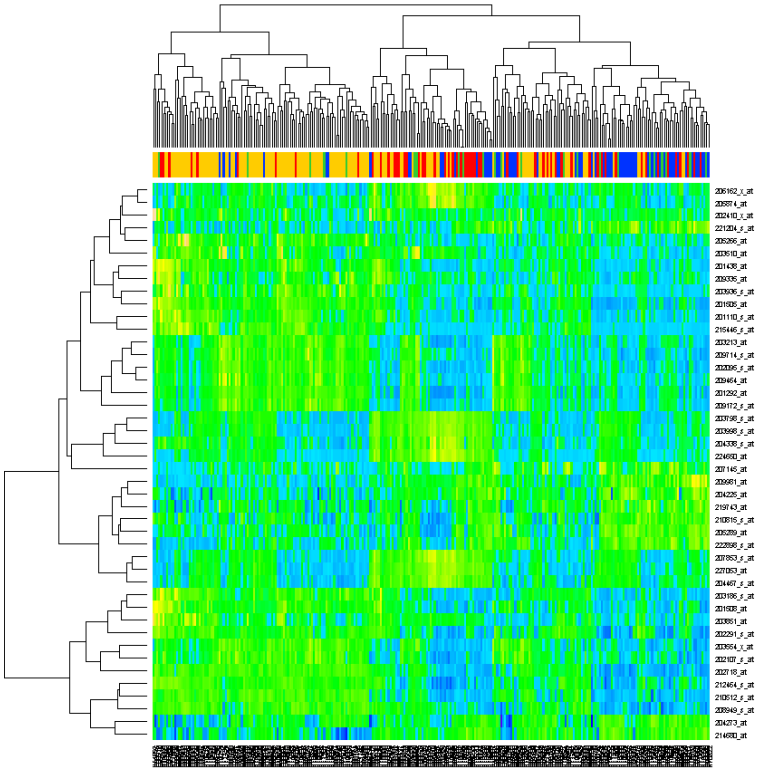

A 44 glioma metagene published by Feije et al. [9] was used to cluster the REMBRANDT data consisting of, as labelled by the top horizontal bar: Astrocytoma (red), GBM (yellow), Mixed (green) and Oligodendroglioma (blue) tumour samples.

7 Discussion

Cancer is a multifactoral disease affecting all levels of the complex biological hierarchy; here intra-cellular molecular biology is of central, but not complete, importance. Other macroscopic factors, such as patient age, are also significant. In most instances the variability in gene expression is unlikely to be the sole factor explaining a complex, high level, clinical covariate such as patient survival time. Despite this there is often an identifiable signal which is significant.

Due to the technical and practical difficulties in collecting high quality drug response data from clinical samples, it has been necessary to employ *in-vitro* drug response data. There are however natural concerns about using *in-vitro* data for drug response prediction, as the cellular biology of these systems is often unrepresentative of the complex *in-vivo* state of a tumour. Our rational is that the presence of a signal above the background noise level must be present, where this is not, then no such differentiation between resistant and sensitive class types will be observed. A further question is to what degree can an expression profile of biopsied tissue from a prospective patient tumour, with a heterogeneous micro-environment, accurately represent the mean profile (in particular the viable tumour cell moiety)? Care must be taken, but this can largely be solved by rigorous multiple sampling[5] or laser-capture microscopy of viable tumour cells. Generally it is accepted that inter-tumour gene expression variability is substantially larger than intra-tumour variability[15,36]; this is particularly so for genes with high variance, for this reason, intra-tumour variability can also be mitigated to some extent by filtering out low-variance genes, as carried out in our work here. With respect to clinical glioma tissue studies such as the TCGA, these employ stringent sample selection criteria that minimizing necrotic tissue sampled. Other studies suggest that intra tumour variability is not prohibitive to expression profiling in these glioma [1,7].

In the dacarbazine and radiation gene signatures, we see by Gene Ontology functional analysis that several DNA damage, replication related genes are enriched in these signatures. This analysis must be extended further to better understand the relationships between genes that constitute resistance. The tumour sub-type classification of the Neurogenesis set of genes which predict good prognosis in gliomas, and conversely the Mesenchymal/Migratory & Cell-Cycle genes predict poor prognosis in glioma, whether there is any interplay with these genes and the therapy received by the patients is unclear.

The classification accuracy is a preliminary step in the process of extrapolating cell survival probability or a probability of response to therapy. The current a binary classification scheme, which will be expanded to produce a variable response level as the model is developed; this will form a further step in the generation of the model and is currently in development.

We are also aiming to incorporate the in-vitro melanoma temozolomide response data this 50 cell line dataset might represent an improvement on the heterogeneous NCI60 cell line for the purpose of estimating resistance and sensitivity signatures. Although this is a different tumour type, the mechanisms of resistance to MITC type drugs appear similar. Additionally, it is a large, uniform dataset may eliminate small class sizes and possible tissue-specific effects which may be problematic in a strategy that uses the NCI60 data. We currently plan to investigate this as soon as we have the independent glioma cell line temozolomide/dacarbazine sensitivity screen as discussed in **[Section 5.2]**.

We have also noted a correlation between dacarbazine and radiation sensitivity across the NCI60 panel when comparing the GI_{50} and LD_{50} values [**Figure 7.1**]. This is reassuring as both therapies essentially act through DNA damage; additionally, this suggests that there are components of these tumours types that are common to the resistance mechanisms to either therapy.

Figure 7.1 Correlation between Dacarbazine and γ-Radiation Sensitivity

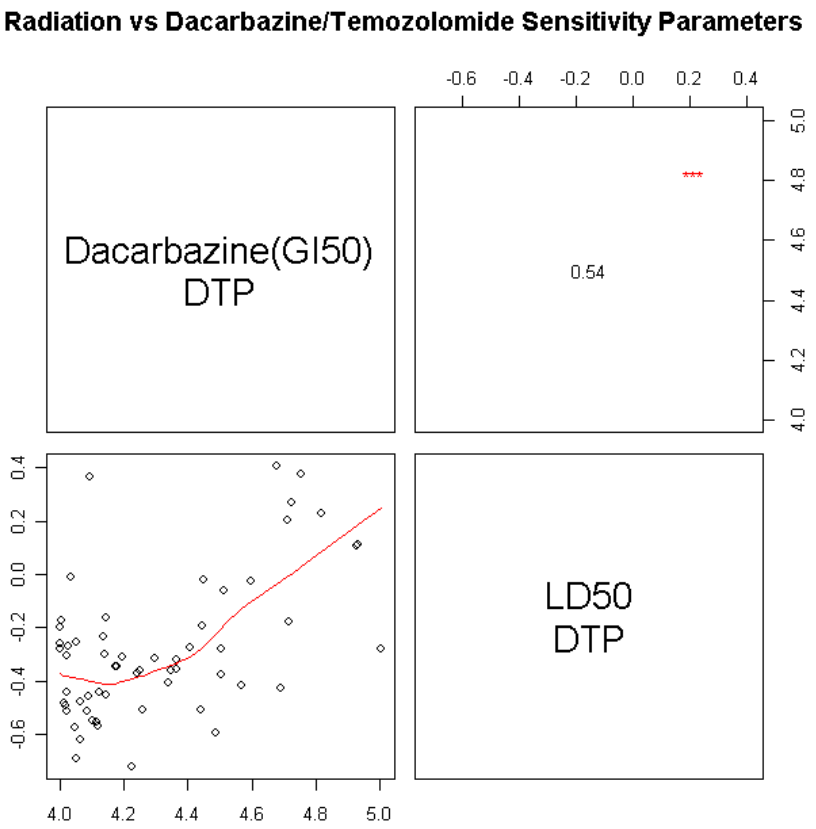

A pairwise plot of correlation between radiation and dacarbazine sensitivity. Dacarbazine and radiation sensitivity is given respectively by -log10(GI_{50}) and -log10(LD_{50}). The diagonal panel show the two parameters, the upper panel displays the Pearson's correlation coefficient (*cor=0.54*) for the plot in the diagonally opposite lower panel (the red line represents a local regression of the points).

A further observation was the lack of increased radiation sensitivity in cell lines were more cells were undergoing mitosis at any particular time, we do not observe a correlation between radiation sensitivity and cell proliferation rates (-LogLD50 [pcor=-0.042]) in the NCI60 panel. We also looked at the amount of cellular DNA as determined by mean ploidy, which might be expected to have an impact on the DNA damaging agent efficacy; this also does not correlate with either radiation or dacarbazine sensitivity (-LogLD50 [pcor=0.012] or –LogGI50 [pcor=0.0046]).

Finally, a large number of the drugs screened against the NCI60 panel are positively correlated with radiation sensitivity -log(SF2) (max pcor=0.78; n=117 with pcor > +5). Conversely, only a small number of drug compounds sensitivity profiles are strongly negatively correlated with radiation sensitivity (min pcor=-0.53; n=2 with pcor < -5). We suggest that for these negatively correlated drugs may have the potentiating or synergistic effects and the relationship between these compounds and radiation deserves further study as they

may represent drug compounds that target cells which are radio-resistant. The strongest negative correlation was for compound NCS:691035 **[Figure 7.2]**.

Figure 7.2 Drug sensitivities with strong negative correlations to radio-sensitivity

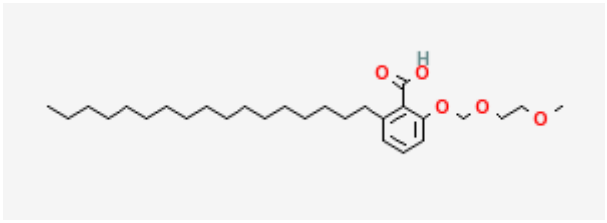

Structure of NCS:691035 from PubChem. 2-heptadecyl-6-(2-methoxyethoxymethoxy)benzoic acid.

8 Addendum

8.1 Appendix

Table 8.1 NCI60 Data

Name	Platform Information	Principal Collaborators	Data Description
	DNA		
DNA: Sequencing	Manufacturer: ABI 3730 Sequencer Platform: Sequencing Molecular Target: DNA Platform Description: Sequencing of the NCI-60 for mutations in known human cancer genes. The coding exons and immediate flanking intron sequences of selected genes from the Cancer Gene Census were PCR-amplified and sequenced.	Wellcome Trust Sanger Institute (M Stratton); Genomics and Bioinf Gp, LMP, CCR, NCI	Raw Data: NA Base-calling method: Mutation surveyor, Chromas, in-house Sanger software Cell Lines: NCI-60
DNA: BAC aCGH	Manufacturer: University of California San Francisco Platform: BAC Clone arrays Molecular Target: DNA Platform Description: DNA samples from tumor cells and from normal controls were labeled with CY3 and CY5, respectively and hybridized to array comprised of 353 unique loci on the bacterial artificial chromosome microarray	UCSF Comp Cancer Ctr(J Gray); Genomics and Bioinf Gp, LMP, CCR, NCI	Raw Data: ratio of sample vs control of DNA copy number Normalization method: Cell Lines: NCI-60
DNA: E-cadherin Methylation	Manufacturer: NA Platform: PCR amplification and sequencing of sodium bisulfite modified DNA. Molecular Target: DNA methylation Platform Description: Genomic DNA (5 micrograms) from each cell line was treated with sodium bisulfite at 50 degrees C for 17 hr using the CpGenome DNA Modification kit from (Chemicon International, Temecula, CA) according to manufacturer's instructions. The DNA was then re-suspended in 125 microliters of 10-mM Tris with 1 mM EDTA pH 7.4 (KD Medical, Columbia, MD). Nested PCR amplification and sequencing of the DNA were carried out using either converted or unconverted DNA as template for the PCR. Primers were based on the E-cad promoter DNA sequence (GenBank accession no. L34545). Two pairs of primers were used. For the bisulfite-converted DNA, the first pair, which amplified a 413-bp deaminated DNA fragment, consisted GATTTTAGGTTTTAGTGAGTT upstream (sequence position -397 to -377) and E-cad-nest2/4 GGA AACAGCTATGACCATGAA CTCCAAAAACCCATAACTAA downstream (sequence position -6 to +16). The second pair was GTAAAACGACGGCCAGTTA TTTAGATTTTAGTAATTTT (upstream, sequence position -319 to -299) and inner primers (with 5' m13 tails) were used to amplify a smaller (335 nucleotide) but higher-quality product. For the unconverted DNA, the same locations of primers were used, with GATCCC AGGTCTTAGTGAGCC, GGAAACAGCTATGACCATGTTCTC CAAGGGCCCATG GCTAA, and GTAAAACGACGGCCAGCCACCT AGACCCTAGCAACTCC. One-strand automated sequencing of the PCR products was performed.	Gene Logic (D Dolginow), SAIC (D Munroe), Johns Hopkins Univ. (A Feinberg); Genomics and Bioinf Gp, LMP, CCR, NCI	Raw Data: sequence tracings Normalization method: Multiple sequence tracings were grouped by bisulfite conversion and sequencing date, calculated as a group mean for each CpG within these groups, and then combined as a mean of these groups. Cell Lines: NCI-60
	RNA		
RNA: Affy HU6800	Manufacturer: Affymetrix Platform: HU6800 Molecular Target: RNA Platform Description: 6,800 probe set array	Whitehead (Broad) (E Lander, T Golub); Genomics and Bioinf Gp, LMP, CCR, NCI	Raw Data: cel files Normalization method: GCRMA, MAS5, RMA Cell Lines: NCI-60
RNA: cDNA Array	Manufacturer: Synteni, now Incyte, Inc. Platform: cDNA array Molecular Target: RNA Platform Description: 9,700 clone two-color flourescence	Stanford (P Brown, D Botstein); Genomics and Bioinf Gp, LMP, CCR, NCI	Raw Data: Two channel sample and pool intensity values. Normalization method: Log2 ratio of sample vs control using Gaussian kernel

			moving-average Cell Lines: NCI-60
RNA: miRNA OSU V3 chip	Manufacturer: Ohio State University Comprehensive Cancer Center Platform: OSU-CCC_hsa-miRNA-chip_v3 For array design, see: V3 design protocol A-MEXP-620 published on ArrayExpress (www.ebi.ac.uk/arrayexpress/) Molecular Target: RNA Platform Description: See: Liu CG, Calin GA, Meloon B, Gamliel N, Sevignani C, Ferracin M, Dumitru CD, Shimizu M, Zupo S, Dono M, Alder H, Bullrich F, Negrini M, and Croce CM. An oligonucleotide microchip for genome-wide microRNA profiling in human and mouse tissues. Proc Natl Acad Sci U S A 2004;101:9740-4.	CCC, OSU (P Blower); Genomics and Bioinf Gp, LMP, CCR, NCI	Raw Data: Two channel sample and background intensity measurements. Normalization method: From the Genepix data, we selected human probes (entries with ID=hsa-[anything]) and median signal intensity minus background for each spot (column labeled 'F635 Median - B635'). After converting any negative values to 1, signal intensities were log2-transformed, and duplicate spots were averaged. Then we performed quantile normalization across the 3 microarray batches, replaced all values less than 5 with the median of such values, and set the value for each control cell line to the mean of its five replicates. Cell Lines: NCI-60
RNA: Oncochip	Manufacturer: NCI Advanced Technology Cen Platform: Oncochip Molecular Target: RNA Platform Description: The Oncochip is a pin-spotted cDNA microarray developed in the Microarray Facility, Advanced Technology Center, National Cancer Institute, NIH, and prepared by Willam C. Reinhold. This glass slide microarray contains 2208 cDNA spots corresponding to 1648 individual human cancer-interesting genes (array lot HS-OC-2p10-101899). Included were 780 spots representing 364 individual genes in replicate.	ATC, CCR, NCI (E Liu); Genomics and Bioinf Gp, LMP, CCR, NCI	Raw Data: Two channel sample and background intensity measurements. Normalization method: Gaussian-kernel fitting method to genrate ratio and fold change values of sample vs control Cell Lines: DU-145/RC-01
RNA: Transporter Array	Manufacturer: Ohio State University Platform: Spotted Array Molecular Target: RNA Platform Description: Spotted 70-mer microarray	OSU (W Sadee); Genomics and Bioinf Gp, LMP, CCR, NCI	Raw Data: Normalization method: Normalization based on robust, locally linear fits (Loess), implemented in the SMA R package Cell Lines: NCI-60
RNA: Affy HG-U133(A,B)	Manufacturer: Affymetrix Platform: HG-U133 Molecular Target: RNA Platform Description: 44,000 probeset 2-chip set	Gene Logic (U Scherf, E Kaljian); Genomics and Bioinf Gp, LMP, CCR, NCI	Raw Data: cel files Normalization method: GCRMA, MAS5, RMA Cell Lines: NCI-60,DU-145/RC-01 59 cell lines - LC:NCI_H23 is excluded
RNA: Affy HG-U95(A-E)	Manufacturer: Affymetrix Platform: HG-U95 Molecular Target: RNA Platform Description: 65,000 probeset 5-chip set	Gene Logic (U Scherf, D Dolginow); Genomics and Bioinf Gp, LMP, CCR, NCI	Raw Data: cel files Normalization method: GCRMA, MAS5, RMA Cell Lines: NCI-60,DU-145/RC-01
Protein			
Protein: Lysate Array	Manufacturer: NCI LMP Genomics and Bioinformatics Group (Nishizuka) Platform: Reverse-phase lysate arrays (RPLA) Molecular Target: Protein Platform Description:	LP, CCR, NCI (L Liotta); CBER, FDA (E	Raw Data: Signal intensity processed by DI25 algorithm (log2)

	Reverse-phase lysate arrays (RPLA) for 176 antibodies. Each array included 64 lysates (60 cancer cells and 4 replicate control pools) in 10 serial two-fold dilutions.	Petricoin); Genomics and Bioinf Gp, LMP, CCR, NCI	Normalization method: DI25 optimization Cell Lines: NCI-60
Drug			
Drug: A118	Manufacturer: Developmental Therapeutics Program, NCI/NIH Platform: Sulforhodamine assay Molecular Target: Platform Description: Negative log10(Gi50) values of Sulforhodamine assay for 118 molecules (also known as the Standard Agents) with known 2D structure, known mechanism of action and have been tested at-least 4 times. Higher values equate to higher sensitivity of cell lines.	LMP, CCR, NCI (K Kohn); DPT, NCI (D Zaharevitz); Genomics and Bioinf Gp, LMP, CCR, NCI	Raw Data: Normalization method: Cell Lines: NCI-60
Drug: A1429	Manufacturer: Developmental Therapeutics Program, NCI/NIH Platform: Sulforhodamine assay Molecular Target: Platform Description: Negative log10(Gi50) values of Sulforhodamine assay for 1429 molecules (also known as the Standard Agents) with known 2D structure, known mechanism of action for many of the drugs and have been tested at-least 4 times. Higher values equate to higher sensitivity of cell lines.	DPT, NCI (D Zaharevitz, S Bates); Genomics and Bioinf Gp, LMP, CCR, NCI	Raw Data: Normalization method: Cell Lines: NCI-60
Drug: A4463	Manufacturer: Developmental Therapeutics Program, NCI/NIH Platform: Sulforhodamine assay Molecular Target: Platform Description: Negative log10(Gi50) values of Sulforhodamine assay for 4463 molecules (also known as the Standard Agents) with known 2D structure and have been tested at-least 2 times. Higher values equate to higher sensitivity of cell lines.	DPT, NCI (D Zaharevitz, S Bates); Genomics and Bioinf Gp, LMP, CCR, NCI	Raw Data: Normalization method: Cell Lines: NCI-60

Table 8.2 NCI-60 Panel Metadata

Name	Origin	Age	Sex	Prior Treatment	Epithelial	Histology	Source	Ploidy	P53	mdr	Doubling Time	Reference
BR:BT_549	Breast	72	F	NA	yes	Papillary infiltrating ductal carcinoma-mammary gland; breast	Metastasis	"3n+/-, Near-triploid (58-80)" 69+/-	?	-45	54	no pub
BR:HS578T	Breast	74	F	NA	yes	Carcinosarcoma-mammary gland; breast	Primary	"2n+, Hyperdiploid (47-57)"	MT	NA	54	"JNCI 58: 1795-1806,1977"
BR:MCF7	Breast	69	F	NA	yes	Adenocarcinoma- mammary gland; breast; metastatic site: pleural effusion;	Pleural effusion	"3n-, Hypotriploid (58-68)"	WT	14	25	"JNCI 51: 1409-1417,1973"
BR:MDA_MB_231	Breast	51	F	NA	yes	Adenocarcinoma-mammary gland; breast; epithelial; metastatic site: pleural effusion;	Pleural effusion	"2n+, Hyperdiploid (47-57)"	MT	29	42	"JNCI 53(3): 661-674,1974"
BR:T47D	Breast	54	F	NA	yes	infiltrating ductal carcinoma	NA	"2n+, Hyperdiploid (47-57)"	MT	19	46	"Eur J Cancer 15:659-679,1979"
CNS:SF_268	CNS	24	F	Rad	no	"Glioblastoma, ud"	NA	"2n+, Hyperdiploid (47-57)"	MT	-38	33	"Acta Neuropathol 75: 92-103, 1987"
CNS:SF_295	CNS	67	F	Rad	no	"Glioblastoma, ud"	NA	"5n+/-,Near-pentaploid (104-115+/-126)"	MT	91	30	"Acta Neuropathol 75: 92-103, 1988"
CNS:SF_539	CNS	34	F	Rad/BCNU/5FU/HU/6MP	no	Glial cell neoplasm	NA	"4n+/-, Near-tetraploid (81-103)" 92+/-	WT	-40	35	"J Neuropathol Exp Neurol 40: 201-229, 1981"
CNS:SNB_19	CNS	47	M	None	no	"Glioblastoma, ud"	NA	"3n+/-, Near-triploid (58-80)" 69+/-	MT	-41	35	"Cancer 47: 255, 1981"

CNS:SNB_75	CNS	NA	F	None	no	Astrocytoma	NA	"2n+, Hyperdiploid (47-57)"	MT	-38	63	-
CNS:U251	CNS	75	M	NA	no	"Glioblastoma,ud"	NA	"2n+, Hyperdiploid (47-57)"	MT	-19	24	"J Neuropathol Exp Neurol 40: 410-427, 1981"
CO:HCT_116	Colon	NA	M	NA	yes	carcinoma-vpd	NA	"2n-, Hypodiploid (35-45)"	?	26	17	"Can Res 41: 1761-1756, 1981"
CO:COLO205	Colon	70	M	NA	yes	Adenocarcinoma	Ascites	"3n, Triploid (69)"	MT	7	24	"Can Res. 38: 1345-1355, 1978"
CO:HCC_2998	Colon	NA	NA	NA	yes	carcinoma	NA	"2n+/-, Near-diploid 46+/- (35-57)"	MT	-5	32	-
CO:HCT_15	Colon	NA	NA	None	yes	Adenocarcinoma p/md	NA	"2n+/-, Near-diploid 46+/- (35-57)"	?	414	21	"Can Res 39: 1020-1025, 1979"
CO:HT29	Colon	44	F	None	yes	Adenocarcinoma-md	Primary	"3n+/-, Near-triploid 69+/- (58-80)"	MT	15	20	"Human Tumor Cells in vitro: 115-159, 1975"
CO:KM12	Colon	NA	NA	None	yes	Adenocarcinome-pd	NA	"2n+/-, Near-diploid 46+/- (35-57)"	MT	-19	24	"Can Res 48: 1943-1948, 1988"
CO:SW_620	Colon	51	M	NA	yes	Carcinoma-ud	NA	"2n+/-, Near-diploid 46+/- (35-57)"	MT	31	20	Can Res 1976 Dec;36(12):4562-9
LC:A549	Non-Small Cell Lung	58	M	NA	yes	Adenocarcinoma-p/md	NA	"3n+/-, Near-triploid 69+/- (58-80)"	WT	10	23	"J Natl Cancer Inst. 51(5):1417-23, 1973"

LC:EKVX	Non-Small Cell Lung	NA	M	NA	yes	Adenocarcinoma-md	NA	"3n+/-, Near-triploid (58-80)" 69+/-	MT	-9	44	-
LC:HOP_62	Non-Small Cell Lung	60	F	None	yes	adenocarcinoma-ud	NA	"4n+, Hypertetraploid (93-103)"	MT	61	39	-
LC:HOP_92	Non-Small Cell Lung	62	M	None	yes	Large cell-ud	NA	"4n+/-,Near-tetraploid 92+/- (81-103)"	MT	-4	80	-
LC:NCI_H226	Non-Small Cell Lung	NA	M	None (non smoker)	yes	Squamous cell carcinoma-vpd	NA	"3n, Triploid (69)"	MT	7	61	"Cancer Res. 40: 3502-3507, 1980"
LC:NCI_H23	Non-Small Cell Lung	NA	M	None	yes	Adenocarcinoma-ud	NA	"2n+, Hyperdiploid (47-57)"	MT	-2	33	"Cancer Res. 40: 3502-3507, 1980"
LC:NCI_H322M	Non-Small Cell Lung	52	M	None	yes	Small Bronchioalveolar Carcinoma cell	NA	"2n+/-, diploid Near- (35-57)" 46+/-	MT	-10	35	-
LC:NCI_H460	Non-Small Cell Lung	NA	M	NA	yes	Large Cell Carcinoma-ud	Pleural effusion	"2n+/-, diploid Near- (35-57)" 46+/-	WT	25	18	"Science 246: 491-494, 1989"
LC:NCI_H522	Non-Small Cell Lung	NA	M	None	yes	Adenocarcinoma-vpd	NA	"2n+/-, diploid Near- (35-57)" 46+/-	MT	16	38	"Can Res 45: 2913-2923, 1985"
LE:CCRF_CEM	Leukemia	4	F	Rad/Mtx/Cyx	no	ALL	NA	"2n+/-, diploid Near- (35-57)" 46+/-	MT	35	27	"Cancer 18: 522-529, 1965"
LE:HL_60	Leukemia	36	M	None	no	Pro myelocytic leukemia	PBL	"2n+/-, diploid Near- (35-57)" 46+/-	MT	-11	29	"Blood 54(3):713-33, 1979"
LE:K_562	Leukemia	53	F	Bisulfan/PiBr	no	CML	Pleural effusion	"3n-, Hypotriploid (58-68)"	MT	-1	20	"Blood 45: 321-334, 1975"

LE:MOLT_4	Leukemia	19	M	VB/6MP/Pred	no	ALL (cells were when patient was in relapse)	PB	"4n, Tetraploid (92)"	WT	10	28	"J. Natl. Cancer Inst. 49: 891-895, 1972"
LE:RPMI_8226	Leukemia	61	M	None	no	Myeloma	PB	"3n-, Hypotriploid (58-68)"	WT	-3	34	"Proc Soc Exp Biol Med 125: 1246-1250, 1967"
LE:SR	Leukemia	11	M	Y	no	Lymphoma	NA	"2n+/-, Near-diploid 46+/- (35-57)"	?	4	29	-
ME:LOXIMVI	Melanoma	58	M	None	no	Malignant amelanotic melanoma	NA	"3n+/-, Near-triploid 69+/- (58-80)"	WT	12	21	"Int J Cancer 41: 442-449, 1988"
ME:M14	Melanoma	NA	NA	NA	no	Melanotic melanoma	NA	"3n+/-, Near-triploid 69+/- (58-80)"	MT	14	26	"Cancer Res 48: 578-582, 1988"
ME:MALME_3M	Melanoma	43	M	None	no	Malignant melanotic melanoma	Metastasis	"4n+/-,Near-tetraploid 92+/- (81-103)"	WT	22	46	"J. Natl. Cancer Inst. 59: 221-226, 1977"
ME:MDA_MB_435	Melanoma	31	F	NA	no	Ductal carcinoma-mammary gland; breast; duct; metastatic site: pleural effusion;	Pleural effusion	"2n+, Hyperdiploid (47-57)"	MT	20	26	"Cancer Res 40:3118-3129,1980 "
ME:MDA_N	Melanoma	31	F	NA	no	Ductal carcinoma-mammary gland; breast; duct; metastatic site: pleural effusion;	Pleural effusion	NA	MT	12	23	-
ME:SK_MEL_2	Melanoma	60	M	None	no	Malignant melanotic melanoma	Metastasis	"4n-, Hypotetraploid (81-91)"	WT	14	46	"Human Tumor Cells in vitro, pp 115-159, 1975"
ME:SK_MEL_28	Melanoma	51	M	None	no	Malignant melanotic melanoma	NA	"4n-, Hypotetraploid (81-91)"	MT	11	35	"PNAS 73: 3278-3282, 1976"

ME:SK_MEL_5	Melanoma	24	F	None	no	Malignant melanotic melanoma	Metastasis	"4n+, Hypertetraploid (93-103)"	WT	12	25	"PNAS, 73: 3278-3282, 1976"
ME:UACC_257	Melanoma	NA	NA	NA	no	Melanotic melanoma	NA	"3n+, Hypertriploid (70-80)"	WT	26	39	-
ME:UACC_62	Melanoma	NA	NA	NA	no	Melanotic melanoma	NA	"3n+/-, Near-triploid 69+/- (58-80)"	WT	8	31	-
OV:IGROV1	Ovarian	47	F	Rad	yes	Cystoadenocarcinoma-pd	NA	"4n+/-,Near-tetraploid 92+/- (81-103)"	MT	20	31	"Can Res 45: 4970-4979,1985"
OV:OVCAR_3	Ovarian	60	F	CyPh/CsPt/Adr	yes	Adenocarcinoma-md	Ascites	"3n+/-, Near-triploid 69+/- (58-80)"	MT	-12	35	"Sem Ocol 11: 285-298, 1984"
OV:OVCAR_4	Ovarian	42	F	CyPh/CsPt/Adr	yes	Adenocarcinoma-md	NA	"3n+/-, Near-triploid 69+/- (58-80)"	MT	-4	41	"Sem Ocol 11: 285-298, 1984"
OV:OVCAR_5	Ovarian	67	F	None	yes	Adenocarcinoma-wd	NA	"2n+, Hyperdiploid (47-57)"	MT	13	49	"Sem Ocol 11: 285-298, 1985"
OV:OVCAR_8	Ovarian	64	F	Ctx/Adr/CsPt/CyPh	yes	Carcinoma-ud	NA	"2n+, Hyperdiploid (47-57)"	MT	7	26	-
OV:NCI_ADR_RES	Ovarian	NA	F	NA	yes	Adenocarinoma	NA	"2n+/-, Near-diploid 46+/- (35-57)"	MT	352	34	"Cancer Res., 46:4087-4090,1986"
OV:SK_OV_3	Ovarian	64	F	Thiotepa	yes	Adenocarcinoma-vpd	Ascites	"4n+/-, Near-tetraploid 92+/- (81-103)"	?	15	49	"Human Tumor Cells in vitro, pp. 115-159, 1975"

PR:DU_145	Prostate	69	M	Androgen independent and unresposive to hormone therapy	yes	prostate; metastatic site: brain; carcinoma (patient with metastatic carcinoma of the prostate and a 3 year history of lymphocytic leukemia.)	Metastasis	"3n+/-, Near-triploid 69+/- (58-80)"	?	4	32	"Int J Cancer 21: 274-281,1978"
PR:PC_3	Prostate	62	M	NA	yes	Adenocarcinoma- prostate; metastatic site: bone;	NA	"4n, Tetraploid (92)"	MT	11	27	Invest Urol 1979 Jul;17(1):16-23
RE:786_0	Renal	58	M	None	yes	Adenocarcinoma	NA	"4n+/-,Near-tetraploid 92+/- (81-103)"	MT	-44	22	"In Vitro 14: 779-786, 1978"
RE:A498	Renal	52	M	NA	yes	Adenocarcinoma	NA	"3n, Triploid (69)"	WT	78	67	"JNCI 51: 1417-1423,1973 "
RE:ACHN	Renal	22	M	Rad/VB/CCNU/Mto/Pred	yes	Renal cell carcinoma-p/md	NA	"2n+/-, Near-diploid 46+/- (35-57)"	WT	120	28	"Cancer Res 42: 4948-4953, 1982"
RE:CAKI_1	Renal	49	M	Rad/HU/5FU/Mtx/Ctx	yes	Clear cell carcinoma	Metastasis	"3n, Triploid (69)"	WT	171	39	"Human Tumor cells in vitro, pp 115-159, 1975"
RE:RXF_393	Renal	54	M	None	yes	hypernephroma-pd	NA	"3n+/-, Near-triploid 69+/- (58-80)"	MT	42	63	"Contrib oncol 42, 1992 "
RE:SN12C	Renal	43	M	None	yes	Renal cell carcinoma-pd	NA	"3n, Triploid (69)"	MT	-86	30	"Cancer Res 46: 4109-4115, 1986"
RE:TK_10	Renal	43	M	None	yes	Renal Spindle cell carcinoma	NA	"4n, Tetraploid (92)"	MT	-4	51	"Cancer Res 46: 3856-3862, 1987"

RE:UO_31	Renal	NA	F	None	yes	cell Renal carcinoma-vpd	NA	Near- 46+/- "2n+/-, diploid (35-57)"	WT	59	42	-

NCI-60 cell line metadata [selected parameters from http://discover.nci.nih.gov/cellminer/celllinequery.do].

Table 8.3 Drug Sensitivity (GI50s)

NSC	45388	362856
Chemical Name	Dacarbazine	Temozolomide
Number of Replicates	**50**	**2**
BR:MCF7	4	4
BR:MDA_MB_231	4	4
BR:HS578T	4	4
BR:BT_549	4	4
BR:T47D	4	4
CNS:SF_268	4.18	4
CNS:SF_295	4.26	4
CNS:SF_539	4.14	4
CNS:SNB_19	4	4
CNS:SNB_75	4.34	4.15
CNS:U251	4	4
CO:COLO205	4	4
CO:HCC_2998	4.23	4
CO:HCT_116	4.41	4
CO:HCT_15	4	4
CO:HT29	4	4
CO:KM12	4	4
CO:SW_620	4.25	4
LE:CCRF_CEM	4.99	4.106
LE:HL_60	4.82	4.068
LE:K_562	4.83	4.12
LE:MOLT_4	4.66	4.078
LE:RPMI_8226	4.74	4
LE:SR	4.67	4
ME:LOXIMVI	5.03	4.086
ME:MALME_3M	4.31	4
ME:M14	4.52	4
ME:SK_MEL_2	5.05	4
ME:SK_MEL_28	4	4
ME:SK_MEL_5	4	4
ME:UACC_257	4.26	4
ME:UACC_62	4.47	4
ME:MDA_MB_435	4.5	4
ME:MDA_N	4	4
LC:A549	4	4
LC:EKVX	4	4
LC:HOP_62	4.51	4
LC:HOP_92	4.37	4
LC:NCI_H226	4	4
LC:NCI_H23	4	4
LC:NCI_H322M	4	4
LC:NCI_H460	4.09	4
LC:NCI_H522	4	4
OV:IGROV1	4	4
OV:OVCAR_3	4.21	4
OV:OVCAR_4	4.49	4
OV:OVCAR_5	4	4
OV:OVCAR_8	4.32	4
OV:SK_OV_3	4.71	4.231
OV:NCI_ADR_RES	4.18	4
PR:PC_3	4	4
PR:DU_145	4.08	4
RE:786_0	4	4
RE:A498	4	4
RE:ACHN	4.14	4
RE:CAKI_1	4.66	4
RE:RXF_393	4	4
RE:SN12C	4.03	4
RE:TK_10	4.36	4
RE:UO_31	4.53	4.131

Drug sensitivity data across the NCI-60 panel. $-\text{Log}_{10}$(GI-50) for Dacarbazine and Temozolomide across NCI-60 panel.

Note Temozolomide only includes 2 replicates and insufficient to determine the accuracy here.

Table 8.4 Radiation Sensitivity Parameters

Cell.Lines	LD_{50}	T2.	SF2	SF5	SF8	Do	n	Casp.8	Casp.16
BR:BT_549	1.575445	58	0.4	0.05	1.50E-02	179	1.03	1.45	1.59
BR:HS578T	1.900039	57	0.48	0.15	3.50E-02	204	1.21	1.8	1.61
BR:MCF7	3.760507	26	0.77	0.32	1.10E-01	275	1.52	3.49	7.17
BR:MDA_MB_231	1.807559	39	0.459	0.094	8.00E-03	150	205	1.47	1.42
BR:T47D	1.01968	53	0.26	0.039	4.70E-03	150	1.03	1.1	1.05
CNS:SF_268	2.048567	34	0.5	0.186	2.27E-02	80	90	1.02	1.08
CNS:SF_295	3.207572	30	0.73	0.214	5.26E-02	144	2.37	2.04	0.96
CNS:SF_539	2.212269	34	0.55	0.215	1.59E-01	320	1.01	1.89	1.34
CNS:SNB_19	1.488374	35	0.38	0.053	2.00E-03	90	12.5	1.75	1.89
CNS:SNB_75	3.222805	40	0.71	0.248	4.60E-02	175	3.92	1.18	1.13
CNS:U251	1.860263	25	0.467	0.061	7.20E-03	150	1.27	1.17	0.96
CO:COLO205	0.432128	23	0.048	0.0011	3.00E-04	95	0.52	1.15	4.49
CO:HCC_2998	2.546552	33	0.67	0.051	4.50E-04	61	241	1.75	1.63
CO:HCT_116	1.877102	18	0.465	0.028	1.90E-03	108	2.85	2.59	3.04
CO:HCT_15	3.258756	21	0.659	0.338	2.01E-01	480	0.98	0.46	1.42
CO:HT29	4.890516	20	0.74	0.5	3.32E-01	725	0.99	1.93	2.17
CO:KM12	2.023962	23	0.505	0.093	3.80E-03	90	24	1.57	0.73
CO:SW_620	2.303432	21	0.575	0.0758	2.51E-04	52	1030	1.04	1.25
LC:A549	3.096174	24	0.68	0.25	5.00E-02	179	4.3	1.26	1.42
LC:EKVX	3.594024	37	0.94	0.183	4.60E-02	200	2.48	2.03	1.33
LC:HOP_62	1.056596	46	0.288	0.091	4.60E-02	238	0.49	1.02	1.36
LC:HOP_92	1.1546	88	0.29	0.033	9.30E-04	85	11.6	0.93	1.06
LC:NCI_H226	2.761197	64	0.631	0.225	1.22E-01	370	1.01	1.38	1.42
LC:NCI_H322M	2.760943	37	0.65	0.17	8.00E-03	90	27.7	1.68	1.67
LC:NCI_H460	5.264815	18	0.749	0.601	2.47E-01	630	1.07	1.24	0.87
LC:NCI_H522	1.711511	50	0.43	0.05	2.60E-03	231	2.7	1.26	1.04
LE:CCRF_CEM	0.767691	27	0.15	0.005	5.96E-05	77	2.4	1.42	1.18
LE:HL_60	0.587631	27	0.085	0.0012	3.50E-06	60	3	1.93	1.24
LE:K_562	0.417653	19	0.0505	0.003	8.50E-04	106	0.33	1.78	2.52
LE:MOLT_4	0.390238	27	0.038	0.0011	2.10E-05	69	0.5	1.47	1.2
LE:RPMI_8226	0.623918	31	0.099	0.00188	4.55E-05	85	1.08	1.95	1.78
LE:SR	0.538624	27	0.068	0.00067	7.44E-06	75	1.13	1.22	1.91
ME:LOXIMVI	0.777927	21	0.184	0.031	2.00E-03	130	0.99	1.64	1.88
ME:M14	2.596092	27	0.621	0.147	1.80E-02	145	4.92	1.32	1.42
ME:MALME_3M	2.27488	35	0.567	0.077	2.00E-03	80	34	1.42	1.07
ME:MDA_MB_435	2.376356	28	0.565	0.176	8.30E-03	140	3.19	2.92	1.7
ME:MDA_N	2.989849	23	0.7	0.18	3.10E-02	171	3.38	1.43	1.88
ME:SK_MEL_2	1.909829	50	0.48	0.081	6.50E-03	120	2.28	1.02	1.1
ME:SK_MEL_28	4.175347	36	0.95	0.31	1.15E-01	280	1.88	1.24	1.42
ME:SK_MEL_5	3.694426	26	0.852	0.24	9.95E-02	275	1.76	1.97	1.56
ME:UACC_257	2.073322	50	0.51	0.17	3.30E-02	475	1.39	3.04	2.22
ME:UACC_62	1.555146	31	0.387	0.035	1.90E-03	100	5.47	1.41	1.81
OV:IGROV1	1.445192	35	0.389	0.14	6.03E-02	285	0.88	1.7	1.32
OV:NCI_ADR_RES	2.210729	34	0.561	0.041	7.10E-03	140	2.09	1.1	1.37
OV:OVCAR_3	2.352249	37	0.577	0.109	1.45E-02	150	2.9	1.56	0.8
OV:OVCAR_4	1.04522	40	0.241	0.0133	9.20E-04	110	1.15	1.1	2.11
OV:OVCAR_5	2.880238	55	0.66	0.201	4.02E-02	180	2.94	1.5	1.12
OV:OVCAR_8	2.305567	25	0.561	0.132	7.40E-03	100	16.1	1.98	1.84
OV:SK_OV_3	2.671564	57	0.66	0.11	2.10E-02	174	2.04	1.34	1.53
PR:DU_145	2.821123	37	0.646	0.205	2.34E-02	140	7.6	1.37	1.39
PR:PC_3	3.042317	39	0.69	0.218	1.62E-02	110	20	1.36	1.26
RE:786_0	1.797503	23	0.457	0.1027	5.90E-03	100	12	3.22	2.97
RE:A498	1.99933	65	0.5	0.08	8.80E-03	139	3.17	1.07	1.58
RE:ACHN	3.918941	31	0.648	0.475	2.78E-01	620	0.96	2.31	2.31
RE:CAKI_1	1.506775	38	0.364	0.02	4.90E-03	108	2.28	1.18	1.21
RE:RXF_393	3.244877	40	0.67	0.315	8.00E-02	225	2.63	1.33	1.29
RE:SN12C	3.523597	30	0.887	0.1903	2.92E-02	165	2.93	1.49	1.52
RE:TK_10	2.077405	34	0.518	0.08	1.47E-02	170	1.66	2.29	1.91
RE:UO_31	1.902122	37	0.477	0.063	9.00E-03	150	1.76	1.02	1.22

Amundson data for radiation resistance (given as survival fraction) across the NCI-60 panel. (LD_{50}) is the dose at 50% survival (calculated from Amundson's data), Doubling time (*T2*) without irradiation. Survival Fractions after 24hrs are given for single radiation doses of 2, 5 and 8 Grays of γ-rays. D_0 is the dose required to reduce survival by 37% (a factor of e) in the linear part of the curve and *n* the extrapolation number, these parameters are used to describe survival curves. Measurements of apoptosis by caspase activity after 8 and 16 Gys are also reported. *Full details of parameters can be found in the publication* [2].

Table 8.5 Genes composing a signature in dacarbazine (sensitive vs. resistant classes)

AffyCode	Gene Names	Gene Ontology
X213564_x_at	lactate dehydrogenase B	oxidation reduction-GO:0055114: :anaerobic glycolysis-GO:0019642: :cellular carbohydrate metabolic process-GO:0044262: :cytoplasm-GO:0005737: :L-lactate dehydrogenase activity-GO:0004459: :binding-GO:0005488: :oxidoreductase activity-GO:0016491
X218967_s_at	phosphotriesterase related	catabolic process-GO:0009056: :metal ion binding-GO:0046872: :zinc ion binding-GO:0008270: :hydrolase activity, acting on ester bonds-GO:0016788
X208758_at	5-aminoimidazole-4-carboxamide ribonucleotide formyltransferase/IMP cyclohydrolase	nucleobase, nucleoside, nucleotide and nucleic acid metabolic process-GO:0006139: :purine nucleotide biosynthetic process-GO:0006164: :IMP biosynthetic process-GO:0006188: :organ regeneration-GO:0031100: :protein binding-GO:0005515: :IMP cyclohydrolase activity-GO:0003937: :phosphoribosylaminoimidazolecarboxamide formyltransferase activity-GO:0004643: :transferase activity-GO:0016740: :hydrolase activity-GO:0016787
X217915_s_at	ribosomal L24 domain containing 1	ribosome biogenesis-GO:0042254: :translation-GO:0006412: :intracellular-GO:0005622: :ribosome-GO:0005840: :nucleus-GO:0005634: :structural constituent of ribosome-GO:0003735
X220865_s_at	prenyl (decaprenyl) diphosphate synthase, subunit 1	ubiquinone biosynthetic process-GO:0006744: :isoprenoid biosynthetic process-GO:0008299: :protein heterotetramerization-GO:0051290: :trans-hexaprenyltranstransferase activity-GO:0000010: :transferase activity-GO:0016740: :protein heterodimerization activity-GO:0046982: :trans-octaprenyltranstransferase activity-GO:0050347
X205053_at	primase, DNA, polypeptide 1 (49kDa)	DNA replication-GO:0006260: :DNA replication, synthesis of RNA primer-GO:0006269: :transcription-GO:0006350: :nucleoplasm-GO:0005654: :alpha DNA polymerase:primase complex-GO:0005658: :protein binding-GO:0005515: :DNA primase activity-GO:0003896: :metal ion binding-GO:0046872: :zinc ion binding-GO:0008270: :transferase activity-GO:0016740: :nucleotidyltransferase activity-GO:0016779
X200763_s_at	ribosomal protein, large, P1	translational elongation-GO:0006414: :translational elongation-GO:0006414: :cytosolic large ribosomal subunit-GO:0022625: :intracellular-GO:0005622: :cytosol-GO:0005829: :ribosome-GO:0005840: :cytoplasm-GO:0005737: :protein binding-GO:0005515: :RNA binding-GO:0003723: :structural constituent of ribosome-GO:0003735
X225326_at	RNA binding motif protein 27	nucleus-GO:0005634: :cytoplasm-GO:0005737: :nuclear speck-GO:0016607: :nucleotide binding-GO:0000166: :RNA binding-GO:0003723: :metal ion binding-GO:0046872: :zinc ion binding-GO:0008270
X201241_at	DEAD (Asp-Glu-Ala-Asp) box polypeptide 1	spliceosome assembly-GO:0000245: :regulation of translational initiation-GO:0006446: :multicellular organismal development-GO:0007275: :nucleotide binding-GO:0000166: :protein binding-GO:0005515: :RNA binding-GO:0003723: :RNA helicase activity-GO:0003724: :ATP binding-GO:0005524: :hydrolase activity-GO:0016787
X208764_s_at	ATP synthase, H+ transporting, mitochondrial F0 complex, subunit C2 (subunit 9)	ion transport-GO:0006811: :proton transport-GO:0015992: :ATP synthesis coupled proton transport-GO:0015986: :membrane-GO:0016020: :mitochondrion-GO:0005739: :integral to membrane-GO:0016021: :mitochondrial proton-transporting ATP synthase complex-GO:0005753: :proton-transporting ATP synthase complex, coupling factor F(o)-GO:0045263: :mitochondrial membrane-GO:0031966: :transporter activity-GO:0005215: :lipid binding-GO:0008289: :hydrogen ion transmembrane transporter activity-GO:0015078
X211666_x_at	ribosomal protein L3	translational elongation-GO:0006414: :cytosolic large ribosomal subunit-GO:0022625: :intracellular-GO:0005622: :cytosol-GO:0005829: :ribosome-GO:0005840: :cytoplasm-GO:0005737: :nucleolus-GO:0005730: :protein binding-GO:0005515: :RNA binding-GO:0003723: :structural constituent of ribosome-GO:0003735
X207438_s_at	snurportin 1	spliceosomal snRNP biogenesis-GO:0000387: :protein import into nucleus-GO:0006606: :transport-GO:0006810: :intracellular protein transport-GO:0006886: :cytosol-GO:0005829: :nucleus-GO:0005634: :nuclear pore-GO:0005643: :cytoplasm-GO:0005737: :RNA cap binding-GO:0000339: :protein transporter activity-GO:0008565
X218512_at	WD repeat domain 12	Notch signaling pathway-GO:0007219: :nucleus-GO:0005634: :protein binding-GO:0005515
X217807_s_at	glioma tumor suppressor candidate region gene 2	intracellular-GO:0005622: :nucleus-GO:0005634
X224723_x_at	hypothetical LOC401397	

X226711_at	forkhead box N2	transcription-GO:0006350: :regulation of transcription, DNA-dependent-GO:0006355: :nucleus-GO:0005634: :cytoplasm-GO:0005737: :transcription factor activity-GO:0003700: :sequence-specific DNA binding-GO:0043565
X205129_at	nucleophosmin/nucleoplasmin, 3	rRNA processing-GO:0006364: :rRNA transcription-GO:0009303: :nucleus-GO:0005634: :nucleolus-GO:0005730: :protein binding-GO:0005515: :nucleic acid binding-GO:0003676
X201716_at	sorting nexin 1	intracellular protein transport-GO:0006886: :endocytosis-GO:0006897: :cell communication-GO:0007154: :membrane-GO:0016020: :cytoplasm-GO:0005737: :endosome-GO:0005768: :Golgi apparatus-GO:0005794: :endosome membrane-GO:0010008: :protein binding-GO:0005515: :protein transporter activity-GO:0008565: :phosphoinositide binding-GO:0035091
X201184_s_at	chromodomain helicase DNA binding protein 4	chromatin assembly or disassembly-GO:0006333: :regulation of transcription from RNA polymerase II promoter-GO:0006357: :chromatin modification-GO:0016568: :chromatin-GO:0000785: :nucleus-GO:0005634: :nucleotide binding-GO:0000166: :DNA binding-GO:0003677: :chromatin binding-GO:0003682: :ATP-dependent DNA helicase activity-GO:0004003: :helicase activity-GO:0004386: :metal ion binding-GO:0046872: :ATP binding-GO:0005524: :transcription factor binding-GO:0008134: :zinc ion binding-GO:0008270: :hydrolase activity-GO:0016787: :hydrolase activity, acting on acid anhydrides, in phosphorus-containing anhydrides-GO:0016818
X221688_s_at	IMP3, U3 small nucleolar ribonucleoprotein, homolog (yeast)	rRNA processing-GO:0006364: :intracellular-GO:0005622: :ribonucleoprotein complex-GO:0030529: :nucleus-GO:0005634: :nucleolus-GO:0005730: :protein binding-GO:0005515: :rRNA binding-GO:0019843
X214662_at	WD repeat domain 43	nucleus-GO:0005634
X201030_x_at	lactate dehydrogenase B	oxidation reduction-GO:0055114: :anaerobic glycolysis-GO:0019642: :cellular carbohydrate metabolic process-GO:0044262: :cytoplasm-GO:0005737: :L-lactate dehydrogenase activity-GO:0004459: :binding-GO:0005488: :oxidoreductase activity-GO:0016491
X211697_x_at	partner of NOB1 homolog (S. cerevisiae)	nucleus-GO:0005634: :nucleolus-GO:0005730: :RNA binding-GO:0003723
X208870_x_at	ATP synthase, H+ transporting, mitochondrial F1 complex, gamma polypeptide 1	ion transport-GO:0006811: :proton transport-GO:0015992: :ATP synthesis coupled proton transport-GO:0015986: :mitochondrial proton-transporting ATP synthase complex, catalytic core F(1)-GO:0000275: :membrane-GO:0016020: :mitochondrion-GO:0005739: :mitochondrial matrix-GO:0005759: :hydrogen ion transporting ATPase activity, rotational mechanism-GO:0046961: :hydrogen ion transporting ATP synthase activity, rotational mechanism-GO:0046933: :ATPase activity-GO:0016887: :ATPase activity-GO:0016887
X200961_at	selenophosphate synthetase 2	selenocysteine biosynthetic process-GO:0016260: :nucleotide binding-GO:0000166: :selenide, water dikinase activity-GO:0004756: :ATP binding-GO:0005524: :selenium binding-GO:0008430: :transferase activity-GO:0016740
X202858_at	U2 small nuclear RNA auxiliary factor 1	nuclear mRNA splicing, via spliceosome-GO:0000398: :nuclear mRNA splicing, via spliceosome-GO:0000398: :RNA splicing-GO:0008380: :nucleus-GO:0005634: :spliceosome-GO:0005681: :Cajal body-GO:0015030: :nucleotide binding-GO:0000166: :protein binding-GO:0005515: :RNA binding-GO:0003723: :metal ion binding-GO:0046872: :zinc ion binding-GO:0008270: :RS domain binding-GO:0050733
X227008_at	HD domain containing 3	catalytic activity-GO:0003824
X211710_x_at	ribosomal protein L4	translational elongation-GO:0006414: :cytosolic large ribosomal subunit-GO:0022625: :intracellular-GO:0005622: :cytosol-GO:0005829: :ribosome-GO:0005840: :protein binding-GO:0005515: :RNA binding-GO:0003723: :structural constituent of ribosome-GO:0003735
X200089_s_at	ribosomal protein L4	translational elongation-GO:0006414: :cytosolic large ribosomal subunit-GO:0022625: :intracellular-GO:0005622: :cytosol-GO:0005829: :ribosome-GO:0005840: :protein binding-GO:0005515: :RNA binding-GO:0003723: :structural constituent of ribosome-GO:0003735
X202325_s_at	ATP synthase, H+ transporting, mitochondrial F0 complex, subunit F6	ion transport-GO:0006811: :proton transport-GO:0015992: :ATP synthesis coupled proton transport-GO:0015986: :mitochondrial proton-transporting ATP synthase complex, coupling factor F(o)-GO:0000276: :membrane-GO:0016020: :mitochondrion-GO:0005739: :transporter activity-GO:0005215: :ATPase activity-GO:0016887: :hydrogen ion transmembrane transporter activity-GO:0015078
X210396_s_at	PI-3-kinase-related kinase SMG-1 pseudogene	
X234339_s_at	glioma tumor suppressor candidate region gene 2	intracellular-GO:0005622: :nucleus-GO:0005634
X201871_s_at	UBX domain protein 1	proteasomal ubiquitin-dependent protein catabolic process-GO:0043161: :proteasome complex-GO:0000502: :cytoplasm-GO:0005737: :polyubiquitin binding-GO:0031593: :ATPase binding-GO:0051117
X218152_at	high-mobility group 20A	transcription-GO:0006350: :regulation of transcription, DNA-dependent-GO:0006355: :chromatin modification-GO:0016568: :nucleus-GO:0005634:

		:nucleolus-GO:0005730: :protein binding-GO:0005515: :transcription factor activity-GO:0003700
X217821_s_at	WW domain binding protein 11	rRNA processing-GO:0006364: :mRNA processing-GO:0006397: :RNA splicing-GO:0008380: :nucleus-GO:0005634: :cytoplasm-GO:0005737: :nuclear speck-GO:0016607: :protein binding-GO:0005515: :single-stranded DNA binding-GO:0003697: :protein phosphatase type 1 regulator activity-GO:0008599
X200963_x_at	ribosomal protein L31	translational elongation-GO:0006414: :cytosolic large ribosomal subunit-GO:0022625: :intracellular-GO:0005622: :cytosol-GO:0005829: :ribosome-GO:0005840: :protein binding-GO:0005515: :RNA binding-GO:0003723: :structural constituent of ribosome-GO:0003735
X203341_at	CCAAT/enhancer binding protein (C/EBP), zeta	transcription-GO:0006350: :regulation of transcription, DNA-dependent-GO:0006355: :transcription from RNA polymerase II promoter-GO:0006366: :nucleus-GO:0005634: :DNA binding-GO:0003677: :binding-GO:0005488
X226456_at	chromosome 16 open reading frame 75	DNA replication-GO:0006260: :nucleus-GO:0005634: :DNA binding-GO:0003677
X203654_s_at	coilin	female germ cell nucleus-GO:0001674: :nucleus-GO:0005634: :nucleoplasm-GO:0005654: :nucleolus-GO:0005730: :Cajal body-GO:0015030: :disulfide oxidoreductase activity-GO:0015036: :protein C-terminus binding-GO:0008022
X219081_at	ankyrin repeat and KH domain containing 1	cytoplasm-GO:0005737: :protein binding-GO:0005515: :RNA binding-GO:0003723
X201880_at	ariadne homolog, ubiquitin-conjugating enzyme E2 binding protein, 1 (Drosophila)	ubiquitin-dependent protein catabolic process-GO:0006511: :ubiquitin ligase complex-GO:0000151: :cytoplasm-GO:0005737: :protein binding-GO:0005515: :metal ion binding-GO:0046872: :zinc ion binding-GO:0008270: :small conjugating protein ligase activity-GO:0019787
X218075_at	achalasia, adrenocortical insufficiency, alacrimia (Allgrove, triple-A)	regulation of nucleocytoplasmic transport-GO:0046822: :nuclear pore-GO:0005643
X201400_at	proteasome (prosome, macropain) subunit, beta type, 3	ubiquitin-dependent protein catabolic process-GO:0006511: :anaphase-promoting complex-dependent proteasomal ubiquitin-dependent protein catabolic process-GO:0031145: :negative regulation of ubiquitin-protein ligase activity during mitotic cell cycle-GO:0051436: :positive regulation of ubiquitin-protein ligase activity during mitotic cell cycle-GO:0051437: :cytosol-GO:0005829: :nucleus-GO:0005634: :cytoplasm-GO:0005737: :proteasome core complex-GO:0005839: :protein binding-GO:0005515: :threonine endopeptidase activity-GO:0004298: :peptidase activity-GO:0008233
X219006_at	chromosome 6 open reading frame 66	mitochondrion-GO:0005739: :calmodulin binding-GO:0005516
X213735_s_at	cytochrome c oxidase subunit Vb	respiratory gaseous exchange-GO:0007585: :membrane-GO:0016020: :mitochondrion-GO:0005739: :mitochondrial envelope-GO:0005740: :mitochondrial inner membrane-GO:0005743: :cytochrome-c oxidase activity-GO:0004129: :metal ion binding-GO:0046872: :zinc ion binding-GO:0008270
X213145_at	F-box and leucine-rich repeat protein 14	ubiquitin-dependent protein catabolic process-GO:0006511
X212716_s_at	eukaryotic translation initiation factor 3, subunit K	regulation of translational initiation-GO:0006446: :cytosol-GO:0005829: :nucleus-GO:0005634: :cytoplasm-GO:0005737: :eukaryotic translation initiation factor 3 complex-GO:0005852: :protein binding-GO:0005515: :translation initiation factor activity-GO:0003743: :ribosome binding-GO:0043022
X218119_at	translocase of inner mitochondrial membrane 23 homolog (yeast)	protein targeting to mitochondrion-GO:0006626: :intracellular protein transport across a membrane-GO:0065002: :membrane-GO:0016020: :mitochondrion-GO:0005739: :integral to membrane-GO:0016021: :mitochondrial outer membrane-GO:0005741: :mitochondrial inner membrane presequence translocase complex-GO:0005744: :mitochondrial intermembrane space-GO:0005758: :protein binding-GO:0005515: :protein transporter activity-GO:0008565: :P-P-bond-hydrolysis-driven protein transmembrane transporter activity-GO:0015450
X200840_at	lysyl-tRNA synthetase	lysyl-tRNA aminoacylation-GO:0006430: :soluble fraction-GO:0005625: :cytoplasm-GO:0005737: :nucleotide binding-GO:0000166: :nucleic acid binding-GO:0003676: :lysine-tRNA ligase activity-GO:0004824: :ATP binding-GO:0005524: :ligase activity-GO:0016874
X221693_s_at	mitochondrial ribosomal protein S18A	translation-GO:0006412: :intracellular-GO:0005622: :mitochondrion-GO:0005739: :ribosome-GO:0005840: :mitochondrial small ribosomal subunit-GO:0005763: :structural constituent of ribosome-GO:0003735
X225892_at	iron-responsive element binding protein 2	metabolic process-GO:0008152: :regulation of translation-GO:0006417: :protoporphyrinogen IX biosynthetic process-GO:0006782: :cellular iron ion homeostasis-GO:0006879: :post-embryonic development-GO:0009791: :regulation of gene expression-GO:0010468: :erythrocyte homeostasis-GO:0034101: :intestinal absorption-GO:0050892: :cytosol-GO:0005829: :cytoplasm-GO:0005737: :RNA binding-GO:0003723: :metal ion binding-GO:0046872: :iron ion binding-GO:0005506: :iron-responsive element binding-

		GO:0030350: :4 iron, 4 sulfur cluster binding-GO:0051539
X205711_x_at	ATP synthase, H+ transporting, mitochondrial F1 complex, gamma polypeptide 1	ion transport-GO:0006811: :proton transport-GO:0015992: :ATP synthesis coupled proton transport-GO:0015986: :mitochondrial proton-transporting ATP synthase complex, catalytic core F(1)-GO:0000275: :membrane-GO:0016020: :mitochondrion-GO:0005739: :mitochondrial matrix-GO:0005759: :hydrogen ion transporting ATPase activity, rotational mechanism-GO:0046961: :hydrogen ion transporting ATP synthase activity, rotational mechanism-GO:0046933: :ATPase activity-GO:0016887: :ATPase activity-GO:0016887
X210501_x_at	eukaryotic translation initiation factor 3, subunit K	regulation of translational initiation-GO:0006446: :cytosol-GO:0005829: :nucleus-GO:0005634: :cytoplasm-GO:0005737: :eukaryotic translation initiation factor 3 complex-GO:0005852: :protein binding-GO:0005515: :translation initiation factor activity-GO:0003743: :ribosome binding-GO:0043022
X200029_at	ribosomal protein L19	translational elongation-GO:0006414: :cytosolic large ribosomal subunit-GO:0022625: :intracellular-GO:0005622: :cytosol-GO:0005829: :ribosome-GO:0005840: :RNA binding-GO:0003723: :structural constituent of ribosome-GO:0003735
X231576_at	NA	
X202329_at	c-src tyrosine kinase	protein amino acid phosphorylation-GO:0006468: :negative regulation of cell proliferation-GO:0008285: :plasma membrane-GO:0005886: :plasma membrane-GO:0005886: :cytoplasm-GO:0005737: :intercellular junction-GO:0005911: :nucleotide binding-GO:0000166: :non-membrane spanning protein tyrosine kinase activity-GO:0004715: :ATP binding-GO:0005524: :protein C-terminus binding-GO:0008022: :transferase activity-GO:0016740
X203677_s_at	TAR (HIV-1) RNA binding protein 2	regulation of transcription from RNA polymerase II promoter-GO:0006357: :intracellular-GO:0005622: :nucleus-GO:0005634: :protein binding-GO:0005515: :double-stranded RNA binding-GO:0003725
X201154_x_at	ribosomal protein L4	translational elongation-GO:0006414: :cytosolic large ribosomal subunit-GO:0022625: :intracellular-GO:0005622: :cytosol-GO:0005829: :ribosome-GO:0005840: :protein binding-GO:0005515: :RNA binding-GO:0003723: :structural constituent of ribosome-GO:0003735
X218438_s_at	mediator complex subunit 28	transcription-GO:0006350: :regulation of transcription, DNA-dependent-GO:0006355: :membrane-GO:0016020: :nucleus-GO:0005634: :cytoplasm-GO:0005737: :protein binding-GO:0005515: :actin binding-GO:0003779
X227711_at	gametocyte specific factor 1	cytoplasm-GO:0005737
X225472_at	HLA-B associated transcript 4	intracellular-GO:0005622: :endoplasmic reticulum-GO:0005783: :protein binding-GO:0005515: :nucleic acid binding-GO:0003676
X224666_at	non-SMC element 1 homolog (S. cerevisiae)	DNA repair-GO:0006281: :DNA recombination-GO:0006310: :response to DNA damage stimulus-GO:0006974: :nucleus-GO:0005634: :metal ion binding-GO:0046872: :zinc ion binding-GO:0008270
X205562_at	ribonuclease P/MRP 38kDa subunit	tRNA processing-GO:0008033: :nucleus-GO:0005634: :nucleolar ribonuclease P complex-GO:0005655: :protein binding-GO:0005515: :ribonuclease P activity-GO:0004526: :hydrolase activity-GO:0016787
X214280_x_at	heterogeneous nuclear ribonucleoprotein A1	nuclear mRNA splicing, via spliceosome-GO:0000398: :nuclear mRNA splicing, via spliceosome-GO:0000398: :RNA export from nucleus-GO:0006405: :transport-GO:0006810: :RNA splicing-GO:0008380: :mRNA transport-GO:0051028: :nuclear import-GO:0051170: :nucleus-GO:0005634: :cytoplasm-GO:0005737: :nucleoplasm-GO:0005654: :spliceosome-GO:0005681: :heterogeneous nuclear ribonucleoprotein complex-GO:0030530: :nucleotide binding-GO:0000166: :protein binding-GO:0005515: :single-stranded DNA binding-GO:0003697: :single-stranded RNA binding-GO:0003727
X201600_at	prohibitin 2	regulation of transcription, DNA-dependent-GO:0006355: :negative regulation of transcription-GO:0016481: :membrane-GO:0016020: :mitochondrion-GO:0005739: :cytoplasm-GO:0005737: :protein binding-GO:0005515: :receptor activity-GO:0004872: :specific transcriptional repressor activity-GO:0016566: :estrogen receptor binding-GO:0030331
X219244_s_at	mitochondrial ribosomal protein L46	mitochondrion-GO:0005739: :ribosome-GO:0005840
X213897_s_at	mitochondrial ribosomal protein L23	translation-GO:0006412: :mitochondrion-GO:0005739: :ribosome-GO:0005840: :mitochondrial large ribosomal subunit-GO:0005762: :nucleotide binding-GO:0000166: :RNA binding-GO:0003723: :structural constituent of ribosome-GO:0003735

X211537_x_at	mitogen-activated protein kinase kinase kinase 7	positive regulation of T cell cytokine production-GO:0002726: :signal transduction-GO:0007165: :protein amino acid phosphorylation-GO:0006468: :transforming growth factor beta receptor signaling pathway-GO:0007179: :activation of NF-kappaB-inducing kinase activity-GO:0007250: :positive regulation of interleukin-2 production-GO:0032743: :T cell receptor signaling pathway-GO:0050852: :positive regulation of T cell activation-GO:0050870: :cytosol-GO:0005829: :nucleotide binding-GO:0000166: :protein binding-GO:0005515: :magnesium ion binding-GO:0000287: :protein serine/threonine kinase activity-GO:0004674: :MAP kinase kinase kinase activity-GO:0004709: :protein tyrosine kinase activity-GO:0004713: :ATP binding-GO:0005524: :transferase activity-GO:0016740
X221494_x_at	eukaryotic translation initiation factor 3, subunit K	regulation of translational initiation-GO:0006446: :cytosol-GO:0005829: :nucleus-GO:0005634: :cytoplasm-GO:0005737: :eukaryotic translation initiation factor 3 complex-GO:0005852: :protein binding-GO:0005515: :translation initiation factor activity-GO:0003743: :ribosome binding-GO:0043022
X211752_s_at	NADH dehydrogenase (ubiquinone) Fe-S protein 7, 20kDa (NADH-coenzyme Q reductase)	mitochondrial electron transport, NADH to ubiquinone-GO:0006120: :electron transport chain-GO:0022900: :transport-GO:0006810: :mitochondrial respiratory chain complex I assembly-GO:0032981: :mitochondrion-GO:0005739: :mitochondrial respiratory chain complex I-GO:0005747: :mitochondrial respiratory chain complex I-GO:0005747: :protein binding-GO:0005515: :NADH dehydrogenase activity-GO:0003954: :metal ion binding-GO:0046872: :iron ion binding-GO:0005506: :NADH dehydrogenase (ubiquinone) activity-GO:0008137: :oxidoreductase activity, acting on NADH or NADPH, quinone or similar compound as acceptor-GO:0016655: :4 iron, 4 sulfur cluster binding-GO:0051539
X226748_at	LysM, putative peptidoglycan-binding, domain containing 2	cell wall catabolic process-GO:0016998
X200909_s_at	ribosomal protein, large, P2	translational elongation-GO:0006414: :translational elongation-GO:0006414: :cytosolic large ribosomal subunit-GO:0022625: :intracellular-GO:0005622: :cytosol-GO:0005829: :ribosome-GO:0005840: :RNA binding-GO:0003723: :structural constituent of ribosome-GO:0003735
X202158_s_at	CUG triplet repeat, RNA binding protein 2	mRNA processing-GO:0006397: :regulation of heart contraction-GO:0008016: :nucleus-GO:0005634: :cytoplasm-GO:0005737: :nucleotide binding-GO:0000166: :protein binding-GO:0005515: :RNA binding-GO:0003723
X226194_at	zinc finger protein 828	intracellular-GO:0005622: :nucleus-GO:0005634: :cytoplasm-GO:0005737: :nucleolus-GO:0005730: :metal ion binding-GO:0046872: :zinc ion binding-GO:0008270
X206218_at	melanoma antigen family B, 2	protein binding-GO:0005515
X222465_at	ribosomal L24 domain containing 1	ribosome biogenesis-GO:0042254: :translation-GO:0006412: :intracellular-GO:0005622: :ribosome-GO:0005840: :nucleus-GO:0005634: :structural constituent of ribosome-GO:0003735
X212740_at	phosphoinositide-3-kinase, regulatory subunit 4	protein amino acid phosphorylation-GO:0006468: :cytosol-GO:0005829: :nucleotide binding-GO:0000166: :protein serine/threonine kinase activity-GO:0004674: :protein tyrosine kinase activity-GO:0004713: :transferase activity-GO:0016740
X201183_s_at	chromodomain helicase DNA binding protein 4	chromatin assembly or disassembly-GO:0006333: :regulation of transcription from RNA polymerase II promoter-GO:0006357: :chromatin modification-GO:0016568: :chromatin-GO:0000785: :nucleus-GO:0005634: :nucleotide binding-GO:0000166: :DNA binding-GO:0003677: :chromatin binding-GO:0003682: :ATP-dependent DNA helicase activity-GO:0004003: :helicase activity-GO:0004386: :metal ion binding-GO:0046872: :ATP binding-GO:0005524: :transcription factor binding-GO:0008134: :zinc ion binding-GO:0008270: :hydrolase activity-GO:0016787: :hydrolase activity, acting on acid anhydrides, in phosphorus-containing anhydrides-GO:0016818
X218859_s_at	ESF1, nucleolar pre-rRNA processing protein, homolog (S. cerevisiae)	transcription-GO:0006350: :regulation of transcription, DNA-dependent-GO:0006355: :nucleus-GO:0005634
X235096_at	Leo1, Paf1/RNA polymerase II complex component, homolog (S. cerevisiae)	transcription-GO:0006350: :regulation of transcription, DNA-dependent-GO:0006355: :nucleus-GO:0005634: :protein binding-GO:0005515
X206854_s_at	mitogen-activated protein kinase kinase kinase 7	positive regulation of T cell cytokine production-GO:0002726: :signal transduction-GO:0007165: :protein amino acid phosphorylation-GO:0006468: :transforming growth factor beta receptor signaling pathway-GO:0007179: :activation of NF-kappaB-inducing kinase activity-GO:0007250: :positive regulation of interleukin-2 production-GO:0032743: :T cell receptor signaling pathway-GO:0050852: :positive regulation of T cell activation-GO:0050870: :cytosol-GO:0005829: :nucleotide binding-GO:0000166: :protein binding-GO:0005515: :magnesium ion binding-GO:0000287: :protein serine/threonine kinase activity-GO:0004674: :MAP kinase kinase kinase activity-GO:0004709: :protein tyrosine kinase activity-GO:0004713: :ATP binding-GO:0005524:

		:transferase activity-GO:0016740
X211025_x_at	cytochrome c oxidase subunit Vb	respiratory gaseous exchange-GO:0007585: :membrane-GO:0016020: :mitochondrion-GO:0005739: :mitochondrial envelope-GO:0005740: :mitochondrial inner membrane-GO:0005743: :cytochrome-c oxidase activity-GO:0004129: :metal ion binding-GO:0046872: :zinc ion binding-GO:0008270
X213366_x_at	ATP synthase, H+ transporting, mitochondrial F1 complex, gamma polypeptide 1	ion transport-GO:0006811: :proton transport-GO:0015992: :ATP synthesis coupled proton transport-GO:0015986: :mitochondrial proton-transporting ATP synthase complex, catalytic core F(1)-GO:0000275: :membrane-GO:0016020: :mitochondrion-GO:0005739: :mitochondrial matrix-GO:0005759: :hydrogen ion transporting ATPase activity, rotational mechanism-GO:0046961: :hydrogen ion transporting ATP synthase activity, rotational mechanism-GO:0046933: :ATPase activity-GO:0016887: :ATPase activity-GO:0016887
X218561_s_at	LYR motif containing 4	
X200867_at	ring finger protein 114	multicellular organismal development-GO:0007275: :spermatogenesis-GO:0007283: :cell differentiation-GO:0030154: :intracellular-GO:0005622: :protein binding-GO:0005515: :metal ion binding-GO:0046872: :zinc ion binding-GO:0008270
X202691_at	small nuclear ribonucleoprotein D1 polypeptide 16kDa	spliceosome assembly-GO:0000245: :spliceosomal snRNP biogenesis-GO:0000387: :RNA splicing-GO:0008380: :small nuclear ribonucleoprotein complex-GO:0030532: :cytosol-GO:0005829: :nucleus-GO:0005634: :cytoplasm-GO:0005737: :nucleoplasm-GO:0005654: :spliceosome-GO:0005681: :protein binding-GO:0005515: :RNA binding-GO:0003723
X209042_s_at	ubiquitin-conjugating enzyme E2G 2 (UBC7 homolog, yeast)	ubiquitin-dependent protein catabolic process-GO:0006511: :post-translational protein modification-GO:0043687: :regulation of protein metabolic process-GO:0051246: :cytosol-GO:0005829: :protein binding-GO:0005515: :ubiquitin-protein ligase activity-GO:0004842: :ligase activity-GO:0016874
X231713_s_at	elongation protein 2 homolog (S. cerevisiae)	transcription-GO:0006350: :regulation of transcription from RNA polymerase II promoter-GO:0006357: :nucleus-GO:0005634: :transcription elongation factor complex-GO:0008023: :DNA binding-GO:0003677: :RNA polymerase II transcription elongation factor activity-GO:0016944
X202157_s_at	CUG triplet repeat, RNA binding protein 2	mRNA processing-GO:0006397: :regulation of heart contraction-GO:0008016: :nucleus-GO:0005634: :cytoplasm-GO:0005737: :nucleotide binding-GO:0000166: :protein binding-GO:0005515: :RNA binding-GO:0003723
X214794_at	proliferation-associated 2G4, 38kDa	transcription-GO:0006350: :rRNA processing-GO:0006364: :regulation of translation-GO:0006417: :cell cycle arrest-GO:0007050: :cell proliferation-GO:0008283: :negative regulation of transcription, DNA-dependent-GO:0045892: :ribonucleoprotein complex-GO:0030529: :nucleus-GO:0005634: :cytoplasm-GO:0005737: :protein binding-GO:0005515: :transcription factor activity-GO:0003700: :RNA binding-GO:0003723
X204599_s_at	mitochondrial ribosomal protein L28	translation-GO:0006412: :regulation of transcription-GO:0045449: :mitochondrion-GO:0005739: :ribosome-GO:0005840: :mitochondrial ribosome-GO:0005761: :transcription factor activity-GO:0003700: :structural constituent of ribosome-GO:0003735: :translation regulator activity-GO:0045182
X218118_s_at	translocase of inner mitochondrial membrane 23 homolog (yeast)	protein targeting to mitochondrion-GO:0006626: :intracellular protein transport across a membrane-GO:0065002: :membrane-GO:0016020: :mitochondrion-GO:0005739: :integral to membrane-GO:0016021: :mitochondrial outer membrane-GO:0005741: :mitochondrial inner membrane presequence translocase complex-GO:0005744: :mitochondrial intermembrane space-GO:0005758: :protein binding-GO:0005515: :protein transporter activity-GO:0008565: :P-P-bond-hydrolysis-driven protein transmembrane transporter activity-GO:0015450
X201913_s_at	Coenzyme A synthase	biosynthetic process-GO:0009058: :coenzyme A biosynthetic process-GO:0015937: :cytoplasm-GO:0005737: :nucleotide binding-GO:0000166: :dephospho-CoA kinase activity-GO:0004140: :pantetheine-phosphate adenylyltransferase activity-GO:0004595: :ATP binding-GO:0005524: :transferase activity-GO:0016740
X205024_s_at	RAD51 homolog (RecA homolog, E. coli) (S. cerevisiae)	double-strand break repair via homologous recombination-GO:0000724: :DNA unwinding during replication-GO:0006268: :DNA repair-GO:0006281: :mitotic recombination-GO:0006312: :response to DNA damage stimulus-GO:0006974: :meiotic recombination-GO:0007131: :protein homooligomerization-GO:0051260: :positive regulation of DNA ligation-GO:0051106: :intracellular-GO:0005622: :nucleus-GO:0005634: :nucleoplasm-GO:0005654: :PML body-GO:0016605: :nucleotide binding-GO:0000166: :damaged DNA binding-GO:0003684: :double-stranded DNA binding-GO:0003690: :single-stranded DNA

		binding-GO:0003697: :protein C-terminus binding-GO:0008022: :identical protein binding-GO:0042802: :single-stranded DNA-dependent ATPase activity-GO:0043142: :sequence-specific DNA binding-GO:0043565
X212244_at	glutamate receptor, ionotropic, N-methyl D-aspartate-like 1A	
X224741_x_at	centromere protein L	chromosome, centromeric region-GO:0000775: :nucleus-GO:0005634: :chromosome-GO:0005694
X230326_s_at	chromosome 11 open reading frame 73	Golgi organization and biogenesis-GO:0007030: :multicellular organismal development-GO:0007275: :lung development-GO:0030324: :cytoplasm-GO:0005737
X228095_at	PHD finger protein 14	protein binding-GO:0005515: :metal ion binding-GO:0046872: :zinc ion binding-GO:0008270
X204145_at	FSHD region gene 1	rRNA processing-GO:0006364: :mRNA processing-GO:0006397: :RNA splicing-GO:0008380: :nucleus-GO:0005634: :spliceosome-GO:0005681: :nuclear speck-GO:0016607
X218317_x_at	GIY-YIG domain containing 2	DNA repair-GO:0006281: :intracellular-GO:0005622: :nuclease activity-GO:0004518

Table 8.6 Genes composing a signature in radiation (sensitive vs. resistant classes)

X207419_s_at	ras-related C3 botulinum toxin substrate 2 (rho family, small GTP binding protein Rac2)	actin cytoskeleton organization and biogenesis-GO:0030036: :signal transduction-GO:0007165: :chemotaxis-GO:0006935: :small GTPase mediated signal transduction-GO:0007264: :positive regulation of cell proliferation-GO:0008284: :regulation of hydrogen peroxide metabolic process-GO:0010310: :cell projection biogenesis-GO:0030031: :regulation of respiratory burst-GO:0060263: :intracellular-GO:0005622: :membrane fraction-GO:0005624: :nuclear envelope-GO:0005635: :cytoplasm-GO:0005737: :nucleotide binding-GO:0000166: :protein binding-GO:0005515: :GTPase activity-GO:0003924: :GTP binding-GO:0005525
X213620_s_at	intercellular adhesion molecule 2	cell-cell adhesion-GO:0016337: :plasma membrane-GO:0005886: :plasma membrane-GO:0005886: :integral to plasma membrane-GO:0005887: :protein binding-GO:0005515: :integrin binding-GO:0005178
X201288_at	Rho GDP dissociation inhibitor (GDI) beta	actin cytoskeleton organization and biogenesis-GO:0030036: :cell motility-GO:0006928: :immune response-GO:0006955: :negative regulation of cell adhesion-GO:0007162: :Rho protein signal transduction-GO:0007266: :multicellular organismal development-GO:0007275: :cytoplasm-GO:0005737: :cytoskeleton-GO:0005856: :cytoplasmic membrane-bounded vesicle-GO:0016023: :protein binding-GO:0005515: :Rho GDP-dissociation inhibitor activity-GO:0005094: :GTPase activator activity-GO:0005096
X218006_s_at	zinc finger protein 22 (KOX 15)	regulation of transcription, DNA-dependent-GO:0006355: :odontogenesis-GO:0042476: :intracellular-GO:0005622: :metal ion binding-GO:0046872: :zinc ion binding-GO:0008270
X224856_at	FK506 binding protein 5	protein folding-GO:0006457: :nucleus-GO:0005634: :cytoplasm-GO:0005737: :protein binding-GO:0005515: :peptidyl-prolyl cis-trans isomerase activity-GO:0003755: :FK506 binding-GO:0005528: :isomerase activity-GO:0016853
X204683_at	intercellular adhesion molecule 2	cell-cell adhesion-GO:0016337: :plasma membrane-GO:0005886: :plasma membrane-GO:0005886: :integral to plasma membrane-GO:0005887: :protein binding-GO:0005515: :integrin binding-GO:0005178
X201721_s_at	lysosomal multispanning membrane protein 5	transport-GO:0006810: :membrane-GO:0016020: :integral to plasma membrane-GO:0005887: :lysosomal membrane-GO:0005765
X223322_at	Ras association (RalGDS/AF-6) domain family member 5	apoptosis-GO:0006915: :intracellular signaling cascade-GO:0007242: :negative regulation of cell cycle-GO:0045786: :cytoplasm-GO:0005737: :microtubule-GO:0005874: :protein binding-GO:0005515: :metal ion binding-GO:0046872: :zinc ion binding-GO:0008270: :diacylglycerol binding-GO:0019992
X204220_at	glia maturation factor, gamma	protein amino acid phosphorylation-GO:0006468: :intracellular-GO:0005622: :mitochondrion-GO:0005739: :nucleus-GO:0005634: :nucleolus-GO:0005730: :actin binding-GO:0003779: :protein kinase inhibitor activity-GO:0004860: :enzyme activator activity-GO:0008047: :growth factor activity-GO:0008083
X201720_s_at	lysosomal multispanning membrane protein 5	transport-GO:0006810: :membrane-GO:0016020: :integral to plasma membrane-GO:0005887: :lysosomal membrane-GO:0005765
X213603_s_at	ras-related C3 botulinum toxin substrate 2 (rho family, small GTP binding protein Rac2)	actin cytoskeleton organization and biogenesis-GO:0030036: :signal transduction-GO:0007165: :chemotaxis-GO:0006935: :small GTPase mediated signal transduction-GO:0007264: :positive regulation of cell proliferation-GO:0008284: :regulation of hydrogen peroxide metabolic process-GO:0010310: :cell projection biogenesis-GO:0030031: :regulation of respiratory burst-GO:0060263: :intracellular-GO:0005622: :membrane fraction-GO:0005624: :nuclear envelope-GO:0005635: :cytoplasm-GO:0005737: :nucleotide binding-GO:0000166: :protein binding-GO:0005515: :GTPase activity-GO:0003924: :GTP binding-GO:0005525
X218005_at	zinc finger protein 22 (KOX 15)	regulation of transcription, DNA-dependent-GO:0006355: :odontogenesis-GO:0042476: :intracellular-GO:0005622: :metal ion binding-GO:0046872: :zinc ion binding-GO:0008270
X203416_at	CD53 molecule	signal transduction-GO:0007165: :plasma membrane-GO:0005886: :integral to membrane-GO:0016021

X204798_at	v-myb myeloblastosis viral oncogene homolog (avian)	regulation of transcription, DNA-dependent-GO:0006355: :nucleus-GO:0005634: :nuclear matrix-GO:0016363: :protein binding-GO:0005515: :DNA binding-GO:0003677: :transcription activator activity-GO:0016563
X204265_s_at	G-protein signaling modulator 3 (AGS3-like, C. elegans)	signal transduction-GO:0007165: :cytoplasm-GO:0005737: :protein binding-GO:0005515: :GTPase activator activity-GO:0005096
X227346_at	IKAROS family zinc finger 1 (Ikaros)	transcription-GO:0006350: :regulation of transcription, DNA-dependent-GO:0006355: :mesoderm development-GO:0007498: :intracellular-GO:0005622: :nucleus-GO:0005634: :DNA binding-GO:0003677: :metal ion binding-GO:0046872: :zinc ion binding-GO:0008270
X225763_at	RCSD domain containing 1	
X204852_s_at	protein tyrosine phosphatase, non-receptor type 7	protein amino acid dephosphorylation-GO:0006470: :cytoplasm-GO:0005737: :protein tyrosine phosphatase activity-GO:0004725: :hydrolase activity-GO:0016787
X209734_at	NCK-associated protein 1-like	plasma membrane-GO:0005886: :integral to plasma membrane-GO:0005887: :membrane fraction-GO:0005624
X215785_s_at	cytoplasmic FMR1 interacting protein 2	apoptosis-GO:0006915: :cell-cell adhesion-GO:0016337: :cytoplasm-GO:0005737: :synaptosome-GO:0019717: :cell junction-GO:0030054: :synapse-GO:0045202: :perinuclear region of cytoplasm-GO:0048471: :protein binding-GO:0005515
X209879_at	selectin P ligand	cell adhesion-GO:0007155: :leukocyte tethering or rolling-GO:0050901: :membrane-GO:0016020: :integral to plasma membrane-GO:0005887: :membrane fraction-GO:0005624: :receptor binding-GO:0005102: :bacterial binding-GO:0008367
X204949_at	intercellular adhesion molecule 3	cell-cell adhesion-GO:0016337: :plasma membrane-GO:0005886: :plasma membrane-GO:0005886: :integral to plasma membrane-GO:0005887: :integrin binding-GO:0005178
X219869_s_at	solute carrier family 39 (zinc transporter), member 8	ion transport-GO:0006811: :metal ion transport-GO:0030001: :zinc ion transport-GO:0006829: :membrane-GO:0016020: :integral to membrane-GO:0016021: :metal ion transmembrane transporter activity-GO:0046873: :zinc ion binding-GO:0008270
X202957_at	hematopoietic cell-specific Lyn substrate 1	regulation of transcription, DNA-dependent-GO:0006355: :intracellular signaling cascade-GO:0007242: :membrane-GO:0016020: :mitochondrion-GO:0005739: :DNA-directed RNA polymerase II, core complex-GO:0005665: :transcription factor activity-GO:0003700: :SH3 domain binding-GO:0017124
X212588_at	protein tyrosine phosphatase, receptor type, C	immunoglobulin biosynthetic process-GO:0002378: :negative regulation of protein kinase activity-GO:0006469: :cell surface receptor linked signal transduction-GO:0007166: :positive regulation of B cell proliferation-GO:0030890: :regulation of S phase-GO:0033261: :positive regulation of protein kinase activity-GO:0045860: :T cell receptor signaling pathway-GO:0050852: :plasma membrane-GO:0005886: :nucleus-GO:0005634: :protein binding-GO:0005515: :transmembrane receptor protein tyrosine phosphatase activity-GO:0005001: :hydrolase activity-GO:0016787: :protein kinase binding-GO:0019901
X207238_s_at	protein tyrosine phosphatase, receptor type, C	immunoglobulin biosynthetic process-GO:0002378: :negative regulation of protein kinase activity-GO:0006469: :cell surface receptor linked signal transduction-GO:0007166: :positive regulation of B cell proliferation-GO:0030890: :regulation of S phase-GO:0033261: :positive regulation of protein kinase activity-GO:0045860: :T cell receptor signaling pathway-GO:0050852: :plasma membrane-GO:0005886: :nucleus-GO:0005634: :protein binding-GO:0005515: :transmembrane receptor protein tyrosine phosphatase activity-GO:0005001: :hydrolase activity-GO:0016787: :protein kinase binding-GO:0019901
X209267_s_at	solute carrier family 39 (zinc transporter), member 8	ion transport-GO:0006811: :metal ion transport-GO:0030001: :zinc ion transport-GO:0006829: :membrane-GO:0016020: :integral to membrane-GO:0016021: :metal ion transmembrane transporter activity-GO:0046873: :zinc ion binding-GO:0008270
X218870_at	Rho GTPase activating protein 15	signal transduction-GO:0007165: :intracellular-GO:0005622: :membrane-GO:0016020: :cytoplasm-GO:0005737: :GTPase activator activity-GO:0005096
X203029_s_at	protein tyrosine phosphatase, receptor type, N polypeptide 2	protein amino acid dephosphorylation-GO:0006470: :plasma membrane-GO:0005886: :integral to plasma membrane-GO:0005887: :cytoplasm-GO:0005737: :protein binding-GO:0005515: :receptor activity-GO:0004872: :transmembrane receptor protein tyrosine phosphatase activity-GO:0005001: :hydrolase activity-GO:0016787

X219634_at	carbohydrate (chondroitin 4) sulfotransferase 11	chondrocyte development-GO:0002063: :respiratory gaseous exchange-GO:0007585: :post-embryonic development-GO:0009791: :carbohydrate biosynthetic process-GO:0016051: :chondroitin sulfate biosynthetic process-GO:0030206: :negative regulation of transforming growth factor beta receptor signaling pathway-GO:0030512: :polysaccharide localization-GO:0033037: :tail morphogenesis-GO:0035121: :regulation of cell proliferation-GO:0042127: :embryonic digit morphogenesis-GO:0042733: :negative regulation of apoptosis-GO:0043066: :developmental growth-GO:0048589: :embryonic viscerocranium morphogenesis-GO:0048703: :embryonic skeletal morphogenesis-GO:0048704: :cartilage development-GO:0051216: :Golgi membrane-GO:0000139: :membrane-GO:0016020: :integral to membrane-GO:0016021: :Golgi apparatus-GO:0005794: :N-acetylgalactosamine 4-O-sulfotransferase activity-GO:0001537: :transferase activity-GO:0016740: :chondroitin 4-sulfotransferase activity-GO:0047756
X208056_s_at	core-binding factor, runt domain, alpha subunit 2; translocated to, 3	transcription-GO:0006350: :regulation of transcription, DNA-dependent-GO:0006355: :cell proliferation-GO:0008283: :cell differentiation-GO:0030154: :Golgi membrane-GO:0000139: :membrane-GO:0016020: :nucleus-GO:0005634: :Golgi apparatus-GO:0005794: :protein binding-GO:0005515: :transcription factor activity-GO:0003700: :metal ion binding-GO:0046872: :zinc ion binding-GO:0008270
X219497_s_at	B-cell CLL/lymphoma 11A (zinc finger protein)	transcription-GO:0006350: :regulation of transcription, DNA-dependent-GO:0006355: :intracellular-GO:0005622: :nucleic acid binding-GO:0003676: :metal ion binding-GO:0046872: :zinc ion binding-GO:0008270
X212587_s_at	protein tyrosine phosphatase, receptor type, C	immunoglobulin biosynthetic process-GO:0002378: :negative regulation of protein kinase activity-GO:0006469: :cell surface receptor linked signal transduction-GO:0007166: :positive regulation of B cell proliferation-GO:0030890: :regulation of S phase-GO:0033261: :positive regulation of protein kinase activity-GO:0045860: :T cell receptor signaling pathway-GO:0050852: :plasma membrane-GO:0005886: :nucleus-GO:0005634: :protein binding-GO:0005515: :transmembrane receptor protein tyrosine phosphatase activity-GO:0005001: :hydrolase activity-GO:0016787: :protein kinase binding-GO:0019901
X213036_x_at	ATPase, Ca++ transporting, ubiquitous	metabolic process-GO:0008152: :ATP biosynthetic process-GO:0006754: :cation transport-GO:0006812: :calcium ion transport-GO:0006816: :membrane-GO:0016020: :integral to membrane-GO:0016021: :nucleus-GO:0005634: :nuclear membrane-GO:0031965: :sarcoplasmic reticulum membrane-GO:0033017: :nucleotide binding-GO:0000166: :protein binding-GO:0005515: :magnesium ion binding-GO:0000287: :calcium ion binding-GO:0005509: :calcium-transporting ATPase activity-GO:0005388: :ATP binding-GO:0005524: :hydrolase activity-GO:0016787: :hydrolase activity, acting on acid anhydrides, catalyzing transmembrane movement of substances-GO:0016820
X220035_at	nucleoporin 210kDa	protein transport-GO:0015031: :mRNA transport-GO:0051028: :intracellular protein transport across a membrane-GO:0065002: :membrane-GO:0016020: :integral to membrane-GO:0016021: :endoplasmic reticulum-GO:0005783: :nucleus-GO:0005634: :nuclear pore-GO:0005643: :endoplasmic reticulum membrane-GO:0005789: :nuclear membrane-GO:0031965: :protein binding-GO:0005515
X216705_s_at	adenosine deaminase	response to hypoxia-GO:0001666: :in utero embryonic development-GO:0001701: :trophectodermal cell differentiation-GO:0001829: :liver development-GO:0001889: :placenta development-GO:0001890: :germinal center B cell differentiation-GO:0002314: :positive regulation of germinal center formation-GO:0002636: :negative regulation of mature B cell apoptosis-GO:0002906: :adenosine catabolic process-GO:0006154: :deoxyadenosine catabolic process-GO:0006157: :nucleotide metabolic process-GO:0009117: :purine ribonucleoside monophosphate biosynthetic process-GO:0009168: :positive regulation of B cell proliferation-GO:0030890: :purine nucleotide salvage-GO:0032261: :regulation of cell-cell adhesion mediated by integrin-GO:0033632: :negative regulation of apoptosis-GO:0043066: :positive regulation of T cell differentiation-GO:0045582: :dATP catabolic process-GO:0046061: :hypoxanthine biosynthetic process-GO:0046101: :inosine biosynthetic process-GO:0046103: :xanthine biosynthetic process-GO:0046111: :alveolus development-GO:0048286: :Peyer's patch development-GO:0048541: :embryonic gut development-GO:0048566: :negative regulation of inflammatory response-GO:0050728: :negative regulation of adenosine receptor signaling pathway-GO:0060169: :membrane-GO:0016020: :lysosome-GO:0005764: :cytosol-GO:0005829: :cytoplasm-GO:0005737: :external side of plasma membrane-GO:0009897: :protein binding-GO:0005515: :adenosine deaminase activity-GO:0004000: :adenosine deaminase activity-GO:0004000:

		:zinc ion binding-GO:0008270: :hydrolase activity-GO:0016787
X226420_at	ecotropic viral integration site 1	multicellular organismal development-GO:0007275: :intracellular-GO:0005622: :protein binding-GO:0005515: :DNA binding-GO:0003677: :metal ion binding-GO:0046872: :zinc ion binding-GO:0008270
X209318_x_at	pleiomorphic adenoma gene-like 1	transcription-GO:0006350: :regulation of transcription, DNA-dependent-GO:0006355: :induction of apoptosis-GO:0006917: :cell cycle arrest-GO:0007050: :positive regulation of transcription from RNA polymerase II promoter-GO:0045944: :intracellular-GO:0005622: :nucleus-GO:0005634: :DNA binding-GO:0003677: :metal ion binding-GO:0046872: :zinc ion binding-GO:0008270
X204153_s_at	MFNG O-fucosylpeptide 3-beta-N-acetylglucosaminyltransferase	pattern specification process-GO:0007389: :Golgi membrane-GO:0000139: :membrane-GO:0016020: :integral to membrane-GO:0016021: :extracellular space-GO:0005615: :Golgi apparatus-GO:0005794: :integral to Golgi membrane-GO:0030173: :transferase activity, transferring glycosyl groups-GO:0016757: :O-fucosylpeptide 3-beta-N-acetylglucosaminyltransferase activity-GO:0033829
X219191_s_at	bridging integrator 2	cytoplasm-GO:0005737: :protein binding-GO:0005515
X223303_at	fermitin family homolog 3 (Drosophila)	cell adhesion-GO:0007155: :plasma membrane-GO:0005886: :podosome-GO:0002102: :cytoplasm-GO:0005737: :protein binding-GO:0005515
X204639_at	adenosine deaminase	response to hypoxia-GO:0001666: :in utero embryonic development-GO:0001701: :trophectodermal cell differentiation-GO:0001829: :liver development-GO:0001889: :placenta development-GO:0001890: :germinal center B cell differentiation-GO:0002314: :positive regulation of germinal center formation-GO:0002636: :negative regulation of mature B cell apoptosis-GO:0002906: :adenosine catabolic process-GO:0006154: :deoxyadenosine catabolic process-GO:0006157: :nucleotide metabolic process-GO:0009117: :purine ribonucleoside monophosphate biosynthetic process-GO:0009168: :positive regulation of B cell proliferation-GO:0030890: :purine nucleotide salvage-GO:0032261: :regulation of cell-cell adhesion mediated by integrin-GO:0033632: :negative regulation of apoptosis-GO:0043066: :positive regulation of T cell differentiation-GO:0045582: :dATP catabolic process-GO:0046061: :hypoxanthine biosynthetic process-GO:0046101: :inosine biosynthetic process-GO:0046103: :xanthine biosynthetic process-GO:0046111: :alveolus development-GO:0048286: :Peyer's patch development-GO:0048541: :embryonic gut development-GO:0048566: :negative regulation of inflammatory response-GO:0050728: :negative regulation of adenosine receptor signaling pathway-GO:0060169: :membrane-GO:0016020: :lysosome-GO:0005764: :cytosol-GO:0005829: :cytoplasm-GO:0005737: :external side of plasma membrane-GO:0009897: :protein binding-GO:0005515: :adenosine deaminase activity-GO:0004000: :adenosine deaminase activity-GO:0004000: :zinc ion binding-GO:0008270: :hydrolase activity-GO:0016787
X207522_s_at	ATPase, Ca++ transporting, ubiquitous	metabolic process-GO:0008152: :ATP biosynthetic process-GO:0006754: :cation transport-GO:0006812: :calcium ion transport-GO:0006816: :membrane-GO:0016020: :integral to membrane-GO:0016021: :nucleus-GO:0005634: :nuclear membrane-GO:0031965: :sarcoplasmic reticulum membrane-GO:0033017: :nucleotide binding-GO:0000166: :protein binding-GO:0005515: :magnesium ion binding-GO:0000287: :calcium ion binding-GO:0005509: :calcium-transporting ATPase activity-GO:0005388: :ATP binding-GO:0005524: :hydrolase activity-GO:0016787: :hydrolase activity, acting on acid anhydrides, catalyzing transmembrane movement of substances-GO:0016820
X207761_s_at	methyltransferase like 7A	metabolic process-GO:0008152: :methyltransferase activity-GO:0008168: :transferase activity-GO:0016740
X55872_at	zinc finger protein 512B	transcription-GO:0006350: :regulation of transcription, DNA-dependent-GO:0006355: :intracellular-GO:0005622: :nucleus-GO:0005634: :DNA binding-GO:0003677: :metal ion binding-GO:0046872: :zinc ion binding-GO:0008270

X226372_at	carbohydrate (chondroitin 4) sulfotransferase 11	chondrocyte development-GO:0002063: :respiratory gaseous exchange-GO:0007585: :post-embryonic development-GO:0009791: :carbohydrate biosynthetic process-GO:0016051: :chondroitin sulfate biosynthetic process-GO:0030206: :negative regulation of transforming growth factor beta receptor signaling pathway-GO:0030512: :polysaccharide localization-GO:0033037: :tail morphogenesis-GO:0035121: :regulation of cell proliferation-GO:0042127: :embryonic digit morphogenesis-GO:0042733: :negative regulation of apoptosis-GO:0043066: :developmental growth-GO:0048589: :embryonic viscerocranium morphogenesis-GO:0048703: :embryonic skeletal morphogenesis-GO:0048704: :cartilage development-GO:0051216: :Golgi membrane-GO:0000139: :membrane-GO:0016020: :integral to membrane-GO:0016021: :Golgi apparatus-GO:0005794: :N-acetylgalactosamine 4-O-sulfotransferase activity-GO:0001537: :transferase activity-GO:0016740: :chondroitin 4-sulfotransferase activity-GO:0047756
X227711_at	gametocyte specific factor 1	cytoplasm-GO:0005737
X211919_s_at	chemokine (C-X-C motif) receptor 4	activation of MAPK activity-GO:0000187: :response to hypoxia-GO:0001666: :response to virus-GO:0009615: :apoptosis-GO:0006915: :signal transduction-GO:0007165: :chemotaxis-GO:0006935: :inflammatory response-GO:0006954: :immune response-GO:0006955: :G-protein coupled receptor protein signaling pathway-GO:0007186: :elevation of cytosolic calcium ion concentration-GO:0007204: :initiation of viral infection-GO:0019059: :interspecies interaction between organisms-GO:0044419: :plasma membrane-GO:0005886: :integral to plasma membrane-GO:0005887: :cytoplasm-GO:0005737: :leading edge-GO:0031252: :protein binding-GO:0005515: :actin binding-GO:0003779: :G-protein coupled receptor activity-GO:0004930: :coreceptor activity-GO:0015026: :C-C chemokine receptor activity-GO:0016493: :C-X-C chemokine receptor activity-GO:0016494: :myosin light chain binding-GO:0032027
X204960_at	protein tyrosine phosphatase, receptor type, C-associated protein	defense response-GO:0006952: :plasma membrane-GO:0005886: :integral to membrane-GO:0016021
X229686_at	purinergic receptor P2Y, G-protein coupled, 8	signal transduction-GO:0007165: :G-protein coupled receptor protein signaling pathway-GO:0007186: :plasma membrane-GO:0005886: :integral to membrane-GO:0016021: :receptor activity-GO:0004872: :G-protein coupled receptor activity-GO:0004930: :purinergic nucleotide receptor activity, G-protein coupled-GO:0045028
X226517_at	branched chain aminotransferase 1, cytosolic	G1/S transition of mitotic cell cycle-GO:0000082: :metabolic process-GO:0008152: :cell proliferation-GO:0008283: :branched chain family amino acid biosynthetic process-GO:0009082: :cytoplasm-GO:0005737: :branched-chain-amino-acid transaminase activity-GO:0004084: :identical protein binding-GO:0042802: :transferase activity-GO:0016740
X205349_at	guanine nucleotide binding protein (G protein), alpha 15 (Gq class)	signal transduction-GO:0007165: :protein amino acid ADP-ribosylation-GO:0006471: :elevation of cytosolic calcium ion concentration-GO:0007204: :muscarinic acetylcholine receptor, phospholipase C activating pathway-GO:0007207: :plasma membrane-GO:0005886: :heterotrimeric G-protein complex-GO:0005834: :nucleotide binding-GO:0000166: :GTPase activity-GO:0003924: :signal transducer activity-GO:0004871: :guanyl nucleotide binding-GO:0019001
X219594_at	ninjurin 2	cell adhesion-GO:0007155: :neuron adhesion-GO:0007158: :nervous system development-GO:0007399: :tissue regeneration-GO:0042246: :membrane-GO:0016020: :integral to plasma membrane-GO:0005887: :protein binding-GO:0005515
X211709_s_at	C-type lectin domain family 11, member A	positive regulation of cell proliferation-GO:0008284: :extracellular region-GO:0005576: :cytoplasm-GO:0005737: :binding-GO:0005488: :sugar binding-GO:0005529: :growth factor activity-GO:0008083
X205164_at	glycine C-acetyltransferase (2-amino-3-ketobutyrate coenzyme A ligase)	amino acid metabolic process-GO:0006520: :biosynthetic process-GO:0009058: :mitochondrial inner membrane-GO:0005743: :acyltransferase activity-GO:0008415: :glycine C-acetyltransferase activity-GO:0008890: :transferase activity, transferring nitrogenous groups-GO:0016769: :pyridoxal phosphate binding-GO:0030170
X204951_at	ras homolog gene family, member H	small GTPase mediated signal transduction-GO:0007264: :T cell differentiation-GO:0030217: :negative regulation of I-kappaB kinase/NF-kappaB cascade-GO:0043124: :regulation of transcription-GO:0045449: :plasma membrane-GO:0005886: :intracellular-GO:0005622: :cytoplasm-GO:0005737: :nucleotide binding-GO:0000166: :protein binding-GO:0005515: :GTPase inhibitor activity-GO:0005095: :GTP binding-GO:0005525: :Rho GTPase binding-GO:0017048: :kinase inhibitor activity-GO:0019210

X244654_at	myosin IG	myosin complex-GO:0016459: :nucleotide binding-GO:0000166: :motor activity-GO:0003774: :actin binding-GO:0003779: :calmodulin binding-GO:0005516: :ATP binding-GO:0005524
X220330_s_at	SAM domain, SH3 domain and nuclear localization signals 1	phosphotyrosine binding-GO:0001784
X211742_s_at	ecotropic viral integration site 2B	plasma membrane-GO:0005886: :integral to plasma membrane-GO:0005887: :cytoplasm-GO:0005737
X202878_s_at	CD93 molecule	phagocytosis-GO:0006909: :cell-cell adhesion-GO:0016337: :macrophage activation-GO:0042116: :interspecies interaction between organisms-GO:0044419: :plasma membrane-GO:0005886: :integral to membrane-GO:0016021: :cytoplasmic membrane-bounded vesicle-GO:0016023: :protein binding-GO:0005515: :calcium ion binding-GO:0005509: :complement component C1q binding-GO:0001849: :receptor activity-GO:0004872: :sugar binding-GO:0005529
X210038_at	protein kinase C, theta	regulation of cell growth-GO:0001558: :membrane protein ectodomain proteolysis-GO:0006509: :intracellular signaling cascade-GO:0007242: :nucleotide binding-GO:0000166: :protein binding-GO:0005515: :magnesium ion binding-GO:0000287: :protein kinase C activity-GO:0004697: :zinc ion binding-GO:0008270: :transferase activity-GO:0016740: :diacylglycerol binding-GO:0019992
X205131_x_at	C-type lectin domain family 11, member A	positive regulation of cell proliferation-GO:0008284: :extracellular region-GO:0005576: :cytoplasm-GO:0005737: :binding-GO:0005488: :sugar binding-GO:0005529: :growth factor activity-GO:0008083
X226219_at	Rho GTPase activating protein 30	signal transduction-GO:0007165: :intracellular-GO:0005622: :GTPase activator activity-GO:0005096
X217028_at	chemokine (C-X-C motif) receptor 4	activation of MAPK activity-GO:0000187: :response to hypoxia-GO:0001666: :response to virus-GO:0009615: :apoptosis-GO:0006915: :signal transduction-GO:0007165: :chemotaxis-GO:0006935: :inflammatory response-GO:0006954: :immune response-GO:0006955: :G-protein coupled receptor protein signaling pathway-GO:0007186: :elevation of cytosolic calcium ion concentration-GO:0007204: :initiation of viral infection-GO:0019059: :interspecies interaction between organisms-GO:0044419: :plasma membrane-GO:0005886: :integral to plasma membrane-GO:0005887: :cytoplasm-GO:0005737: :leading edge-GO:0031252: :protein binding-GO:0005515: :actin binding-GO:0003779: :G-protein coupled receptor activity-GO:0004930: :coreceptor activity-GO:0015026: :C-C chemokine receptor activity-GO:0016493: :C-X-C chemokine receptor activity-GO:0016494: :myosin light chain binding-GO:0032027
X206067_s_at	Wilms tumor 1	negative regulation of transcription from RNA polymerase II promoter-GO:0000122: :transcription-GO:0006350: :regulation of transcription, DNA-dependent-GO:0006355: :negative regulation of cell cycle-GO:0045786: :intracellular-GO:0005622: :transcription factor activity-GO:0003700: :metal ion binding-GO:0046872: :zinc ion binding-GO:0008270
X213720_s_at	SWI/SNF related, matrix associated, actin dependent regulator of chromatin, subfamily a, member 4	negative regulation of transcription from RNA polymerase II promoter-GO:0000122: :blastocyst growth-GO:0001832: :blastocyst hatching-GO:0001835: :methylation-dependent chromatin silencing-GO:0006346: :glial cell fate determination-GO:0007403: :keratinocyte differentiation-GO:0030216: :forebrain development-GO:0030900: :hindbrain development-GO:0030902: :embryonic hindlimb morphogenesis-GO:0035116: :epidermis morphogenesis-GO:0048730: :heterochromatin-GO:0000792: :nucleus-GO:0005634: :nucleoplasm-GO:0005654: :SWI/SNF complex-GO:0016514: :nucleotide binding-GO:0000166: :chromatin binding-GO:0003682: :transcription factor activity-GO:0003700: :transcription coactivator activity-GO:0003713: :helicase activity-GO:0004386: :ATP binding-GO:0005524: :transcription factor binding-GO:0008134: :identical protein binding-GO:0042802: :hydrolase activity-GO:0016787: :hydrolase activity, acting on acid anhydrides, in phosphorus-containing anhydrides-GO:0016818: :protein N-terminus binding-GO:0047485

X209201_x_at	chemokine (C-X-C motif) receptor 4	activation of MAPK activity-GO:0000187: :response to hypoxia-GO:0001666: :response to virus-GO:0009615: :apoptosis-GO:0006915: :signal transduction-GO:0007165: :chemotaxis-GO:0006935: :inflammatory response-GO:0006954: :immune response-GO:0006955: :G-protein coupled receptor protein signaling pathway-GO:0007186: :elevation of cytosolic calcium ion concentration-GO:0007204: :initiation of viral infection-GO:0019059: :interspecies interaction between organisms-GO:0044419: :plasma membrane-GO:0005886: :integral to plasma membrane-GO:0005887: :cytoplasm-GO:0005737: :leading edge-GO:0031252: :protein binding-GO:0005515: :actin binding-GO:0003779: :G-protein coupled receptor activity-GO:0004930: :coreceptor activity-GO:0015026: :C-C chemokine receptor activity-GO:0016493: :C-X-C chemokine receptor activity-GO:0016494: :myosin light chain binding-GO:0032027
X207957_s_at	protein kinase C, beta	protein amino acid phosphorylation-GO:0006468: :calcium ion transport-GO:0006816: :cellular calcium ion homeostasis-GO:0006874: :intracellular signaling cascade-GO:0007242: :lipoprotein transport-GO:0042953: :plasma membrane-GO:0005886: :plasma membrane-GO:0005886: :cytosol-GO:0005829: :nucleus-GO:0005634: :cytoplasm-GO:0005737: :nucleotide binding-GO:0000166: :protein binding-GO:0005515: :calcium ion binding-GO:0005509: :protein kinase C activity-GO:0004697: :calcium channel regulator activity-GO:0005246: :ATP binding-GO:0005524: :zinc ion binding-GO:0008270: :transferase activity-GO:0016740: :diacylglycerol binding-GO:0019992
X234973_at	solute carrier family 38, member 5	plasma membrane-GO:0005886: :integral to membrane-GO:0016021
X228153_at	ring finger protein 144B	protein ubiquitination during ubiquitin-dependent protein catabolic process-GO:0042787: :apoptosis-GO:0006915: :ubiquitin ligase complex-GO:0000151: :membrane-GO:0016020: :protein binding-GO:0005515: :ubiquitin-protein ligase activity-GO:0004842: :metal ion binding-GO:0046872: :zinc ion binding-GO:0008270: :ligase activity-GO:0016874
X201695_s_at	nucleoside phosphorylase	nucleobase, nucleoside, nucleotide and nucleic acid metabolic process-GO:0006139: :inosine catabolic process-GO:0006148: :DNA modification-GO:0006304: :nucleoside metabolic process-GO:0009116: :urate biosynthetic process-GO:0034418: :positive regulation of T cell proliferation-GO:0042102: :positive regulation of alpha-beta T cell differentiation-GO:0046638: :cytosol-GO:0005829: :purine-nucleoside phosphorylase activity-GO:0004731: :purine-nucleoside phosphorylase activity-GO:0004731
X204513_s_at	engulfment and cell motility 1	actin cytoskeleton organization and biogenesis-GO:0030036: :apoptosis-GO:0006915: :phagocytosis, engulfment-GO:0006911: :cell motility-GO:0006928: :Rac protein signal transduction-GO:0016601: :plasma membrane-GO:0005886: :cytosol-GO:0005829: :cytoplasm-GO:0005737: :cytoskeleton-GO:0005856: :protein binding-GO:0005515: :SH3 domain binding-GO:0017124
X204338_s_at	regulator of G-protein signaling 4	inactivation of MAPK activity-GO:0000188: :regulation of G-protein coupled receptor protein signaling pathway-GO:0008277: :negative regulation of signal transduction-GO:0009968: :signal transducer activity-GO:0004871: :GTPase activator activity-GO:0005096: :calmodulin binding-GO:0005516
X203761_at	Src-like-adaptor	cytoplasm-GO:0005737: :endosome-GO:0005768: :protein binding-GO:0005515: :SH3/SH2 adaptor activity-GO:0005070
X204285_s_at	phorbol-12-myristate-13-acetate-induced protein 1	release of cytochrome c from mitochondria-GO:0001836: :induction of apoptosis-GO:0006917: :caspase activation-GO:0006919: :cell structure disassembly during apoptosis-GO:0006921: :virus-infected cell apoptosis-GO:0006926: :response to dsRNA-GO:0043331: :mitochondrion-GO:0005739: :protein binding-GO:0005515
X213539_at	CD3d molecule, delta (CD3-TCR complex)	cell surface receptor linked signal transduction-GO:0007166: :plasma membrane-GO:0005886: :integral to membrane-GO:0016021: :cytoplasm-GO:0005737: :T cell receptor complex-GO:0042101: :transmembrane receptor activity-GO:0004888: :protein heterodimerization activity-GO:0046982
X200953_s_at	cyclin D2	G1/S transition of mitotic cell cycle-GO:0000082: :positive regulation of protein amino acid phosphorylation-GO:0001934: :regulation of cell cycle-GO:0051726: :positive regulation of cell proliferation-GO:0008284: :positive regulation of cyclin-dependent protein kinase activity-GO:0045737: :cell division-GO:0051301: :cyclin-dependent protein kinase holoenzyme complex-GO:0000307: :nucleus-GO:0005634: :protein binding-GO:0005515: :protein kinase binding-GO:0019901

X204116_at	interleukin 2 receptor, gamma (severe combined immunodeficiency)	signal transduction-GO:0007165: :immune response-GO:0006955: :interspecies interaction between organisms-GO:0044419: :membrane-GO:0016020: :integral to plasma membrane-GO:0005887: :protein binding-GO:0005515: :receptor activity-GO:0004872: :interleukin-2 receptor activity-GO:0004911: :interleukin-4 receptor activity-GO:0004913: :interleukin-7 receptor activity-GO:0004917
X209083_at	coronin, actin binding protein, 1A	phagolysosome formation-GO:0001845: :calcium ion transport-GO:0006816: :cell motility-GO:0006928: :actin filament organization-GO:0007015: :regulation of actin polymerization and/or depolymerization-GO:0008064: :positive regulation of cell migration-GO:0030335: :leukocyte chemotaxis-GO:0030595: :cell-substrate adhesion-GO:0031589: :uropod organization and biogenesis-GO:0032796: :positive regulation of T cell proliferation-GO:0042102: :T cell homeostasis-GO:0043029: :innate immune response-GO:0045087: :positive chemotaxis-GO:0050918: :negative regulation of actin nucleation-GO:0051126: :plasma membrane-GO:0005886: :immunological synapse-GO:0001772: :phagocytic cup-GO:0001891: :nucleus-GO:0005634: :cytoplasm-GO:0005737: :lamellipodium-GO:0030027: :cortical actin cytoskeleton-GO:0030864: :cytoplasmic vesicle-GO:0031410: :filamentous actin-GO:0031941: :phagocytic vesicle-GO:0045335: :actin filament binding-GO:0051015: :protein C-terminus binding-GO:0008022: :protein homodimerization activity-GO:0042803: :phosphoinositide 3-kinase binding-GO:0043548
X215714_s_at	SWI/SNF related, matrix associated, actin dependent regulator of chromatin, subfamily a, member 4	negative regulation of transcription from RNA polymerase II promoter-GO:0000122: :blastocyst growth-GO:0001832: :blastocyst hatching-GO:0001835: :methylation-dependent chromatin silencing-GO:0006346: :glial cell fate determination-GO:0007403: :keratinocyte differentiation-GO:0030216: :forebrain development-GO:0030900: :hindbrain development-GO:0030902: :embryonic hindlimb morphogenesis-GO:0035116: :epidermis morphogenesis-GO:0048730: :heterochromatin-GO:0000792: :nucleus-GO:0005634: :nucleoplasm-GO:0005654: :SWI/SNF complex-GO:0016514: :nucleotide binding-GO:0000166: :chromatin binding-GO:0003682: :transcription factor activity-GO:0003700: :transcription coactivator activity-GO:0003713: :helicase activity-GO:0004386: :ATP binding-GO:0005524: :transcription factor binding-GO:0008134: :identical protein binding-GO:0042802: :hydrolase activity-GO:0016787: :hydrolase activity, acting on acid anhydrides, in phosphorus-containing anhydrides-GO:0016818: :protein N-terminus binding-GO:0047485
X210754_s_at	v-yes-1 Yamaguchi sarcoma viral related oncogene homolog	signal transduction-GO:0007165: :protein amino acid phosphorylation-GO:0006468: :interspecies interaction between organisms-GO:0044419: :plasma membrane-GO:0005886: :plasma membrane-GO:0005886: :Golgi apparatus-GO:0005794: :membrane raft-GO:0045121: :nucleotide binding-GO:0000166: :protein binding-GO:0005515: :non-membrane spanning protein tyrosine kinase activity-GO:0004715: :receptor signaling protein tyrosine kinase activity-GO:0004716: :ATP binding-GO:0005524: :transferase activity-GO:0016740
X208885_at	lymphocyte cytosolic protein 1 (L-plastin)	actin filament bundle formation-GO:0051017: :ruffle-GO:0001726: :phagocytic cup-GO:0001891: :cytosol-GO:0005829: :cytoplasm-GO:0005737: :actin filament-GO:0005884: :calcium ion binding-GO:0005509: :actin filament binding-GO:0051015: :identical protein binding-GO:0042802
X203408_s_at	SATB homeobox 1	negative regulation of transcription from RNA polymerase II promoter-GO:0000122: :establishment and/or maintenance of chromatin architecture-GO:0006325: :regulation of transcription, DNA-dependent-GO:0006355: :nucleus-GO:0005634: :double-stranded DNA binding-GO:0003690: :transcription factor activity-GO:0003700: :sequence-specific DNA binding-GO:0043565

X213160_at	dedicator of cytokinesis 2	membrane raft polarization-GO:0001766: :establishment of T cell polarity-GO:0001768: :formation of immunological synapse-GO:0001771: :actin cytoskeleton organization and biogenesis-GO:0030036: :chemotaxis-GO:0006935: :positive thymic T cell selection-GO:0045059: :negative thymic T cell selection-GO:0045060: :alpha-beta T cell proliferation-GO:0046633: :lymphocyte chemotaxis-GO:0048247: :membrane-GO:0016020: :cytosol-GO:0005829: :cytoplasm-GO:0005737: :cytoskeleton-GO:0005856: :endomembrane system-GO:0012505: :electron carrier activity-GO:0009055: :protein binding-GO:0005515: :guanyl-nucleotide exchange factor activity-GO:0005085: :heme binding-GO:0020037: :Rac GTPase activator activity-GO:0030675: :Rac guanyl-nucleotide exchange factor activity-GO:0030676: :T cell receptor binding-GO:0042608
X222895_s_at	B-cell CLL/lymphoma 11B (zinc finger protein)	transcription-GO:0006350: :regulation of transcription, DNA-dependent-GO:0006355: :intracellular-GO:0005622: :nucleus-GO:0005634: :nucleic acid binding-GO:0003676: :metal ion binding-GO:0046872: :zinc ion binding-GO:0008270
X225285_at	branched chain aminotransferase 1, cytosolic	G1/S transition of mitotic cell cycle-GO:0000082: :metabolic process-GO:0008152: :cell proliferation-GO:0008283: :branched chain family amino acid biosynthetic process-GO:0009082: :cytoplasm-GO:0005737: :branched-chain-amino-acid transaminase activity-GO:0004084: :identical protein binding-GO:0042802: :transferase activity-GO:0016740
X226016_at	CD47 molecule	cell adhesion-GO:0007155: :integrin-mediated signaling pathway-GO:0007229: :positive regulation of cell proliferation-GO:0008284: :positive regulation of cell-cell adhesion-GO:0022409: :positive regulation of T cell activation-GO:0050870: :plasma membrane-GO:0005886: :plasma membrane-GO:0005886: :integral to plasma membrane-GO:0005887: :protein binding-GO:0005515
X237215_s_at	transferrin receptor (p90, CD71)	cellular iron ion homeostasis-GO:0006879: :endocytosis-GO:0006897: :plasma membrane-GO:0005886: :extracellular region-GO:0005576: :integral to plasma membrane-GO:0005887: :endosome-GO:0005768: :cytoplasmic membrane-bounded vesicle-GO:0016023: :melanosome-GO:0042470: :perinuclear region of cytoplasm-GO:0048471: :receptor activity-GO:0004872: :transferrin receptor activity-GO:0004998
X224579_at	solute carrier family 38, member 1	ion transport-GO:0006811: :sodium ion transport-GO:0006814: :glutamine transport-GO:0006868: :plasma membrane-GO:0005886: :integral to membrane-GO:0016021: :membrane fraction-GO:0005624: :axon-GO:0030424: :sodium:amino acid symporter activity-GO:0005283: :neutral amino acid transmembrane transporter activity-GO:0015175: :L-glutamine transmembrane transporter activity-GO:0015186: :symporter activity-GO:0015293: :sodium ion binding-GO:0031402
X204249_s_at	LIM domain only 2 (rhombotin-like 1)	multicellular organismal development-GO:0007275: :nucleus-GO:0005634: :metal ion binding-GO:0046872: :zinc ion binding-GO:0008270
X224927_at	KIAA1949	cytoplasm-GO:0005737: :cytoskeleton-GO:0005856: :actin binding-GO:0003779
X214728_x_at	SWI/SNF related, matrix associated, actin dependent regulator of chromatin, subfamily a, member 4	negative regulation of transcription from RNA polymerase II promoter-GO:0000122: :blastocyst growth-GO:0001832: :blastocyst hatching-GO:0001835: :methylation-dependent chromatin silencing-GO:0006346: :glial cell fate determination-GO:0007403: :keratinocyte differentiation-GO:0030216: :forebrain development-GO:0030900: :hindbrain development-GO:0030902: :embryonic hindlimb morphogenesis-GO:0035116: :epidermis morphogenesis-GO:0048730: :heterochromatin-GO:0000792: :nucleus-GO:0005634: :nucleoplasm-GO:0005654: :SWI/SNF complex-GO:0016514: :nucleotide binding-GO:0000166: :chromatin binding-GO:0003682: :transcription factor activity-GO:0003700: :transcription coactivator activity-GO:0003713: :helicase activity-GO:0004386: :ATP binding-GO:0005524: :transcription factor binding-GO:0008134: :identical protein binding-GO:0042802: :hydrolase activity-GO:0016787: :hydrolase activity, acting on acid anhydrides, in phosphorus-containing anhydrides-GO:0016818: :protein N-terminus binding-GO:0047485

X209685_s_at	protein kinase C, beta	protein amino acid phosphorylation-GO:0006468: :calcium ion transport-GO:0006816: :cellular calcium ion homeostasis-GO:0006874: :intracellular signaling cascade-GO:0007242: :lipoprotein transport-GO:0042953: :plasma membrane-GO:0005886: :plasma membrane-GO:0005886: :cytosol-GO:0005829: :nucleus-GO:0005634: :cytoplasm-GO:0005737: :nucleotide binding-GO:0000166: :protein binding-GO:0005515: :calcium ion binding-GO:0005509: :protein kinase C activity-GO:0004697: :calcium channel regulator activity-GO:0005246: :ATP binding-GO:0005524: :zinc ion binding-GO:0008270: :transferase activity-GO:0016740: :diacylglycerol binding-GO:0019992
X224848_at	cyclin-dependent kinase 6	G1 phase of mitotic cell cycle-GO:0000080: :positive regulation of cell-matrix adhesion-GO:0001954: :protein amino acid phosphorylation-GO:0006468: :cell cycle-GO:0007049: :regulation of gene expression-GO:0010468: :regulation of gene expression-GO:0010468: :hemopoiesis-GO:0030097: :gliogenesis-GO:0042063: :cell dedifferentiation-GO:0043697: :regulation of erythrocyte differentiation-GO:0045646: :negative regulation of osteoblast differentiation-GO:0045668: :positive regulation of fibroblast proliferation-GO:0048146: :negative regulation of epithelial cell proliferation-GO:0050680: :cell division-GO:0051301: :cyclin-dependent protein kinase holoenzyme complex-GO:0000307: :ruffle-GO:0001726: :nucleus-GO:0005634: :cytoplasm-GO:0005737: :nucleotide binding-GO:0000166: :cyclin-dependent protein kinase activity-GO:0004693: :ATP binding-GO:0005524: :transferase activity-GO:0016740: :cyclin binding-GO:0030332
X205270_s_at	lymphocyte cytosolic protein 2 (SH2 domain containing leukocyte protein of 76kDa)	immune response-GO:0006955: :transmembrane receptor protein tyrosine kinase signaling pathway-GO:0007169: :mast cell activation-GO:0045576: :cytokine secretion-GO:0050663: :cytosol-GO:0005829: :cytoplasm-GO:0005737: :protein binding-GO:0005515
X202746_at	integral membrane protein 2A	plasma membrane-GO:0005886: :integral to membrane-GO:0016021: :cytoplasm-GO:0005737
X219528_s_at	B-cell CLL/lymphoma 11B (zinc finger protein)	transcription-GO:0006350: :regulation of transcription, DNA-dependent-GO:0006355: :intracellular-GO:0005622: :nucleus-GO:0005634: :nucleic acid binding-GO:0003676: :metal ion binding-GO:0046872: :zinc ion binding-GO:0008270
X204890_s_at	lymphocyte-specific protein tyrosine kinase	cellular zinc ion homeostasis-GO:0006882: :induction of apoptosis-GO:0006917: :caspase activation-GO:0006919: :cell surface receptor linked signal transduction-GO:0007166: :intracellular signaling cascade-GO:0007242: :Ras protein signal transduction-GO:0007265: :response to drug-GO:0042493: :peptidyl-tyrosine phosphorylation-GO:0018108: :hemopoiesis-GO:0030097: :T cell differentiation-GO:0030217: :interspecies interaction between organisms-GO:0044419: :positive regulation of gamma-delta T cell differentiation-GO:0045588: :protein amino acid autophosphorylation-GO:0046777: :B cell receptor signaling pathway-GO:0050853: :positive regulation of T cell receptor signaling pathway-GO:0050862: :positive regulation of T cell activation-GO:0050870: :regulation of lymphocyte activation-GO:0051249: :plasma membrane-GO:0005886: :plasma membrane-GO:0005886: :pericentriolar material-GO:0000242: :cytosol-GO:0005829: :cytoplasm-GO:0005737: :Golgi apparatus-GO:0005794: :membrane raft-GO:0045121: :nucleotide binding-GO:0000166: :glycoprotein binding-GO:0001948: :non-membrane spanning protein tyrosine kinase activity-GO:0004715: :protein serine/threonine phosphatase activity-GO:0004722: :ATP binding-GO:0005524: :protein C-terminus binding-GO:0008022: :transferase activity-GO:0016740: :protein kinase binding-GO:0019901: :SH2 domain binding-GO:0042169: :CD4 receptor binding-GO:0042609: :CD8 receptor binding-GO:0042610: :phosphoinositide 3-kinase binding-GO:0043548: :ATPase binding-GO:0051117
X211372_s_at	interleukin 1 receptor, type II	immune response-GO:0006955: :membrane-GO:0016020: :integral to membrane-GO:0016021: :receptor activity-GO:0004872: :interleukin-1, Type II, blocking receptor activity-GO:0004910

X204891_s_at	lymphocyte-specific protein tyrosine kinase	cellular zinc ion homeostasis-GO:0006882: :induction of apoptosis-GO:0006917: :caspase activation-GO:0006919: :cell surface receptor linked signal transduction-GO:0007166: :intracellular signaling cascade-GO:0007242: :Ras protein signal transduction-GO:0007265: :response to drug-GO:0042493: :peptidyl-tyrosine phosphorylation-GO:0018108: :hemopoiesis-GO:0030097: :T cell differentiation-GO:0030217: :interspecies interaction between organisms-GO:0044419: :positive regulation of gamma-delta T cell differentiation-GO:0045588: :protein amino acid autophosphorylation-GO:0046777: :B cell receptor signaling pathway-GO:0050853: :positive regulation of T cell receptor signaling pathway-GO:0050862: :positive regulation of T cell activation-GO:0050870: :regulation of lymphocyte activation-GO:0051249: :plasma membrane-GO:0005886: :plasma membrane-GO:0005886: :pericentriolar material-GO:0000242: :cytosol-GO:0005829: :cytoplasm-GO:0005737: :Golgi apparatus-GO:0005794: :membrane raft-GO:0045121: :nucleotide binding-GO:0000166: :glycoprotein binding-GO:0001948: :non-membrane spanning protein tyrosine kinase activity-GO:0004715: :protein serine/threonine phosphatase activity-GO:0004722: :ATP binding-GO:0005524: :protein C-terminus binding-GO:0008022: :transferase activity-GO:0016740: :protein kinase binding-GO:0019901: :SH2 domain binding-GO:0042169: :CD4 receptor binding-GO:0042609: :CD8 receptor binding-GO:0042610: :phosphoinositide 3-kinase binding-GO:0043548: :ATPase binding-GO:0051117

9 References

Reference List

[1] D. Albino, *et al.*, "Identification of low intratumoral gene expression heterogeneity in neuroblastic tumors by genome-wide expression analysis and game theory," **113**(6), 1412 (2008).

Ref Type: Journal

[2] S. A. Amundson, *et al.*, "Integrating global gene expression and radiation survival parameters across the 60 cell lines of the National Cancer Institute Anticancer Drug Screen," Cancer Res. **68**(2), 415 (2008).

Ref Type: Journal

[3] J. P. Annereau, *et al.*, "Analysis of ATP-binding cassette transporter expression in drug-selected cell lines by a microarray dedicated to multidrug resistance," **66**(6), 1397 (2004).

Ref Type: Journal

[4] C. K. Augustine, *et al.*, "Genomic and molecular profiling predicts response to temozolomide in melanoma," **15**(2), 502 (2009).

Ref Type: Journal

[5] B. Bachtiary, *et al.*, "Gene expression profiling in cervical cancer: an exploration of intratumor heterogeneity," **12**(19), 5632 (2006).

Ref Type: Journal

[6] S. Bao, *et al.*, "Glioma stem cells promote radioresistance by preferential activation of the DNA damage response," Nature **444**(7120), 756 (2006).

Ref Type: Journal

[7] Preter K. De, *et al.*, "Application of laser capture microdissection in genetic analysis of neuroblastoma and neuroblastoma precursor cells," **197**(1-2), 53 (2003).

Ref Type: Journal

[8] O. P. Erpolat, *et al.*, "Outcome of newly diagnosed glioblastoma patients treated by radiotherapy plus concomitant and adjuvant temozolomide: a long-term analysis," **95**(2), 191 (2009).

Ref Type: Journal

[9] W. A. Freije, *et al.*, "Gene expression profiling of gliomas strongly predicts survival," Cancer Res. **64**(18), 6503 (2004).

Ref Type: Journal

[10] H. S. Friedman, T. Kerby, and H. Calvert, "Temozolomide and treatment of malignant glioma," **6**(7), 2585 (2000).

Ref Type: Journal

[11] K. S. Garman, J. R. Nevins, and A. Potti, "Genomic strategies for personalized cancer therapy," **16 Spec No. 2**, R226-R232 (2007).

Ref Type: Journal

[12] E. J. Hall and A. J. Giaccia, *radiobiology for the radiologist*, 6th ed. (Lippincott Williams & Wilkins, 2006).

[13] M. E. Hegi, *et al.*, "MGMT gene silencing and benefit from temozolomide in glioblastoma," **352**(10), 997 (2005).

Ref Type: Journal

[14] M. E. Hegi, *et al.*, "Correlation of O6-methylguanine methyltransferase (MGMT) promoter methylation with clinical outcomes in glioblastoma and clinical strategies to modulate MGMT activity," J. Clin. Oncol. **26**(25), 4189 (2008).

Ref Type: Journal

[15] K. M. Jochumsen, *et al.*, "Gene expression in epithelial ovarian cancer: a study of intratumor heterogeneity," **17**(5), 979 (2007).

Ref Type: Journal

[16] T. Kanzawa, *et al.*, "Inhibition of DNA repair for sensitizing resistant glioma cells to temozolomide," **99**(6), 1047 (2003).

Ref Type: Journal

[17] J. Lamb, "The Connectivity Map: a new tool for biomedical research," **7**(1), 54 (2007).

Ref Type: Journal

[18] E. Lee, *et al.*, "Inferring pathway activity toward precise disease classification," **4**(11), e1000217 (2008).

Ref Type: Journal

[19] Y. Lee, *et al.*, "Gene expression analysis of glioblastomas identifies the major molecular basis for the prognostic benefit of younger age," **1**, 52 (2008).

Ref Type: Journal

[20] S. Madhavan, *et al.*, "Rembrandt: helping personalized medicine become a reality through integrative translational research," **7**(2), 157 (2009).

Ref Type: Journal

[21] National Cancer Institute, "REpository for Molecular BRAin Neoplasia DaTa (REMBRANDT),"in 2005).

[22] NCI-NCGRI, "Controlled TCGA Data Access,"in 2009).

[23] NCI-NIH, "Developmental Therapeutics Program (DTP): Screening Procedures,"in 2009).

[24] C. Nieder, M. Adam, and A. L. Grosu, "Combined modality treatment of glioblastoma multiforme: the role of temozolomide," **1**(1), 43 (2006).

Ref Type: Journal

[25] C. L. Nutt, *et al.*, "Gene expression-based classification of malignant gliomas correlates better with survival than histological classification," Cancer Res. **63**(7), 1602 (2003).

Ref Type: Journal

[26] J. Pittman, *et al.*, "Integrated modeling of clinical and gene expression information for personalized prediction of disease outcomes," Proc. Natl. Acad. Sci. U. S. A **101**(22), 8431 (2004).

Ref Type: Journal

[27] S. M. Pollard, *et al.*, "Glioma stem cell lines expanded in adherent culture have tumor-specific phenotypes and are suitable for chemical and genetic screens," **4**(6), 568 (2009).

Ref Type: Journal

[28] A. Potti, *et al.*, "Genomic signatures to guide the use of chemotherapeutics," **12**(11), 1294 (2006).

Ref Type: Journal

[29] A. Potti, *et al.*, "A genomic strategy to refine prognosis in early-stage non-small-cell lung cancer," **355**(6), 570 (2006).

Ref Type: Journal

[30] J. N. Rich, *et al.*, "Gene expression profiling and genetic markers in glioblastoma survival," Cancer Res. **65**(10), 4051 (2005).

Ref Type: Journal

[31] U. T. Shankavaram, *et al.*, "Transcript and protein expression profiles of the NCI-60 cancer cell panel: an integromic microarray study," **6**(3), 820 (2007).

Ref Type: Journal

[32] U. T. Shankavaram, *et al.*, "CellMiner,"in 2009).

[33] R. H. Shoemaker, "The NCI60 human tumour cell line anticancer drug screen," **6**(10), 813 (2006).

Ref Type: Journal

[34] S. C. Short, *et al.*, "Dose- and time-dependent changes in gene expression in human glioma cells after low radiation doses," **168**(2), 199 (2007).

Ref Type: Journal

[35] R. Stupp, *et al.*, "Radiotherapy plus concomitant and adjuvant temozolomide for glioblastoma," **352**(10), 987 (2005).

Ref Type: Journal

[36] K. Trautmann, *et al.*, "Expression profiling of gastric cancer samples by oligonucleotide microarray analysis reveals low degree of intra-tumor variability," **11**(38), 5993 (2005).

Ref Type: Journal

[37] Rijn J. van, *et al.*, "Survival of human glioma cells treated with various combination of temozolomide and X-rays," **47**(3), 779 (2000).

Ref Type: Journal

[38] L. Wang, *et al.*, "Survival prediction in patients with glioblastoma multiforme by human telomerase genetic variation," J. Clin. Oncol. **24**(10), 1627 (2006).

Ref Type: Journal